The role of glutathionperoxidase 4 (GPX4) in hematopoiesis and leukemia

von Kira Célénie Stahnke

Inaugral- Dissertation zur Erlangung der Doktorwürde der Tierärztlichen Fakultät der Ludwig-Maximilians-Universität

München

The role of glutathionperoxidase 4 (GPX4) in hematopoiesis and leukemia

von Kira Célénie Stahnke

aus Dortmund

München 2016

Aus dem
Veterinärwissenschaftlichen Department der Tierärztlichen Fakultät
der **Ludwig-Maximilians-Universität München**
Lehrstuhl für Molekulare Tierzucht und Biotechnologie

Arbeit angefertigt unter der Leitung von
Univ.-Prof. Dr. Eckhard Wolf

Angefertigt am
Institut für Experimentelle Tumorforschung
Universitätsklinikum Ulm
Mentor: Prof. Dr. Christian Buske

Gedruckt mit Genehmigung der Tierärztlichen Fakultät der
Ludwig-Maximilians-Universität München

Dekan:	Univ.-Prof. Dr. Joachim Braun
Berichterstatter:	Univ.-Prof. Dr. Eckard Wolf
Korreferent/en:	Priv.-Doz. Dr. Bianka Schulz

Tag der Promotion: 06.02.2016

Table of contents

List of Abbreviations

aa	Amino acids
AEL	Acute erythroid leukemia
AIDS	Acquired immune deficiency syndrome
AKT	Protein kinase B
ALL	Acute lymphoblastic leukemia
AML	Acute myeloid leukemia
Amp	Ampicillin
APL	Promyelocytic leukemia
ATO	Arsenic trioxide
bFGF	Basic fibroblast growth factor
BM	Bone marrow
BSA	Bovine serum albumin
bZIP domaine	Basic leucine zipper domain
CaT	Catalase
CBF	Core binding factor
CC	Cytokine cocktail
CEBPA	CCAAT/enhancer binding protein alpha
CFC	Colony forming cell
CLL	Chronic lymphoid leukemia
CLP	Common lymphoid progenitor
CM-H2DCFDA	Dichlorofluorescein diacetate
CML	Chronic myeloid leukemia
CMP	Common myeloid progenitor
$C_{T^{\wedge}}$	Cycle threshold
Cu	Copper
DEPC	Diethyldicarbonat
DHA	Dehydroascorbine acid
DMEM	Dulbecco's Modified Eagle's medium
DMSO	Dimethyl sulfoxide
DNA	Deoxyribonucleic acid
dNTP	Deoxyribonucleotide triphosphate
EBF	Early B-cell factor
EcRB	Ecdysone receptor
EDTA	Ethylenediaminetetraacetic acid
EGF	Epidermal growth factor
EKLF	Erythrocyte Krüppel-like factor
EtOH	Ethanol
FACS	Fluorescence activated cell sorting
FBS	Fetal bovine serum
FC	Fragment crystallizable

Fe	Iron
FIT-C	Fluoresceinisothiocyanat
Fli	Friend leukemia integration
Flt3	FSM like thyrosin kinase 3
FoxO	Forkhead box O
GATA 1	GATA binding factor
GFI	Growth factor independent
GFP	Green fluorecent protein
GLCL	Glutamate-cysteine-ligase
GM-CSF	Granulocyte-macrophage colony stimulating factor
GMP	Granulocyte macrophage progenitor
GPCR	G protein coupled receptor
Gpx	Glutathione peroxidase
GR	Glutathionereductase
GSH	L-gammaglutamyl-L-cysteinglycine
h	Hour
H_2O_2	Hydrogen peroxide
HBSS	Hank's balanced salt solution
HClO	Hypochlorous acid
HEPES	Hydroxyethylpiperacin-ethansulfonacid
HIV	Human immunodeficiency virus
HPC	Hematopoietic progenitor cells
HSC	Hematopoetic stem cell
IFN	Interferon
IGF	Insulin-like growth factor
IL	Interleukin
IRF	Interferon regulatory factor
ITD	Internal tandem duplication
kb	Kilobase
kDa	Kilo Dalton
LB	Luria-Bertani
Lef	Lymphoid enhancer factor
LOX	Lipoxygenase
LSC	Leukemic stem cell
LSK	Lineage- ska1+ c-kit- cells
M	Molar (mol/L)
MAP(K)	Mitogen activated protein (kinase)
mCSF	Murine stem cell factor
MEP	Megakaryocytic erythrocytic progenitor
min	Minute
ml	Milliliter
MLL	Mixed lineage leukemia

MNC	Mononuclear cell
MPP	Multipotent progenitor
n.s.	Not significant
NAC	N-acetyl cysteine
NADPH	Nicotinamide adenine dinucleotide phosphate
NaOH	Sodium hydroxide
NF-κB	Nuclear factor kappa light chain enhancer
NK	Normal karyotype
nm	Nano meter
NO	Nitrate monoxide
NPM	Nucleophosmin
Ox-LDL	Oxidized low density lipoprotein
Pax	Paired box protein
PB	Peripheral blood
PBS	Phosphate buffered saline
PCR	Polymerase chain reaction
PDGF	Platelet derived growth factor
PEITC	Beta-phenylethyl isothiocyanate
PHGpx	Phospholipid hydroxyperoxide glutathione peroxidase
pMIG	MSCV-IRES-(E)GFP plasmid
Prx	Peroxiredoxin
PS	Phospholipid phosphatidylserine
PU 1	Purine rich box binding protein
qRT-PCR	Quantitative reverse transcription PCR
Ras	Rat sarcoma
RNA	Ribonucleic acid
ROS	Reactive oxygen species
rpm	Rounds per minute
RPMI	Roswell park memorial institute
RT	Room temperature
RUNX	Stem cell level runt related transcription factor
SC	Stem cell
SCL	Stem cell leukemia factor
scr	Scrambled
SD	Standard deviation
SDS	Sodium dodecyl sulfate
sec	Second
SEM	Standard error of mean
shRNA	Short hairpin RNA
SOD	Superoxid dismutase
STAT 5	Signal transducer and activator of transcription
TBS	Tris buffered saline

TCF	T-cell specific transcription factor
TEMED	Tetramethylethylendiamin
TKD	Thyrosine kinase domain
TNF	Tumor necrosis factor
Trx (R)	Thioredoxin (-reductase)
µg	Microgram
µl	Microliter
V	Volt
VCM	Virus containing medium
VEGF	Vascular endothelial growth factor
WHO	World health organization
WNT	Wingless-Int1
WT	Wild type

Species	**Gene**	**Protein**
Human	*GPX4*	GPX4
Mouse	*Gpx4*	GPX4

1 Introduction

1.1 ROS and oxidative stress in physiology and pathology

1.1.1 Sources of Reactive Oxygen Species

Life originally evolved under anaerobic circumstances. The more sophisticated species developed mechanisms to generate energy from oxidative respiration instead of fermentation. This method of generating energy implicates the single electron reduction of oxygen to water (Figure 1). The leakage of electrons during this reaction generates partially reduced oxygen species that are more reactive and more toxic than molecular oxygen itself. Oxygen species appear as inevitable by-products of the normal metabolism and their toxicity is handled during phylogenesis by the development of several antioxidative defense mechanisms. Reactive Oxygen Species (ROS) include superoxide anion (O_2^-), hydrogen peroxide (H_2O_2), the highly reactive hydroxyl radical (HO°), singlet oxygen ($^1O_2$), peroxyl radical (RO_2°), alkoxyl radical (RO°) and hydroperoxyl radical (HO_2°) (Imlay, 2008).

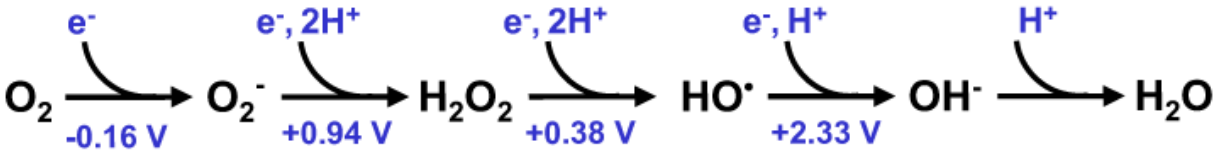

Figure 1: ROS are inevitable by-products of the normal metabolism via the single electron reduction of O_2 to H_2O. The redox state of oxygen with standard reduction potentials. The standard concentration of oxygen was regarded as 1M (Imlay, 2008).

The terms ROS and free radicals are often used as equivalents. Both can react with a number of biomolecules and are able to start a chain reaction that forms more free radicals. This reaction can only be stopped by the reaction with a radical scavenger, a primary antioxidant or by the interaction of free radicals with each other. All of these reactions lead to elimination of an unpaired electron (Nordberg & Arnér, 2001).

ROS are generated by both endogenous and exogenous sources. The most important endogenous source is the respiratory chain located in the mitochondria. Besides there are several other potential sources for ROS such as xanthine oxidase, cytochrome P450 based enzymes, NADPH oxidases, dysfunctional NO synthases and inflammatory cells (Shah AM, 2004).

ROS molecule	**Main source**
Superoxide ($O_2^{\circ -}$)	Leakage of electrons from the electron transport chain Activated phagocytes Xanthine oxidase Flavoenzymes
Hydrogen peroxide (H_2O_2)	From $O_2^{\circ -}$ via superoxide dismutase (SOD) NADPH-oxidase (neutrophils) Glucose oxidase Xanthine oxidase
Hydroxyl radical (°OH)	From $O_2^{\circ -}$ and H_2O_2 via transition metals (Fe or Cu)
Nitric oxide (NO)	Nitric oxide synthases

Table 1: Major ROS molecules and their sources (modified from Nordberg & Arner, 2001)

Exogenous sources for ROS are environmental factors like UV light, ionizing irradiation, inflammatory cytokines and pathogens that directly or indirectly increase the cellular ROS levels (Waris & Ahsan, 2006).

During phylogenesis several systems were developed to eliminate ROS from those sources. A frail balance exists between the formation of ROS and the antioxidative defense mechanisms that cause the difference between physiological ROS levels and oxidative stress induced by high ROS levels.

1.1.2 Physiological role of ROS

Research over the last two decades has shown that ROS play a role in physiologic and pathologic states.

One important physiologic role of ROS is the direct antibacterial effect. Activated phagocytes produce HCLO and °OH, two highly reactive ROS molecules that are toxic to bacteria and therefore have a direct antimicrobial effect (oxidative burst). The NADPH oxidase complex produces those molecules. Another antimicrobial molecule is hypochlorous acid. HClO disturbs the DNA replication of bacteria (Nordberg & Arnér, 2001). Besides the direct effect on bacteria ROS enhance the response of lymphocytes to antigens (Dröge, 2002).

Changes in ROS level also affect the carotid body that acts as oxygen sensor and controls ventilation and the production of certain hormones such as erythropoietin, VEGF and insulin like growth factor II (IGF-II) (Marian Valko et al., 2007).

Furthermore ROS play a pivotal role in redox-responsive signaling pathways that control numerous physiological functions. ROS may strengthen the function of redox-sensitive proteins, lead to a loss of function or switch the protein to another function (Trachootham et al., 2006).

In addition ROS play a major role in receptor-mediated cell signaling pathways (Veal, Day, & Morgan, 2007). They act as second messenger in mitogen–activated protein kinases (MAPKs) signaling pathways (Mulder, 2000). In that way ROS are able to mediate cellular functions such as proliferation and apoptosis (Dröge, 2002; M Valko, Rhodes, Moncol, Izakovic, & Mazur, 2006). This has been proven for a variety of receptors.

For example ROS play a role in activated growth factor signaling including epidermal growth factor (EGF) receptor, platelet-derived growth factor (PDGF) receptor, and vascular endothelial growth factor (VEGF) (Neufeld, Cohen, Gengrinovitch & Poltorak, 1999). Other cell surface receptors which are modulated by hydrogen peroxide (H_2O_2) are basic fibroblast growth factor (bFGF) (Lo & Cruz, 1995), granulocyte-macrophage colony stimulating factor (GM-CSF) (Sattler et al., 1999), cytokines like interleukin-1 (IL-1) (Krieger-Brauer & Kather, 1995), interleukin-3 (IL-3) (Sattler et al., 1999), interferon γ (IFN-γ) (Lo & Cruz, 1995), tumor necrosis factor-α (TNF-α) (Krieger-Brauer & Kather, 1995; Lo & Cruz, 1995), T cell receptor (Tatla, Woodhead, Foreman, & Chain, 1999) and GTP-binding protein (G-Protein)-coupled receptors (GPCRs) like angiotensin II (Griendling & Ushio-Fukai, 2000).

Hydrogen peroxide may also stimulate insulin and glucose transport and lipid synthesis in adipocytes (May & de Haën, 1979).

ROS as a second messenger are present everywhere in the organism most of the time in a balance between ROS formation and antioxidative mechanisms but because of their toxicity have a potential role in pathologies.

1.1.3 Oxidative stress, principle pathology of ROS

Oxidative stress appears if there is an imbalance in between ROS formation and the clearance of antioxidative mechanisms. Ongoing oxidative stress leads to damage of macromolecules (DNA, RNA, protein, lipids) by free radicals and to an increased inflammatory response due to TNF-α, INF-Ɣ and Il-1-β (Yang et al., 2007).

1.1.3.1 Oxidative stress in diseases

Studies have proven a role for ROS and ROS related stress for diabetes mellitus, uremia, atherosclerosis, hyperlipidemia, rheumatoid arthritis, respiratory distress syndrome, human immunodeficiency virus (HIV) infection and cystic fibrosis (Chinta & Andersen, 2008; Niwa, 2007; Ozben, 2007; M Valko et al., 2006). It is also known that ROS play a role in aging (Campisi & Vijg, 2009). In addition to that, oxidative stress is known to be part of a number of other pathological conditions and diseases like macula degeneration (Winkler, Boulton, Gottsch, & Sternberg, 1999), cataracts (Truscott, 2000), septic shock (Andresen et al., 2008), neurodegenerative diseases like Parkinson and Alzheimer disease, cardiovascular diseases, ischemia/reperfusion and most of all in the development of cancer (Dalle-Donne, Rossi, Colombo, Giustarini, & Milzani, 2006; Dhalla, Temsah, & Netticadan, 2000; Jenner, 1996; Sayre, Smith, & Perry, 2001)

1.1.3.2 Oxidative stress in cancer

A redox imbalance caused by oxidative stress is found in various cancer cells. This imbalance can cause DNA mutations through oxidative damage. ROS induced DNA damage includes single- or double-stranded DNA breaks, purine, pyrimidine or deoxyribose modifications and DNA cross-links. The DNA damage may lead to arrest or induction of transcription and signal transduction affecting apoptosis and cell cycle pathways. Furthermore it

causes replication errors and genomic instability. All of these events are involved in carcinogenesis (Marian Valko et al., 2007).

In particular ROS act as a carcinogen as they facilitate tumor promotion and progression. The tumor promoting effect is explained via the signaling cascades that were discussed above. Chronic oxidative stress can block the regulation of signaling pathways in a way that leads to a permanent activation and therefore to permanent proliferation of the affected cells (Schumacker, 2006). Even normal cells show higher proliferation and expression of genes related with growth when they are treated with hydrogen peroxide or superoxide (Dröge, 2002). Tumor cells in culture are known to produce more ROS compared to normal cells (Szatrowski & Nathan, 1991) and the event of malignant transformation is directly followed by an increased ROS production of the cells (Trachootham et al., 2006).

Following the "multi hit model of carcinogenesis" in which tumorigenesis is caused by the accumulation of a variety of events (J. V Sutherland & Bailar, 1984) it is difficult to dissect the role of ROS in this complex process. In addition it is not quite clear which came first. Whether ROS are required for tumor initiation or are caused by the development of tumors and are required for tumor growth and maintenance. Regarding that elevated ROS levels even lead to apoptosis/necrosis and therefore are destructive for tumor cells (Figure 2) it is clear that ROS can not be identified as neither "good" nor "bad". Further investigation of their role in specific tumors and of the antioxidative mechanisms that balance the cellular ROS levels is needed. This may eventually lead to the identification of targets for anti cancer therapy (Schumacker, 2006).

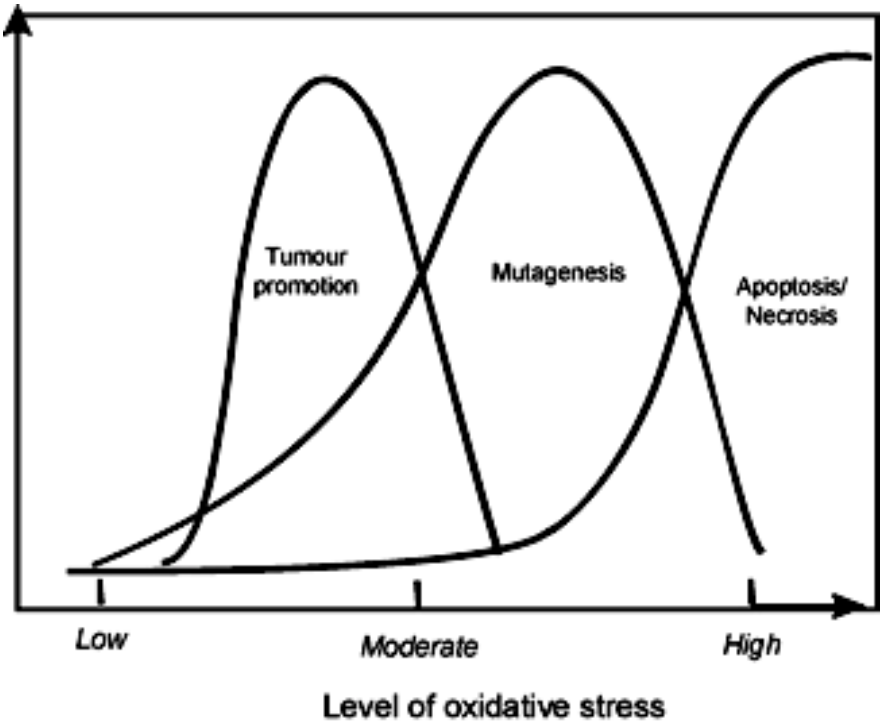

Figure 2 The dose-dependend effect of relationship between levels of oxidative stress and tumor promotion, mutagenesis and apoptosis/necrosis (Marian Valko et al., 2007).

1.2 Antioxidative mechanisms

Antioxidants are substances that significantly delay or inhibit oxidation of substrates when present at low concentration, compared to amount of oxidizable substrate (Halliwell, B a. G., 1989).

During the adaption of life to an aerobic world the organism developed strategies to eliminate single electrons that leak from the mitochondrial chain. These mechanisms are defensive or reparative and are able to eliminate ROS from intracellular and extracellular compartments. A number of DNA repair enzymes are available in the organism but antioxidants show a more specific and more effective way to protect cells from damaging radicals. The antioxidant system of mammalians includes endogenous, exogenous, enzymatic and non-enzymatic antioxidants (Karihtala & Soini, 2007).

The classification into enzymatic and non-enzymatic antioxidants is sometimes problematic. Non-enzymatic antioxidants may act as substrates for enzymes and therefore interfere with the enzymatic system. Bearing this in mind the classification though is used in the present work.

1.2.1 Non-enzymatic antioxidant mechanisms

Several low molecular weight compounds act as antioxidants such as vitamine E, where α-tocopherol is the most potent biological and antioxidant form of the vitamin that is incorporated into the membrane bilayer and acts together with β-carotine against lipidperoxidation (Burton & Traber, 1990). Another important vitamin in this system is vitamin C (ascorbic acid) which acts synergistically with vitamin E in order to regenerate vitamin E (Packer, Slater, & Willson, 1979).
Other non-enzymatic antioxidants are serum albumin (Roche, Rondeau, Singh, Tarnus, & Bourdon, 2008), ceruloplasmin-transferrin (Asetskaia et al., 1990), metallothioneins (Viarengo, Burlando, Ceratto, & Panfoli, 2000), bilirubin (Stocker, Yamamoto, McDonagh, Glazer, & Ames, 1987), glucose (Piwkowska, Rogacka, Audzeyenka, Jankowski, & Angielski, 2011), N-acetyl-cysteine (NAC), a by-product of glutathione that contains cysteine and plays a role in glutathione maintenance and metabolism (Kerksick & Willoughby, 2005), metabolic intermediates and small molecules.
System X_c is a transmembranic antiporter of the anionic forms of cystine and glutamate. Its activity is important for the maintenance of intracellular Glutathione levels and the redox balance between cystine and cysteine in the extracellular compartment (Sato et al., 2002).
Glutathione (L-gammaglutamyl-L-cysteinylglycine; GSH) is one of the most important intracellular antioxidants. It is thiol-based and present in all living aerobic cells in millimolar concentrations. It works as a sulfhydryl but is also able to detoxify radicals via conjugations catalyzed by glutathione S-transferase or directly as for example in glutathionperoxidase (GPX) catalyzed reactions. Oxidized glutathione is reduced by glutathione-reductase (GR) a NADPH-dependend flavoenzyme. Glutathione is related to a number of enzymes and antioxidant mechanisms of which the most important are summarized in Figure 3.

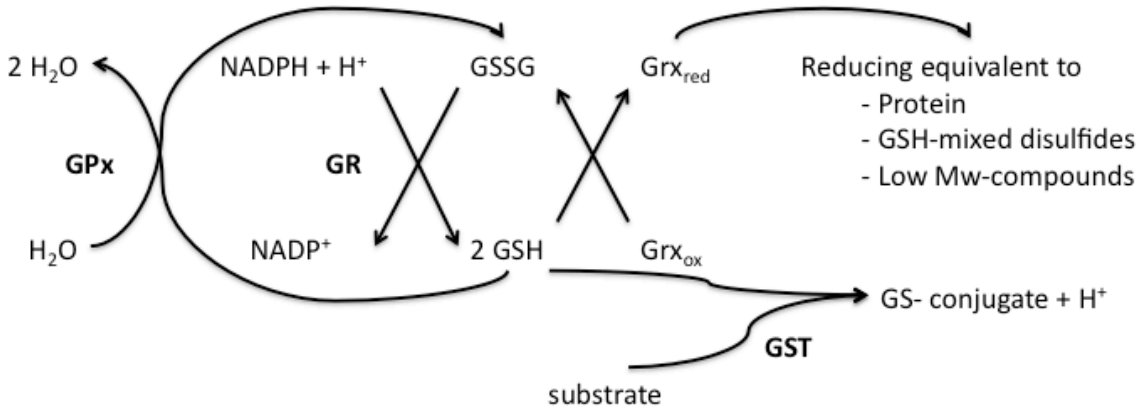

Figure 3: schematic summary of the major glutathione-associated antioxidant systems. Hydrogen peroxide is reduced by glutathione peroxidases (GPX) by oxidation of two molecules of glutathione (GSH) forming glutathione disulfide (GSSG) that subsequently can be reduced by glutathione reductase (GR) under consumption of NADPH. Glutathione also reduces glutaredoxins (GRX) that in their turn reduce various substrates. Specific for glutaredoxins is the reduction of glutathione mixed disulfides such as glutathionylated proteins. Glutathione S-transferase (GST) catalyze the conjugation of glutathione with other molecules, thereby functioning as an intermediate step in the detoxification of miscellaneous toxic substances (Nordberg & Arnér, 2001).

1.2.2 Enzymatic antioxidant mechanisms

Antioxidants and cell redox state modulating enzymes are summarized in Table 2.

Enzyme/protein	Abbreviation	Primary antioxidant function
Catalase	CAT	Reduces hydrogen peroxide to water and oxygen
Mitochondrial superoxide dismutase	mSOD	Dismutates superoxide anions to hydrogen peroxide and molecular oxygen
Cytosolic superoxide dismutase	cSOD	Dismutates superoxide anions to hydrogen peroxide and molecular oxygen
Glutamate-cysteine ligase	GLCL	Catalyzes the first production step of GSH
Glutathione	GSH	See below
Glutathione peroxidase	GPX	Reduces hydrogen peroxide (and lipidperoxides), GSH as substrate
Glutathione reductase	GR	
Peroxiredoxin	Prx	Reduces the oxidized form of GSH
Thioredoxin reductase	TrxR	Reduces peroxides to corresponding alcohol Catalyzes the reduction of Trx

Table 2: Summary of certain human antioxidant and other redox state modulating enzymes (Karihtala & Soini, 2007).

Superoxide dismutase (SOD)

Superoxide dismutases were the first ROS-metabolizing enzymes that were discovered and further investigated. Two metal containing SOD isoenzymes are able to metabolize $O_2^{\circ -}$ to hydrogen peroxide in eukaryotic cells, the mitochondrial Mn-SOD and the cytosolic Cu/Zn-SOD. SOD catalyzes the following reaction:

$$\mathbf{2O_2^{\circ -} + 2H^+ \rightarrow \quad H_2O_2 + O_2}$$

(Karihtala & Soini, 2007).

Catalases

The heme-containing group of Catalases is mostly located in peroxisomes of mammalian cells and catalyzes the following reaction:

$2H_2O \rightarrow O_2 + 2H_2O$

In addition Catalases are able to detoxify substrates like phenols and alcohols.

Catalase binds NADPH and therefore protects itself from inactivation and increases its efficiency. The inhibition of Catalase is thought to be the cause of the hemolysis that appears in the disease of 6-phosphate dehydrogenase deficiency (Karihtala & Soini, 2007).

Peroxiredoxins (Prx; thioredoxin peroxidases)

So far about 13 peroxiredoxins are known that are able to directly reduce peroxides (hydrogen peroxide, alkyl hydroperoxides). Oxidized Prx formed by the catalytic cycle is regenerated through thioredoxin and thioredoxin seems to be a specific reductant of Prx in the mammalian mitochondrion. It is known that P53 induced apoptosis can be inhibited by peroxiredoxins (Nordberg & Arnér, 2001).

Thioredoxin (*TRX*)

Thioredoxins are thiol-containing antioxidants. Their antioxidant function is due to reversible oxidation of the catalytic site to the cysteine disulfide.

$Trx\text{-}(SH)_2 + X\text{-}S_2 \rightarrow Trx\text{-}S_2 + X(SH)_2$

The oxidized form is reduced back via TrxR under the consumption of 1 NADPH. Besides the primary antioxidative effect Trx plays a role in other physiologic processes. It is for example an efficient growth factor, inhibits apoptosis and activates transcription factors such as NF-κB and activator protein-2 (Karihtala & Soini, 2007). Three variants of human TRX encoded on different genes have bee characterized. TRX1, a 12 Da protein, TRX2 enzyme located in the mitochondrium and spTRX a variant that is highly expressed in spermatozoa. TRX is involved in some clinical issues. For example it protects the lens from oxidative stress and this way is able to protect it from cataract. It is considered to have a protective effect in acute ischaemic heart disease and increased plasma levels of TRX were found in hepatocellular carcinoma, AIDS, Sjörgens Syndrome, rheumatoid arthritis and other diseases (Nordberg & Arnér, 2001).

Glutathionperoxidases (Gpx)

Glutathionperoxidases are glutathiondependend enzymes that reduce H_2O and alky peroxidase to H_2O. There are 7 isoforms existing of which GPX1-4 and hGPX 6 are Selenoproteins. GPX5, GPX7 and mGPX6 are non-selenium containing Cys homologues. Gpx 2 (gastrointestinal GPX) and GPX3 (plasma GPX) are mainly found in the gastrointestinal tract and in the kidney. GPX3 is considered to be regenerated by the Trx system. It is still discussed whether GPX plays an important role under physiological circumstances or if it only becomes important in state of oxidative stress. Knock out mice that are lacking Gpx1 for example show normal phenotype and are even able to deal with hypoxia and oxidative stress (Nordberg & Arnér, 2001). The present work focuses on the glutathionperoxidase isoform Gpx 4.

Glutathionperoxidase 4/Phospholipid Hydroperoxide Glutathione peroxidase (Gpx4/PHGpx)

GPX4 is a selenium dependent phospholipid peroxidase that protects cell membranes against lipidperoxidation. In contrast to other members of the GPX protein family that show a tetrameric form it has a monomeric structure and is less dependend on glutathione than the other glutathionperoxidases. GPX4 catalyzes the following reaction:

2 glutathione + lipid-hydroperoxide → glutathione disulfid + lipidalcohol + H_2O

GPX4 is in contrast to other members of the familiy not only able to reduce small hydrophilic peroxides but also to reduce more complex peroxides such as phospholipid or cholesterol hydroperoxides. This even holds true if they are incorporated into membranes or lipoproteins. If enough glutathione is present GPX4 uses it as reducing equivalent. But in case glutathione is limited like in developing sperm cells GPX4 is able to accept thiol groups of proteins as reducing equivalent (Ufer & Wang, 2011).

The gene is ubiquitously expressed in all tissues and is located on chromosome 19 in humans and chromosome 10 in mouse. It is a 22,17 DA protein in humans. In mice the protein weight is 20,47 DA. The GPX4 protein is found in almost all subcellular components, as there are the cytoplasm, the nucleus, mitochondria and the endoplasmatic reticulum. (Marcus Conrad, Schneider, Seiler, & Bornkamm, 2007). In mammals there are 3 different isoforms existing that can be characterized by their specific N-terminal sequences (Figure 4). They are described as mitochondrial, cytosolic and nuclear isoform (Savaskan, Ufer, Kühn, & Borchert, 2007).

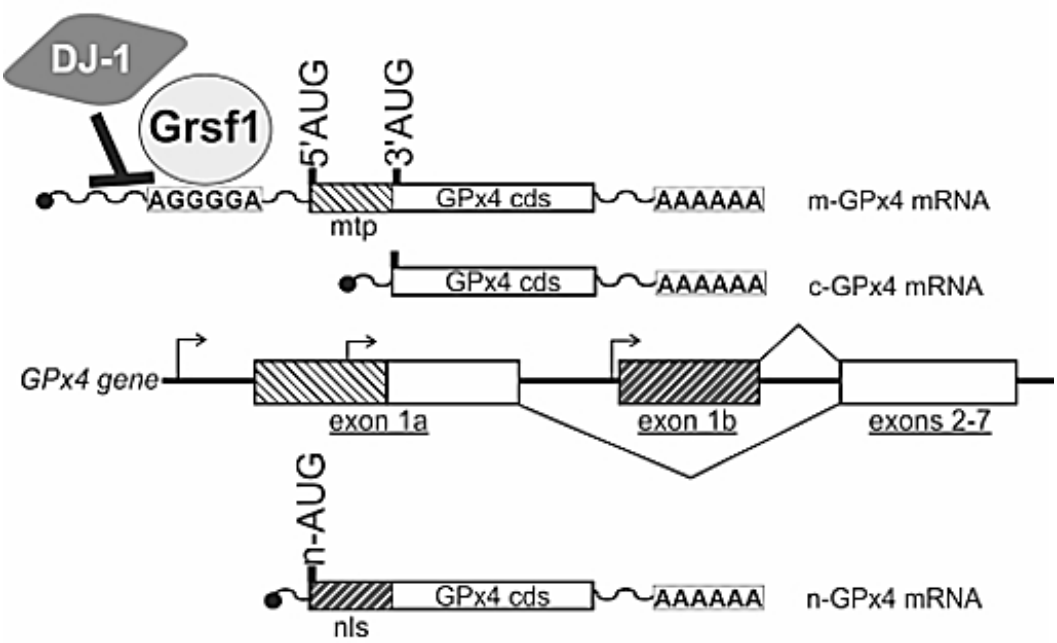

Figure 4 Coding multiplicity of the *Gpx4* gene. The *Gpx4* gene gives rise to three isoenzymes designated *m-Gpx4, c-Gpx4 and n-Gpx4*. They can be distinguished by their N-terminal sequences that determine their subcellular localization (mtp, mitochondrial targeting peptide (light hatching); nls, nuclear localization sequence (dark hatching)). The mammalian *Gpx4* gene consists of seven exons and contains three windows of transcriptional (arrows) and translational (5ÁUG, 3ÁUG, n-AUG) initiation, that are specific to the isoenzymes. Two protein factors (DJ-1, Grsf1) have been identified that affect post-transcriptional regulation of the *Gpx4* gene. Cds coding sequence (Ufer & Wang, 2011).

Ursini et al. (1982) were the first who extracted the GPX4 protein from a pig liver and later described it as a protein containing one mole of selenium per one mole protein (Ursini, Maiorino, Valente, Ferri, & Gregolin, 1982). So far a variety of functions were identified in vitro as well as in vivo. Maiorino et al. described that selenocysteine is indispensable for full GPX4 activity (M Maiorino et al., 1995). GPX4 reduces hydroperoxy ester lipids that are generated by 15-lipoxygenase (Banning et al., 2004) and a knock down of PHGPx leads to an up-regulation of the arachidon acid metabolism caused by 12-lipoxigenase and cyclooxygenase 1 (C. J. Chen, Huang, Lin, & Chang, 2000; C.-J. Chen, Huang, & Chang, 2003). GPX4 is able to polymerisate in vitro without glutathione when H_2O_2 is present (Mauri et al., 2003).

Concerning the different isoforms of GPX4 it is known that the cytosolic form if overexpressed leads to a decreased leukotriene formation in RBL-2H3 cells (H Imai et al., 1998) and lowers NFκB (nuclear factor kappa-light-chain-enhancer of activated B-cells) activation induced from interleukin-1 in endothelial cells (Brigelius-Flohé, Friedrichs, Maurer, Schultz, &

Streicher, 1997). Overexpression of *Gpx4* in RBL-2H3 cells leads to some protection against oxidative stress (Arai et al., 1999) and lowers the prostaglandin D2 production (Sakamoto, Imai, & Nakagawa, 2000). Experiments with porcine GPX4 showed that it prevents NFκB activation, oxLDL-induced proliferation and apoptosis induced by linoleic acid (Brigelius-Flohé et al., 2000).

The mitochondrial form is basically expressed in somatic tissues during embryonic development (Borchert et al., 2006; Pushpa-Rekha, Burdsall, Oleksa, Chisolm, & Driscoll, 1995; Schneider et al., 2006) and the transfer into mitochondria is only possible in presence of a leader sequence (Arai et al., 1996). It protects cells from damages caused by lipid hydroperoxides (Yagi et al., 1996; Yagi, Shidoji, Komura, Kojima, & Ohishi, 1998) and the overexpression in RBL-2H3 cells leads to a high stress resistance (Arai et al., 1999). In addition mitochondrial GPX4 migrates in the mitochondria from the matrix to the outer membrane (Haraguchi et al., 2003). It prevents apoptosis induced by hypoglycemia (Hirotaka Imai et al., 2003) and geranylgeranoic acid (Shidoji et al., 2006).

The nuclear isoform of GPX4 is mainly present in sperm nuclei and is therefore often named snGPX (Godeas et al., 1996; Pfeifer et al., 2001). It is expressed in the nucleus of late spermatids (Borchert, Savaskan, & Kuhn, 2003; Matilde Maiorino et al., 2003; Moreno, Laux, Brielmeier, Bornkamm, & Conrad, 2003; Nakamura, Imai, Tsunashima, & Nakagawa, 2003).

Functions of GPX4 were studied in vivo and using knock-out models. It was shown that a loss of PHGPx lead to death at embryonic day 7,5 in homozygote knock-out mice (Hirotaka Imai et al., 2003; Yant et al., 2003). Heterozygote mice had a shorter survival after the exposure to irradiation and were more sensitive to oxidative and genotoxic stress (Yant et al., 2003). Mice that overexpress human *GPX4* are protected against oxidative stress induced apoptosis (Ran et al., 2004). *GPX4* is highly expressed in testis and spermatogenetic cells (M Maiorino et al., 1998; Roveri et al., 1992) and is an important structural protein of the sperm midpiece mitochondrial capsule (Ursini et al., 1982). Sutherland at al. claimed a possible involvement of GPX4 in the 12-lipoxygenase pathway in human platelets (M. Sutherland, Shankaranarayanan, Schewe, & Nigam, 2001). A knock down of mitochondrial *Gpx4* in ex-vivo cultivated embryos led to neuronal degeneration in the middle of gestation. Embryos in the same experiment that carry a knock-down of nuclear *Gpx4* showed abnormal heart formation at the same time point (Borchert et al., 2006). Knock-out mice for nuclear *Gpx4* showed a normal phenotype but had a retarded chromatin condensation of male germ cells (M Conrad et al., 2005).

1.3 Antioxidant mechanisms in tumorigenesis and as target for anti cancer drugs

The role of ROS in cancer is ambiguous. Malignant cells use ROS signaling to drive proliferation and tumor progression. This need for a higher basal ROS level can be used to target tumor cells with either augmenting ROS generation or weaken antioxidant defense mechanisms of the cell. In that case tumor cells die through the same system they need to survive (Schumacker, 2006). Along this line targeting the antioxidant mechanisms seems to be a promising approach in anti-cancer therapy. In particular as antioxidant mechanisms are upregulated in malignant cells, pointing to their protective role for cancer cells. It was shown that if the Glutathion dependend sytem is targeted with beta-phenylethyl isothiocyanate (PEITC) in cancer cells it is possible to selectively kill tumor cells by increased ROS accumulation. High ROS levels cause oxidative mitochondrial damage, inactivate redox sensitive molecules and cause massive cell death. In mouse models mice with tumors that were treated with PEITC showed a prolonged survival (Figure 5) (Trachootham et al., 2006). A knock down of the antioxidant enzyme thioredoxin reductase 1 (*Trx1*) in mouse lung carcinoma (LLC1) cells led to a recovered non-malignant phenotype. Reduced expression in mice led to slower tumor progression and less metastasis (Yoo, Xu, Carlson, Gladyshev, & Hatfield, 2006).

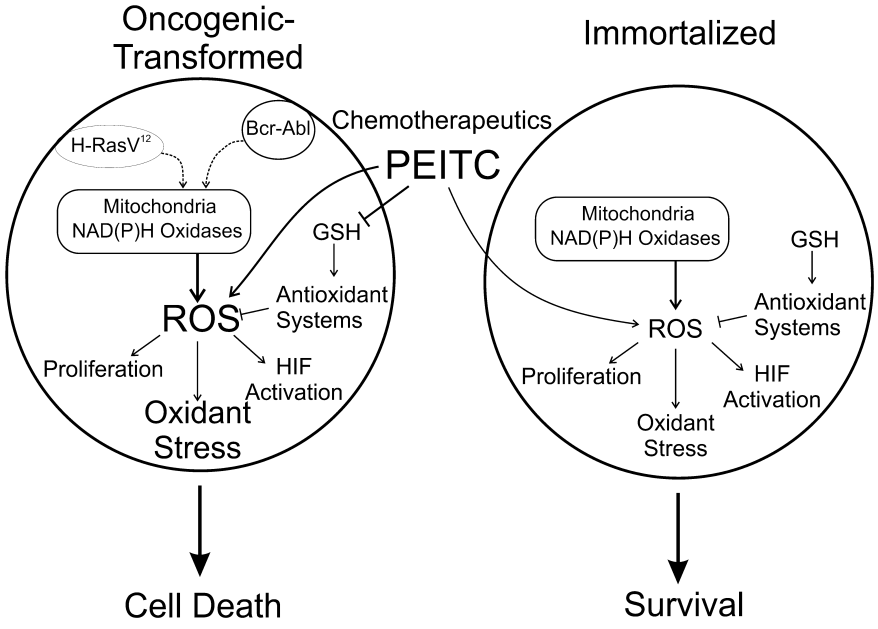

Figure 5 Oncogenic transformation, oxidant stress and cell survival in response to chemotherapeutic agents that augment ROS production (Schumacker, 2006)

The effect of Arsenic trioxide (ATO), an anti cancer drug particularly used against acute promyelocytic leukemia (APL) and solid tumors is based on the inhibition of TrxR (Lu, Chew, & Holmgren, 2007).

Glutathionperoxidase 4 in cancer

It is known that GPX4 is able to protect Burkitt's lymphoma cells from death due to oxidative stress (Brielmeier et al., 2001) and the overexpression of cytosolic or mitochondrial *GPX4* in pancreatic tumor cell lines causes growth inhibition in tumor transplantation experiments (Liu et al., 2006; Trachootham et al., 2006). It was shown that Doxohexaenoic acid (DHA) causes cytotoxic effects in a variety of tumors via lipidperoxidation. It leads to a downregulation of the GPX4 protein in human cancer cell lines and a knockdown of *GPX4* in an ovarian cancer cell line enhanced the cytotoxic effect of DHA (Ding & Lind, 2007). Heterozygous knock-out mice *Gpx4* (+/-) had a delayed occurrence of fatal lymphomas (Ran et al., 2007) and GPX4 plays an important role in the regulation of tumor angiogenesis and vessel maturation through controlling 12/15-lipoxygenase (LOX) activity (Schneider et al., 2010). All these findings suggest a protective role of GPX4 for malignant cells against accumulation of ROS and give raise to the idea that it might be possible to reverse this protective effect by targeting GPX4.

1.4 Normal and malignant hematopoiesis

Mature hematopoietic cells in the peripheral bloodstream have a very limited life span. Leucocytes and thrombocytes live for 12-14 days, red blood cells circle in the bloodstream for 120 days. This system requires a permanent regeneration of these cells in the bloodforming organs. The most important organ is the bone marrow but liver and spleen are also involved in the process of hematopoiesis during embryogenesis or during pathologic processes. In vertebrates one can distinguish between two phases of hematopoiesis, primitive (embryonic) and definitive (adult) hematopoiesis (Liao et al., 2002).

1.4.1 Normal hematopoiesis

Postpartal hematopoiesis

Postpartal (adult) blood formation takes place in the bone marrow. Extramedullar hematopoiesis only occurs as phathologic compensatory phenomenon caused by insufficient bone marrow function. It is observed in hematological diseases like myelofibrosis, polycythemia vera, leukemia, lymphoma or after irradiation of the bone marrow. In this case all organs that were involved in the fetal hematopoiesis are able to step in (Haidar, Mhaidli, & Taher, 2010).

Hematopoietic stem cells

The constant release of bloodcells from the bone marrow depends on a rare population of progenitor cells called hematopoietic stem cells (HSCs). These cells have the ability to self-renew and the potential for multilineage differentiation, the hematopoietic stem cells (HSCs) (Cumano & Godin, 2007). HSCs are on top of a hematopoietic hierarchy (Figure 6) and can be subdivided into long-term self-renewing HSCs, short-term self-renewing HSCs and multipotent progenitors. Long term HSCs are on top of the hierarchy and have the ability of long-term self-renewal and multilineage differentiation. Short time HSCs have less self-renewing potential and are able to differentiate into all hematopoietic cell types. Multipotent progenitors lost their ability of self renewal but still even though they have lineage specific surface markers have the potential to differentiate into cells of other lineages (Challen & Goodell, 2011).
HSCs give rise to the different hematopoietic lineages. The lymphoid lineage of which common lymphoid progenitors (CLPs) give rise to all further differentiated lymphoid cells and the myeloid lineage with common myeloid progenitors (CMPs) as precursors of all myeloid cells. GMPs (granulocyte macrophage progenitor) and erythroid (MEP, megakaryocyte erythrocyte progenitor) cells (Reya, Morrison, Clarke, & Weissman, 2001) (Figure 6). Specific cell surface markers, proteins that are specifically expressed on the surface of the cells are used to identify the different progenitor cells.

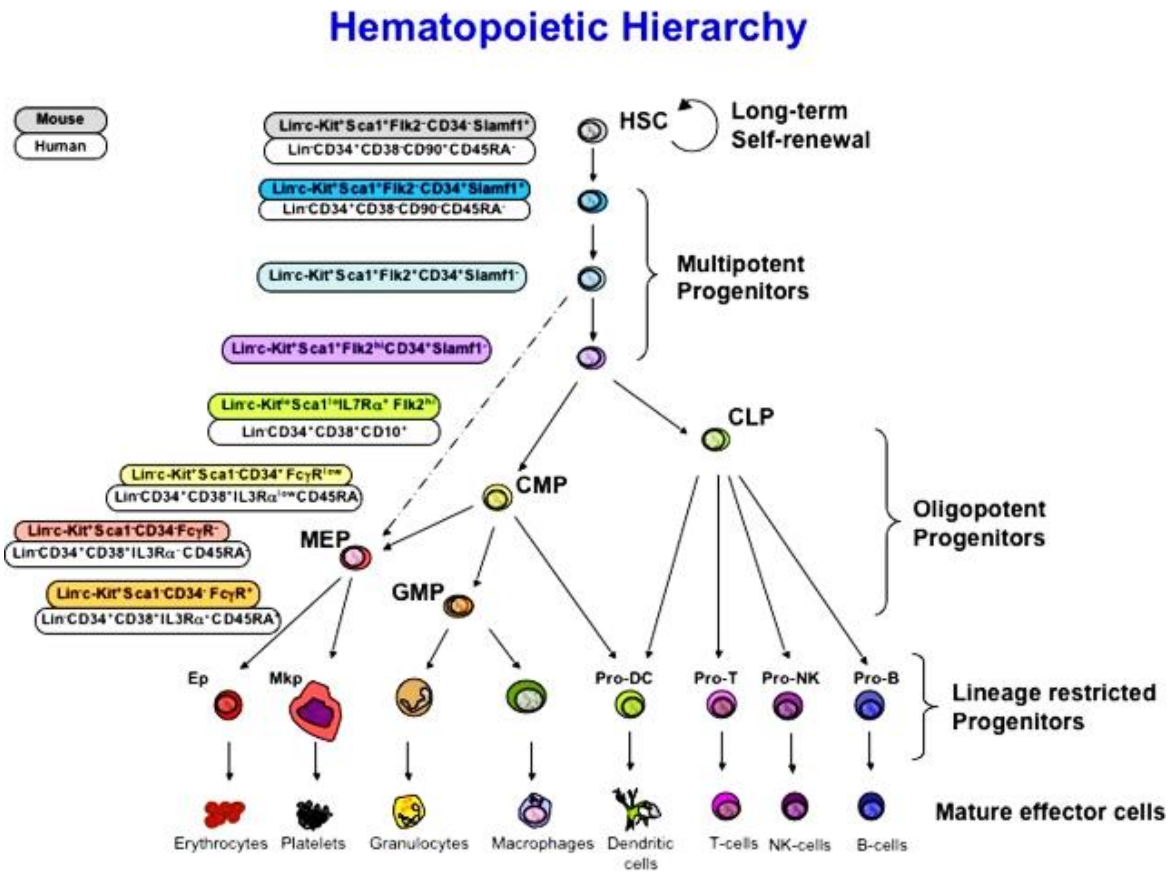

Figure 6: Hematopoietic and progenitor cell lineages and their surfacemarkers in human and mouse (Weissman & Shizuru, 2008).

Myeloid lineage

Common myeloid progenitors (CMP) give rise to the erythroid lineage that starts from Megakayoblasts, Proerythroblasts and to the actual myeloid lineage that developes basophil, neutrophil and eosinophil granulocytes as well as macrophages.

All members of the myeloid lineage are part of the immune response and develope according to the immunesituation of the body. PU.1 plays a role in the specification of the myeloid versus the lymphoid lineage. It is present in B-lmphocytes and myelocytes and is able to drive HSCs into differentiation towards the myeloid lineage. The mechanism is upregulation of myeloid specific cell surface marker genes and downregulation of cell-surface markers specific for progenitor cells, thrombocytes and GATA-1. Long term-activation of PU.1 leads to a development of the myeloid lineage, whereas short time activation leads to the development of immature eosinophils (Nerlov & Graf, 1998). Other involved transcription factors are CCAAT-enhancer-binding proteins, growth-factor-independent 1 (GFI1), interferon-regulatory factor 8 (IRF8), stem-cell level runt-related

transcription factor 1 (RUNX1), stem-cell leukemia factor (SCL), JUNB, Ikaros and MYC (Figure 7) (Rosenbauer & Tenen, 2007).

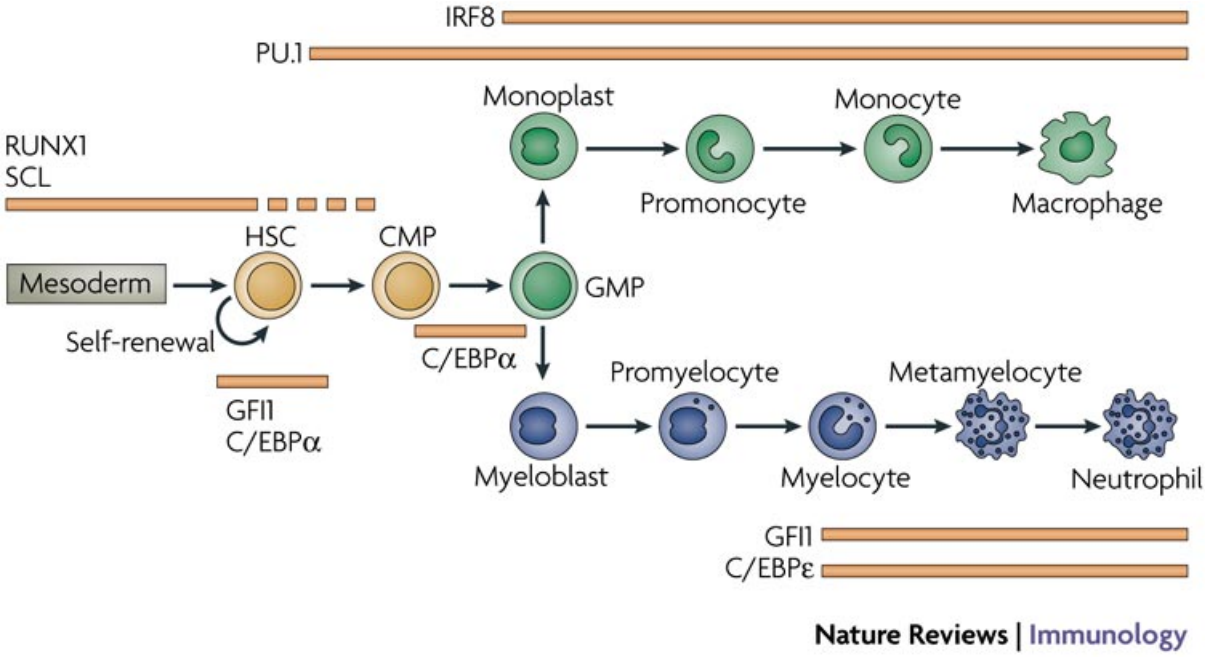

Figure 7 Stem cell differentiation in the myeloid lineage and the required transcriptionfactors (Rosenbauer & Tenen, 2007).

1.5 Malignant hematopoiesis - leukemia

Leukemia is a neoplastic disease of the hematopoietic system that is characterized by the massive occurrence of immature leucocytes in the peripheral blood. Those so-called blast cells derive from different lineages. Cancer stem cell theory implies that specific subpopulations of cells exist, which are able to initiate and maintain tumors. Self-renewing leukemic stem cells (LSCs) drive leukemias. LSCs are assumed to be abnormal stem cells (Gentles, Plevritis, Majeti, & Alizadeh, 2010).

Leukemia is both cytogenetically as well as molecularly a very heterogeneous disease. In other malignancies inherited mutations are found in the majority of the cases. In leukemia mutations appear sporadic as consequence of acquired somatic mutations in the hematopoietic progenitor cells (Dash & Gilliland, 2001).

Neoplasias of all hematopoietic lineages are classified according to the system of the World Health Organization (WHO). This system classifies leukemias according to the lineage that is affected (myeloid, lymphoid, histiocytic/dendritic) and seperates neoplasia caused by a precursor cell from those consisting of functionally mature cells (Vardiman, 2010).

Furthermore according to the US national cancer institute leukemia can be categorized by on the rate of their progress and the affected lineage (Table 3).

Affected lineage	Acute	Chronic
Myeloid	Acute myeloid leukemia (AML)	Chronic myeloid leukemia (CML)
Lymphoid	Acute lymphoid leukemia (ALL)	Chronic lymphoid leukemia (CLL)

Table 3: Most common types of leukemia classified after the lineage and the rapidness of the diseases progress (www.cancer.gov).

Because of the complexity and heterogeneity of leukemia and as the present study was performed focusing on AML only this subtype will be discussed further.

Acute myeloid leukemia (AML)

AML includes a heterogeneous group of hematopoietic malignancies in which the proliferation and maturation of myeloid blasts arrests in the bone marrow as well as in the peripheral blood (Cammarata et al., 2010). It is diagnosed if more than 20% of the cells in the peripheral blood are myeloid blasts (Gilliland & Tallman, 2002). AML is the most frequent type of acute leukemia in adults with an incidence of 3.6 per 100'000 men and woman per year. The median age at point of diagnosis is 66 years (www.cancer.gov). AML can be classified according to the French-American-British (FAB) classification into subtypes based on the cell type and maturity of the cells (Table 4).

FAB subtype	Nomenclature	% of adult AML patients
M0	Undifferentiated acute myeloblastic leukemia	5%
M1	Acute myeloblastic leukemia with minimal maturation	15%
M2	Acute myeloblastic leukemia with maturation	25%
M3	Acute promyelocytic leukemia (APL)	10%
M4	Acute myelomonocytic leukemia	20%
M4 eos.	Acute myelomonocytic leukemia with eosinophilia	5%
M5	Acute monocytic leukemia	10%
M6	Acute erythroid leukemia	5%
M7	Acute megakaryoblastic leukemia	5%

Table 4 French-American-British (FAB) classification of AML.

The current and more detailed classification is made by the world health organization (WHO). This classification is based on genetic- and immunophenotype as well as on cytochemistry and cell morphology. In addition, the classification considers clinical prognosis and outcome.

WHO classification of myeloid neoplasms and acute leukemia
Myoproliferative neoplasms (MPN)
Myeloid and lymphoid neoplasms associated with eosinophilia and abnormalities of PDGFRA, PDGFRB, or $FGFR_1$
Myelodysplastic syndrome (MDS)
Acute myeloid leukemia and related neoplasms
AML with recurrent genetic abnormalities
AML with t(8;21)(q22;q22); RUNX1-RUNX1T1
AML with inv.(16)(p13.1q22) or t(16;16)(p13.1;q22); CBFB-MYH1 1
APL with t(15;17)(q22;q12); PML-RARA
AML with t(9;11)(p22;q23); MLLT3-MLL
AML with t(6;9)(p23;q34); DEK-NUP214
AML with inv(3)(qq21;q26.2) or t(3;3)(q21;q26.2); RPN1-EVI1
AML (megakaryoblastic) with 1(1;22)(p13;q13); RBM15-MKL1
Provisional entity: AML with mutated NPM1
Provisional entity: AML with mutated CEBPA
Acute myeloid leukemia with myelodysplasia related changes
Therapy-related myeloid neoplasms
Acute myeloid leukemia, not otherwise specified
AML with minimal differentiation
AML without maturation
AML with maturation
Acute myelomonocytic leukemia
Acute monoblastic/monocytic leukemia
Acute erythroid leukemia
Pure erythroid leukemia
Erythroleukemia, erythroid/myeloid
Acute megakaryoblastic leukemia
Acute basophilic leukemia
Acute panmyelosis with myelofibrosis
Myeloid sarcoma
Myeloid proliferation related to Down syndrome
Transient abnormal myelopoiesis
Myeloid leukemia associated with Down syndrome
Blastic plasmacytoid dendritic cell neoplasm
Acute leukemias of ambiguous lineage
B lymphoblastic leukemia/lymphoma
T lymphoblastic leukemia/lymphoma

Table 5: WHO classification of myeloid neoplasms and acute leukemia (modified from Vardiman et al., 2009)

AML like most malignancies is a multistep disease in which several independent factors and events lead to tumorigenesis (Raskind, Steinmann, & Najfeld, 1998). Those factors can be genetically determined or can appear in form of mutations due to a number of internal and external influences. Around 25% of AML show a chromosomal translocation, which usually are correlated to good prognosis. 40-50% show a normal karyotype and have a variety of molecular abnormalities (Cammarata et al., 2010).

AML with Chromosomal Translocations

The diagnosis of chromosomal abberation nowadays has a major effect on the choice of therapy. Of more than 100 cloned translocations some have the same targets for signal transduction and transcriptional pathways.

Loss of function of the heterodimeric transcription factor core-binding factor (CBF) is found in 20-25% of AML. It is for example targeted by the chromosomal inversion inv(16)(p13q22) that leads to CBFβ-SMMHC and by the translocation t(8;12)(q22;q22) that results in the AML1-ETO fusion protein. The transcription inhibitor PML/RARα that recruits the nuclear co-repressor complex (NCoR) aberantly is affected by the translocation t(15;17)(q22;q12) that is strictly associated with acute promyelocytic leukemia (APL). It leads to the PML/RARα fusion gene and appears in 93% of APL (Gilliland & Tallman, 2002). Another transcription factor that under physiologic circumstances is responsible for normal hematopoiesis is the rearrangement of the mixed lineage leukemia (MLL) protein that is found in 10% of de novo AML (Cozzio et al., 2003)(**Figure 8**).

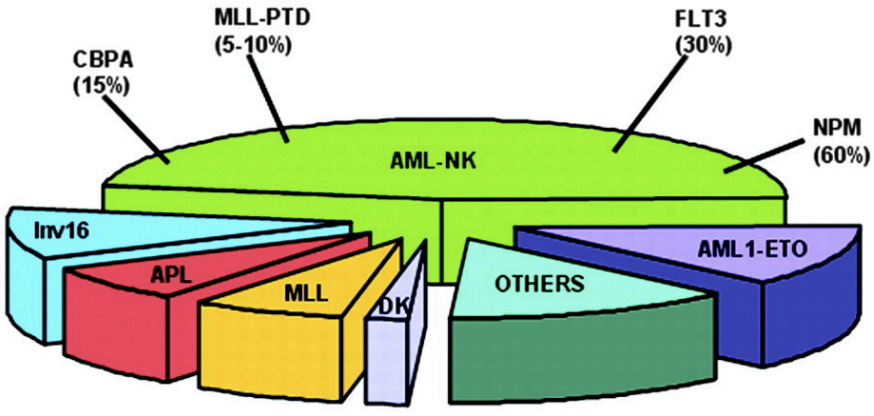

Figure 8 Genetic alterations in adult AML. Cytogenetic alterations in adult AML and frequency of gene mutations in AML with normal karyotype (AML NK) (modified from (Falini, Nicoletti, Martelli, & Mecucci, 2007).

AML1-ETO

The translocation t(8;21) that leads to the AML1-ETO fusion protein (also named RUNX1/MTG8) is found in about 15% of all AMLs. 40% of these are classified as FAB M2 (Petrie & Zelent, 2007). In this translocation the AML1 gene on chromosome 21, also known as RUNX1 fuses with the ETO gene that is also referred to as RUNX1T1 on chromosome 8. Patients with this translocation show specific biological characteristics and have a better prognosis after chemotherapy than most of the other AML patients. The t(8;21) translocation is most common in younger patients and children and not very often found in patients at an age of more than 60 years.

AML1-ETO alone is not able to induce leukemia in mice. It downregulates DNA repair enzymes and with a second event appearing may cause leukemogenesis. Several splice variants of the AML1-ETO gene are found in patients. All of them are variants in the ETO part of the molecule (Figure 9). The AML1-ETO9a variant contains an alternative ETO9a exon and codes for a 575 amino acid protein that lacks the NHR3 and NHR4 domains and on itself is able to cause leukemia in a mouse model. Coexpression of full-length AML1-ETO and AML1-ETO9a leads to an earlier onset of leukemia in the mouse model and blocks the myeloid differentiation at earlier stages. One splicing variant that is expressed in primary human AML cells contains an alternative exon at the C-terminal. It reduces repressor activity and may form multimeres. ETO-exon 6a if integrated gives rise to two different transcripts of different length. AML1-ETO alone is again not leukemogenic but has affects on the full-length fusion protein.

The effects of all molecular variants of the AML1-ETO fusion protein depend on the interaction and balance of these isoforms (Reikvam, Hatfield, Kittang, Hovland, & Bruserud, 2011).

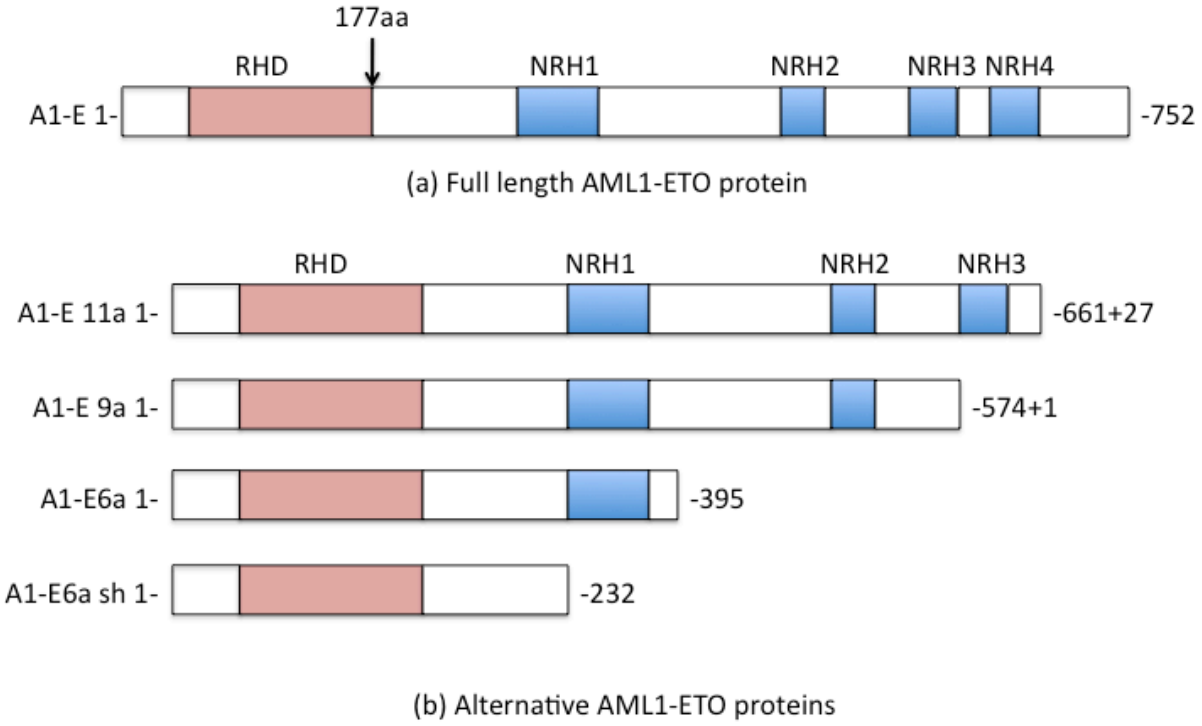

Figure 9 Alternative AML1-ETO proteins. Domain organization of the full-length and alternative AML1-ETO fusion proteins. (a) Full-length AML1-ETO protein with most of the ETO (RUNX1T1) gene fused into the N-terminal 177aa of AML1 (RUNX1) gene. This construct gives rise to a transcript coding for a protein of 752 amino acids. (b) Different fusion transcripts that arise due to alternative exon usage and splicing that give rise to truncated proteins lacking NHR domains. The protein size (amino acids, aa) and the number of aminoacids that were not part of the original sequence are given on the right. These alternative transcripts can be coexpressed with the full-length transcript and effect the leucemogenic capabilities (modified from Reikvam et al., 2011).

Normal Karyotype AML (Mutations)

The second group of AML carries none of the aberrations that are detectable by cytogenetic analysis and are therefore classified as normal karyotype AML (AML NK) (Wen et al., 2012). This group includes CEBPA (15%), MLL-PTD (5-10%), Flt3 and NPM mutations as single mutation or in combination with each other (29%).

A major group of normal karyotype AML is associated with NPM1 and Flt3-ITD mutations. The tyrosinkinase FLT3 (FMS-like tyrosine kinase 3) internal tandem duplication (ITD) mutation or point mutations of the

thyrosin kinase domain (FLT3-TKD) lead to a constant activity of the receptor and result in a permanent activation of STAT5, downstream MAP kinase and AKT signaling that then causes a depression of apoptosis and dysregulated proliferation of cells. FLT3 mutations in general imply a poor prognosis (Fathi & Chen, 2011).

In 60% of normal karyotype AML a mutation of the cytoplasmatic nucleophosmin (NPM) can be found (Falini et al., 2007). NPM1 is able to shuttle across different cell compartments. It plays a role in the regulation of tumor suppressor $p14^{ARF}$ and p53 and has an impact on the cellular response in apoptosis pathways. A mutation of the NPM1 gene leads to a restriction of the intercompartimental traffic and therefore causes an accumulation of NPM1 in the cytoplasm. NPM1 mutated leukemias with Flt3 wildtype show a better prognosis than those with FLT3-ITD mutation (Falini & Martelli, 2011). In 19% of normal karyotype AML, a NPM1 mutation is combined with FLT3-ITD, and is associated with poor prognosis (Falini et al., 2007) (Figure 10).

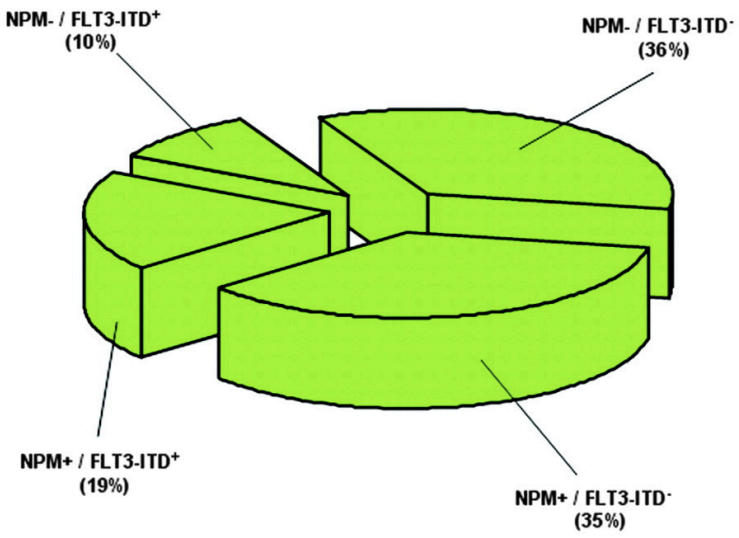

Figure 10 Relationship between NPM1 mutations and FLT3-ITD in normal karyotype AML (modified from Falini et al., 2007).

ROS in hematopoiesis and leukemogenesis

ROS in hematopoiesis

Studies have shown that ROS level play an essential role in the maintenance of quiescence and self-renewal potential of hematopoietic stem cells (HSC). The essential component of ROS regulation in HSCs seems to be the bone marrow niche (Eliades, Matsuura, & Ravid, 2012). A low oxygenic niche in the bone marrow provides long term protection of HSCs from ROS and selects for HSCs that may reside in this niche (Jang & Sharkis, 2007). The most sensitive blood cells that are affected by oxidative stress are red blood cells and stem cells. ROS accumulation leads to hemolysis and impairs the process of erythroid cell formation. Hematopoietic stem cells have a very low metabolism. Therefore accumulation of DNA damage and activation of senescense mechanisms caused by increased ROS develop slowly. Despite all the risks of oxygen stress and high ROS level, the presence of ROS and their strict regulation is essential for normal hematopoiesis (Ghaffari, 2008). An important regulator of ROS in stem cells is the transcription factor FoxO. This factor is upregulated in the bone marrow and its targets are antioxidative mechanisms such as Gpx3. FoxO knockout mice show increased ROS levels in the hematopoietic system without affecting the myeloid lineage. A loss of FoxO 1, 3 and 4 decreases the number of stem cells and increases ROS levels as well (Ghaffari, 2008; Tothova et al., 2007).

ROS in leukemia

High ROS levels are observed in AML and CML and could be correlated to several oncogenes and translocations. For example the ectopic expression of BCR/ABL, a translocation between chromosome 9 and 22 that causes chronic myeloid leukemia and is also found in many other types of leukemia leads to increased ROS levels in cell lines (Kim et al., 2005; Sattler et al., 1999). Patients with a mutation of the receptor tyrosin kinase Flt3-ITD show higher ROS levels in the hematopoietic precursors (Sallmyr et al., 2008; Sinenko et al., 2010). The aggressiveness of the disease and poor prognosis in patients carrying this mutation might be due to genomic instability, DNA damage and misrepair that is caused by elevated ROS levels (Sallmyr et al., 2008). In a drosophila model the AML1-ETO translocation led to the expansion of hematopoietic precursors that showed high ROS levels. Furthermore the activation of antioxidative mechanisms and targeting of their regulators (inactivation of EcRB1, activation of FoxO and superoxide dismutase-2 (SOD2)) was able to reverse this phenotype by reducing the ROS levels in precursor cells (Sinenko et al., 2010). These findings point to an important role of antioxidative mechanisms in leukemogenesis.

1.6 Aims of the present study

Reactive oxygen species play a major role in cell proliferation, cell signaling and apoptosis pathways. The manipulation and regulation of this system is a promising target for anti-cancer drugs. It is known that GPX4 plays a role in malignant diseases and that targeting the oxidative system via GPX4 has affects on survival and impairs tumor growth.

The aim of the present study was to delineate the role of GPX4 in hematopoiesis and in leukemia in order to test a potential role of GPX4 as a target for anti-cancer therapy. We hypothesized that GPX4 has a major influence on cell proliferation and apoptosis in leukemic cells. To prove this we chose an in vitro knockdown model in AML cells carrying the AML1-ETO fusion gene. This gene is present in 15% of all AML patients who at the same time show a high expression of *GPX4.*

2 Materials and Methods

2.1 Materials

2.1.1 Reagents

Reagent	Company
1Kb DNA ladder	NEB
Agarose	Sigma
Ammonium persulfate (APS)	Sigma
BSA bovine serum albumin (50g)	Boehringer
BSA liquid	NEB
Chloroform	Ambion
Complete, Mini Protease Inhibitor Cocktail Tablets	Roche
DEPC treated H_2O	Life technologies
DMSO	Sigma
DNAzol	Invitrogen
ECL Western Blot Detecting reagents	GE healthcare
EcoRI buffer	NEB
EDTA	VWR
Ethanol	Sigma
Ficoll-Hypaque	Sigma
Gel loading dye, blue (6x)	Bio Labs
Gel red	Biotium
Glycerol	Sigma
Glycine	Sigma
H_2O dest.	Gibco
HEPES	Sigma
Isopropanol	Sigma
IVIg (10%) (hsIgG)	Privigen
LB- Agar	Roth
Methanol	Sigma
Methocult	Stemcell

N-Acetylcystein	Sigma
NH_4Cl	Stemcell
PhosphoStop Phosphatase Ínhibitor Cocktail Tabletten	Roche
Propidium Iodide (PI) live-death cell stain	BD
Quick-Load 100bp DNA ladder	NEB
RetroNectin (Recombinant Human Fibronectin)	Takara Bio Inc.
Rotiphorese Gel A und B	Roth
SDS	Applichem
Spectra Multicolour broad range protein ladder	Fermentas
ß-mercaptoethanol (laemmli)	Sigma
Sytox Blue live-dead cell stain	Invitrogen
TBS	Applichem
TEMED	Applichem
Tris	USB
Trizol	Invitrogen
Tween	Applichem
Wasserstoffperoxid	Fischar
Immersol 518 N	Zeiss

2.1.2 Cell culture

Reagent	**Company**
Chloroquin	Sigma
Destilled H_2O	Gibco
DMEM	PAN Biotech
DMSO	Sigma
Dulbecco's PBS (1x)	PAA
FBS Gold	PAN Biotech
Fibronectin, murine, lyophilzed, 1mg	Biopur
Hexadimethrine bromide (Polybrene)	Sigma
Lipofectamine 2000	Invitrogen
Optimem	Gibco

Penicillin/Streptomycin	Gibco
Phosphatase I und II	Roche
Protamine sulfate	Sigma
Proteaseinhibitor Cocktail	Sigma
rh hu GMCSF	ImmunoTools
rh Il3	ImmunoTools
RPMI	PAN Biotech
Trypan Blue Solution	Fluka Sigma Aldrich
Trypsin/EDTA	Gibco

2.1.3 Disposables

Product	**Company**
14ml Polypropylene Round Bottom tube	Falcon
6-Well plates	Falcon
Blunt end needles	Stemcell Technologie
Cell culture dishes	Corning
Cell scraper, 25 cm sterile	Sarstedt
Cell strainer 40um	BD Biosciences
CFC dish 35mm	Greiner
Cryo tubes	VWR
Facs tubes with and without filter	Greiner bio-one
Falcon 50ml	BD Biosciences
Filter cards Shandon (white)	Thermo Scientific
MicroAmp®Fast Optical 96-Well Plate	ABI
Microscope slides	VWR
Nitrocellulose Trans-Blot	Bio Rad
PCR softtubes	VWR
Petri dish 100 x 20mm	BD
Pipettes	Corning
Suspension cell flask	BD
Syringe filters 45 and 22 um	Millipore
Syringes 5, 10 ml	BD
Tips	Eppendorf
Tubes	Eppendorf

Uvette	Eppendorf
Western Gel cassette	Invitrogen
Whatmann paper 0,34 mm	VWR

2.1.4 Kits

Product	Company	Catalognumber
Annexin V: PE Apoptosis Kit	BD	559763
CM-H_2DCFDA	Invitrogen	C6827
DC Protein Assay	Bio-Rad	500-0006
Mammalian transfection Kit	Clontech	631312
Maxi prep 25	Quiagen	12163
Platinum Taq Polymerase	Invitrogen	10966-034
Super Script III	Invitrogen	18080-051
Taq man Master mix	Applied Biosystems	4364343

2.1.5 Equipment

Product	Company
BioPhotometer plus	Eppendorf
Blotting chamber	OWL
Brutschrank Galaxy 170S	New Brunswick (Eppendorf Company)
Brutschrank Heraeus	Thermo scientific
Centrifuge 5415 R	Eppendorf
Cytospin 4	Thermo Scientific
Easy sep magnet	Stemcell Technology
Entwickler	AGFA Curix 60
Facs aria	BD
Facs Fortessa	BD
Gel chamber	OWL
Microscope Axiovert 40c Hellfeld	Zeiss
Microskope eclipse Ti-S	Nikon
MSC-Advantage Flow	Thermo scientific

Multifuge x3R	Thermo scientific
NanoDrop Spectrophotometer	Thermo scientific
Neubauer improved Zählkammer	Zeiss
PH meter	Mettler Toledo
Pipette	Eppendorf
Platform rocker PMR-30	Grant-bio
Power supply	VWR
Taq man	Applied Biosystems
Thermo block	Eppendorf
Thermo cycler	Peq Lab
UV Transilluminator Ceroview	VWR
Vi-cell- cell counter	Beckmann Coulter
Vortex Genie 2	Scientific Industries
Water bath 1003 14L	GFL
Western Gel chamber DCX 700	C.B.S. Scientific

2.1.6 Cell lines and culture conditions

2.1.6.1 Human leukemia cell lines

Cell line	Karyotype	Medium
EOL-1	AML (eosinophilic) carries a MLL partial tandem duplication and the fusion FIP1L1-PDGFRA	RPMI, 10% FBS
HL-60	AML FAB M2	RPMI, 1ß% FBS
K562	CML, cells carry the philadelphia chromosome with a BCR-ABL b3-a2 fusion gene	RPMI, 10% FBS
Kasumi	AML FAB M2 carry t(8;21) AML1-ETO fusion Gene	RPMI, 20% FBS, 1%PS
MOLM-13	APL= AMLFAB M3 carry internal tandem duplication ofFLT3	RPMI, 10% FBS

Cell line	Karyotype	Medium
MONO-MAC-6	AML FAB M5 carry t(9;11) (p22;q23) leading to MLL-AF9 fusion gene	RPMI, 10% FBS, amM L-gluthamine, 1mM sodium pyruvate, 10ug/ml hs insulin
MV4-11	Acute monocytic leukemia	RPMI, 10% FBS
NB-4	APL= AML FAB M3 carry the t(15;17) PML-RARA fusion gene	RPMI, 10% FBS
OCI-AML-3	AML FAB M4, NPM gene mutation	Alpha-MEM, 20% FBS
OCI-AML-5	AML FAB M4	Alpha-MEM, 20% FBS, 10% vol conditioned medium of cell line
SKNO 1	AML FAB M2 carry t(8;21) AML1-ETO fusion Gene; p35 mutation	RPMI, 10% FBS, 1% PS hGMCSF 10 ng/ml
THP-1	Acute monocytic Leukemia T(9;11)(p21;q32) leading to MLL-AF9 fusion gene	RPMI, 10% FBS
U-937	Human histiocytic lymphoma	RPMI, 10% FBS, 1%PS

2.1.6.2 Mouse cell lines

Cell line	Cell type	Medium
32D	Mouse myeloid cell line	RPMI, 10% FBS, 1% PS mIL_3 10 ng/ml

All cell lines were received from DSMZ (Deutsche Sammlung von Mikroorganismen und Zellkulturen)

2.1.6.3 Mouse cell lines established from leukemic mice

Cell line	Karyotype	Medium
CalmAF10	Calm AF10 fusion Gene	DMEM, 10% FBS, 1 % PS
Cdx2 101-394	Expression of the homeobox gene Cdx2	RPMI, 20% FBS, 10ng/ml mIl3
Cdx2 3997	Expression of the homeobox gene Cdx2	DMEM, 15% FBS, 10ng/ml mIl3
Cdx2 78-251	Expression of the homeobox gene Cdx2	RPMI, 20& FBS, 19ng/ml mIl3
HoxA9	Expression of HoxA9	DMEM, 15% FBS, mIl3 10ng/ml
Meis1-AML1-ETO	Expression of Meis1 and the AML1-ETO fusion gene	DMEM, 10% FBS, mIl3 10ng/ml

These cell lines were established in our lab from the bone marrow of primary leukemic mice that were lethally irradiated and transplanted with bone marrow that was transduced with the respective vector.

2.1.6.4 Packaging cell lines

Cell line	Viral system	Medium
Phoenix ampho (Allelebiotech ABP RVC 10001)	Retroviral packaging cellline	DMEM, 10% FBS
Lenti-X 293T (Clontech 632180)	Lentiviral packaging cellline	DMEM, 10% FBS

2.1.7 Antibodies for FACS-staining

Tag	Antigen
Alexa 700	C-kit
APC	c-kit
APC	CD 34
APC cy7	Il7Ra
E660	CD34
Eflur450	Strepavidin
PE	Flk 2
PE-Cy7	Sca-1
Percp cy5.5	C-kit
APC-cy7	FC 16/32
PE	C-kit

Biotin labeled antibodies for lineage depletion

Antigen	Cat.No°
B220	01122D
CD5	01032D
CD8a	01042D
Gr-1	01212D
Mac-1	01712D
Ter119	09082D

All Antibodies were received from BD biosciences, Franklin Lake, USA

2.1.8 Primer for Standard PCR

Tag		PCR Primer Sequence 5´→ 3	Product Length (b)
mGpx4	For	ACTCCCCGTGGAACTGTCAGCTTTGTGC	180
	Rev	GGATCTAAGGATCACAGAGCTGAGGCTGC	
hsAML-1ETO	For	ATGACCTCAGGTTTGTCGGTCG	220
	Rev	TGAACTGGTTCTTGGAGCCTCCT	
hsAML-1ETO9a	For	ATGACCTCAGGTTTGTCGGTCG	448
	Rev	TCGGGTGAAATGTCATTGCC	
EGFP	For	For CCACGTTGTGAGTTGGATAG	120
	Rev	Rev ATGAACTTCAGGGTCAGCTT	

2.1.9 shRNA hairpin Sequences

shGPX4:

CCGGGTGAGGCAAGACCGAAGTAAACTCGAGTTTACTTCGGTCTTGCCTCACTT TTTG

scramble:

CCTAAGGTTAAGTCGCCCTCGCTGAGCGAGGGCGACTTAACCTTAGG

2.1.10 Plasmids

EGFP: murine stem cell virus derived vector. A bi-cistronic vector with an internal ribosomal entry site (IRES) and an *EGFP* cassette 3' of the IRES (the vector was kindly provided by Prof. Dr. R. K. Humphries, Vancouver, Canada)

For retroviral gene transfer into murine cells plasmids were used in which the gene products *AML1-ETO* and *AML1-ETO9a* were subcloned into the multiple cloning site of the modified MSCV 2.1 vector (Pineault et al., 2003), upstream of the internal ribosomal entry site (IRES) and the enhanced green fluorescent protein (*EGFP*) gene (Figure 11).

Figure 11 constructs used for retroviral gene transfer into murine cells. Backbone vector is the modified MSCV 2.1 vector.

For lentiviral knock down of *GPX4* in human cell lines pLKO.1 puro vector (Addgene) was used to introduce shRNA into the cells (Figure 12).

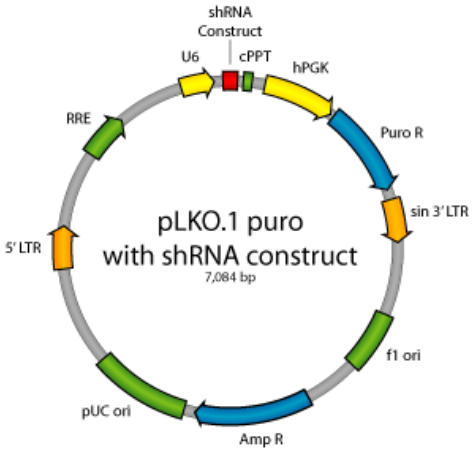

Figure 12: vector map of the pLKO.1puro lenti vector provided by Addgene.

For the introduction of the shRNA into HEK293T LentiX cells and virus production psPAX2 and pMD2 expression vectors were used as helper plasmids (both provided by Addgene).

2.1.11 Assays for qRT-PCR

All assays for qRT-PCR were performed using the Taqmann 7900HT system. The sytem was purchased from Applied Biosystems, Foster City, CA, USA.

Gene Symbol	Assay ID/Product No
Murine	
Gpx4	Mm00515041_m1
GAPDH (housekeeping gene)	4352932E
Human	
GPX4	Hs00157812_m1
TBP (housekeeping gene)	433769F

2.1.12 Antibodies for detection of protein

Target	Antibody	Company	Cat.No
GPX4, Gpx4	mouse monoclonal IgG	Santa Cruz	Sc-166437
β-Actin	mouse monoclonal β-Actin (C4)	Santa Cruz	Sc47778
Mouse IgG	Goat-anti-mouse-IgG-HRP	Santa Cruz	Sc2060

2.1.13 Enzymes

Restriction enzymes

EcoRI, BamHI, NotI (New England BioLabs, Ipswich, MA, USA)

Enzymes for PCR were purchased as kits (see chapter 2.1.4)

2.1.14 Patient samples

Mononuclear cells from AML patients were prepared from diagnostic bone marrow or peripheral blood (PB). All AML cases were classified according to the French-American-British criteria and the World Health Organization classification (Varela, Chuang, Woll, & Bennett, n.d.). The study was approved by the ethic committees of all participating institutions and informed consent was obtained from all patients before they entered the study in accordance with the Declaration of Helsinki (http://www.wma.net/e/policy/b3.htm). As control, bone marrow mononuclear cells (BM MNCs; Lonza, Visp, Switzerland) from healthy individuals were analyzed. Cytomorphology, cytochemistry, cytogenetics and molecular genetics were applied in all cases as described.

2.1.15 Mouse strains

Parental generations and experimental mice were bred in the animal facility of the University of Ulm.

Donors of primary bone marrow cells were >12 weeks old (C57Bl/6Ly-Peb3b x C3H/HeJ) F1 mice.

2.1.16 Software and statistical analysis

For statistical analysis and figures Prism Graph Pad 6 was used. FACS data was analyzed using Flowjo. Pictures were taken from the microscope using the program infinity analyze and were arranged with Iphoto and PowerPoint. All other software used was part of Microsoft office for Mac 2008.
Data was analyzed using the student's t-test. Differences with p-values of 0.05 and less were considered as significant. Bars in figures indicate Mean ± SEM.

2.2 Methods

2.2.1 Isolation of DNA

1 x 10^6 cells were suspended in 1 ml DNAzol (Invitrogen) and 500µl of 100% ethanol (EtOH) was added. Samples were mixed for 1 min and then centrifuged for 1 min at 8000 rpm. The supernatant was removed and the pellet was washed with 1 ml of 75% EtOH twice. Afterwards EtOH was removed and the samples were air dried for 10 min. DNA was dissolved in 20 to 50 µl of 8 mM sodium hydroxide (NaOH).

2.2.2 Isolation of RNA

RNA extraction was performed with Invitrogen Trizol® Reagent. 1.6 x 10^6 cells were homogenized in 1ml Trizol, transfered to 1.5 ml microfuge tubes and frozen down at -80 °C. For extraction samples were thawed on ice and incubated at room temperature for 5 min. The samples were shaken to homogenize them. Then 500 µl chloroform was added and everything was mixed by vortex. After 3 min. incubation at room temperature (RT) the samples were centrifuged at 4 °C with 8000 rpm for 15 min. Afterwards the now clear upper phase containing RNA was transferred into a new tube. RNA was precipitated with 500 µl isopropanol. After 10 min. incubation at RT the samples were spun down for another 10 minutes at 4 °C with 8000 rpm. The pellet was washed with 75% ethanol 2 times and then dissolved in 30 µl DEPC treated RNase free water. To dissolve the RNA pellet completely the samples were incubated 10 minutes at 55 °C. RNA was stored at -80 °C.

2.2.3 cDNA synthesis

For cDNA synthesis Invitrogen Superscipt III enzyme was used. The synthesis was performed according to manufacturer's instructions using random hexamer primers.

DNase treatment was performed before the synthesis to prevent contamination with genomic DNA in the later analysis. 2 µg of RNA was diluted with DEPC treated H_2O up to 16 µl. 2 µl of 10x DNase I buffer and 2 µl DNase I were added to each sample and incubated for 30 min at 37°C. After incubation 2 µl of 25 mM EDTA was added per sample and everything was incubated at 65°C for 10 min.

For synthesis, 1 µg of RNA was used per sample in a reaction volume of 10 µl. After adding primers and dNTPs the samples were heated for 5 min at 50 °C to denaturate the RNA completely and then cooled down on ice. The cDNA synthesis was performed under the following conditions:

10 min	25°C for primer annealing
50 min	50°C for synthesis of DNA
5 min	85°C for inactivation of reverse transcriptase

Afterwards mRNA was digested by adding 1 µl RNase per sample and incubation for 20 min at 37°C. cDNA was stored at -20 °C.

2.2.4 Quantification of RNA and DNA

RNA and DNA concentrations were determined using a Thermo Scientific NanoDrop spectrophotometer at a wavelength of 260 nm. At this wavelength the absorption peak of nucleic acids can be expected. For quality control the samples were also measured at a wavelength of 280 nm where the absorption peak of amino acids lays.

2.2.5 Standard PCR (polymerase chain reaction)

For the amplification of defined DNA regions standard PCR was performed using Invitrogen Taq DNA Polymerase.

Reaction compounds and conditions were used as followed:

	Volume (µl)
10 x buffer –Mg	2.50
$MgCl_2$ 50 mM	0.75
dNTP mix 10 mM	0.50
Forward Primer	0.50
Reverse Primer	0.50
Taq polymerase 5 U/ul	0.10
Template DNA	1.00
H_2O	ad 25.0

Step	**No Cycle(s)**	**Temp. (°C)**	**Time (s)**
Denaturation	1	94	120
Denaturation		94	30
Annealing	ps	ps	ps
Extension		72	30
Extension	1	72	120

Table 6 cycler program for standard PCR ps= product/primer-specific parameter

Primer	Annealing (°C)	No Cycles	Elongation (s)
Gpx4	63	35	50
AML1-ETO	58	30	60
MIG	58	35	120
AML1-ETO 9a	58	30	80

Table 7 Product/Primer specific parameters for standard PCR

2.2.6 Quantitative RT-PCR

For real-time PCR Applied Biosystems 7900HT Fast Real-Time PCR system was used in 96 well plates. For each reaction 10 µl AmpliTaq Gold® Master mix, 8 µl of DEPC treated H_2O and 1 µl of primer mix were added into one well. Primers were purchased from Applied Biosystems. Taqman was running 10 min at 95°C for Enzyme activation followed by 45 cycles of 15 sec. at 95°C for denaturation and 1 min at 60°C for annealing and extending. The color detected was FAM™ at a wavelenghth of 530 nm. ROX™ a color at a wavelength of 610 nm was used as control dye for passive reference.

The house keeping genes GAPDH for murine and TBP for human samples were used for normalization. All primers were controlled by a water control Results were exported using RQ manager and ΔCT was calculated using Microsoft Excel.

2.2.7 Agarose gel electrophoresis

Preparative and analytical separation of PCR products or plasmids was done by agarose gel electrophoresis. 15 µl of PCR Product was mixed with 2.5 µl gel loading dye, blue (6x) (NEB) and loaded on an agarose gel containing 10 000 x GelRed (VWR). Depending on the size of the expected PCR products 1 % to 2 % gels were used. As marker 0.5 µg of a 100 bp or 1kb DNA ladder (both NEB) were loaded. The electrophoretic separation was carried out depending on the size of the gel for 60 to 90 min at 90-120 V.

2.2.8 Extraction of protein from whole cells

For extraction of total protein 1 x 10^6 cells of the human cell lines and 4 x 10^6 cell of the mouse cell lines were collected by centrifugation and washed with 5 ml cold PBS. The cells were then lysed in 200 µl (human cell lines) and 350 µl (mouse cell lines) Ripa buffer, incubated on ice for 30 min and then centrifuged for 15 min at 13 0000 rpm. The clear lysate was transferred into a fresh tube and for storage kept at -80 °C.

Ripa lysis buffer:

50 mM Tris HCl, pH 7.5

150 mM NaCl

0.5 % sodium-deoxycholate

1% NP-40

0.1% SDS

1 mM EDTA

10% glycerol

10 µl phosphatse inhibitor I and II (100 x) and 100 µl protease inhibitor (10 x) were added per 1 ml Ripa buffer

2.2.9 Extraction of nuclear and cytoplasmatic protein

6 x 10^7 cells were washed twice in cold PBS and transferred into 2 ml microfuge tubes. Samples were spinned down and taken up in 200 µl Dignam A Buffer. Then the samples were incubated on ice for 30 min and vortexed from time to time. After spinning the clear lysate which contains the cytosolic fraction was transferred into a new tube, 10% glycerol was added and the sample was snap frozen in liquid nitrogen and stored at -80°C.

The remaining pellet containing the nuclear fraction was washed with 500 µl Dignam A buffer 3 times and taken up in 150 µl Dignam B buffer. Samples were incubated on ice for 30 min and vortexed from time to time. Then they were snap frozen with liquid nitrogen and thawed 3 times. Finally samples were centrifuged and the supernatant containing the nuclear protein was stored at -80°C.

Dignam A buffer:

20 mM Tris pH 8.0

20 mM KCl

1M $MgCl_2$

Phosphatase Cocktail I und II (100 x)

Protease Inhibitor Cocktail (10 x)

0.5 mM DTT

Dignam B Buffer

40 mM Tris pH 8.0

50 % glycerol

840 mM NaCl

3 mM $MgCl_2$

0.4 mM EDTA

Phosphatase Cocktail I and II (100 x)

Protease Inhibitor (10 x)

0.5 mM DTT

2.2.10 Detection of protein

The amount of protein was detected performing a Bradford Assay (Bradford, 1976) using BioRad protein assay reagent. The stock solution was diluted 1:5 with distilled H_2O shortly before usage.

1 µl of each sample was added to 100 µl 150 mM NaCl and filled up to 1 ml with diluted Bio Rad solution. After 5 min of incubation the absorbance was measured at 595 nm by BioPhotometer plus (Eppendorf).

For calibration a serial dilution with BSA (bovine serum albumin) was performed at concentrations of 1, 2, 5, 8 and 10 ng and measured as described before. Based on the extinction a calibration line was created and the protein concentration of the samples was calculated using the formula.

Protein µg/µl= A_λ/m

2.2.11 Immunoblot

Western blot was performed using 30 µg of protein. The proper volume of protein was filled up to 25 µl with H_2O and 4.5 µl 6 x Laemmli buffer was added in order to reduce disulfide bonds, denature proteins and subunits and stain the samples for easier loading and following on the gel. Samples were incubated at 95 °C for 2 minutes for degradation. Proteins were separated in a 10 % SDS-polyacrylamide gel at 120 V. Semi-dry blotting using the blotting buffer described below on a nitrocellulose membrane was performed for 50 min. at 300 mA. The membrane was blocked with TBS containing 5% Milk for 1h. Afterwards the membrane was incubated overnight at 4°C with Gpx4 antibody (1:2000) and ß-actin antibody (1:6000) in TBS containing 5% milk.

The next day the membrane was washed three times 5 min. in TBS and one time 10 min in TBS containing 1% Tween20. The second antibody (anti mouse) was added in TBS 5% milk, incubated on a shaker for 1.5 hours and then washed 2 x 10 min with TBS and 2 x 5 min with TBS plus 1% Tween20.

2 ml of ECL Western Blot detecting reagent A and B each were poured over the Membrane for 1 minute prior to developing.

Western blots were developed on Amersham Hyperfilm ECL (GE healthcare) using an Agfa Crurix developer. Exposure time of the membrane to the film was inbetween 1 and 8 minutes.

Separating gel: 2.7 ml H_2O

2.5 ml 1.5M Tris pH 8.8

3.24 ml Rotiporese Gel A

1.35 ml Rotiporese Gel B

100µl 10% SDS

100µl 10%APS

4µl TEMED

Stacking gel: 1.87 ml H_2O

380 µl 1.5 M Tris pH 6.8

487 µl Rotiporese Gel A

203 µl Rotiporese Gel B

30 µl 10% SDS

30 µl 10% APS

3 µl TEMED

Electrophoresis-buffer 5x:

15.1 g Tris base

94 g glycine

50 ml 10% SDS

adjusted to 1000ml with H_2O

Blotting buffer:

2.9 g glycine

5.8 g Tris base

0.37 g SDS

200 ml methanol

adjusted to 1000 ml with H_2O

Laemmli buffer (6x):

1.2 g SDS

6 mg bromophenol blue

4.7 ml glycerol

1.2 ml Tris 0.5 M, pH 6.8

2.1 ml H_2O

0.9 g DTT

2.2.12 Heat shock transformation of DH5α competent E. coli cells

For introduction of plasmid DNA into E. coli 100 µl of DHα competent cells per plasmid were thawed on ice. 1 ng of plasmid was added and cells were incubated on ice for 30 minutes. Heat shock transformation was performed in an eppendorf thermomixer at 42 °C for 45 seconds directly followed by incubation on ice for 2 minutes. 900 µl SOC media was added and cells were incubated with shaking for 1 hour at 37°C.

100 µl of the cell suspension was plated on LB-Agar plates containing 1% ampicillin for selction of E.colis containing the introduced plasmid that carries an ampicillin resistence. Plates were incubated over night at 37°C in a Thermo Scientific Heraeus Incubator. Bacterial plates were stored up to 3 months at 4 °C.

2.2.13 Isolation of plasmid DNA (Miniprep, Maxiprep)

For isolation of plasmid DNA one colony of transfected bacteria was precultured shaking at 200 rpm and 37 °C in 5 ml LB medium containing 100 µg ampicillin per ml for 8 hours. For miniprep this preculture was used. For maxiprep the preculture was added to 500 ml LB medium containing 100 µg Ampicillin per ml and incubated overnight at the conditions described before. The elution of plasmid DNA from the bacteria was performed using Quiagen plasmid maxi kit for large amounts of DNA and Quiagen plasmid mini kit for small amounts of DNA. The preparation was performed following the users manual instructions. Amount and purity of the DNA were determined photometrically as described in section 2.2.4.

2.2.14 Restriction analysis

To test the successful transformation and preparation of the plasmids the plasmid was cut with appropriate restriction enzymes and analyzed via agarose gel electrophoresis. Control digestion was performed at 37 °C for 3h in a total volume of 50 µl.

Restriction analysis buffer:

2 µl of plasmid

1 µl of each required enzyme

1 µl Eco buffer

0.5 µl BSA

44.5 µl H_2O

2.2.15 Sequencing

Plasmids were commercially sequenced by GATC Biotech AG (Konstanz).

2.2.16 General culture conditions

Mammalian cell lines were cultured in the appropriate medium containing the required supplements (2.1.6). Cells were passaged at ratios of 1:10 to 1:5 every 2 to 3 days and were cultivated in a humified atmosphere at 37 °C with 5% CO_2.

2.2.17 Freezing and thawing of mammalian cells

Around $1x10^7$cells were washed with PBS. Adherent cells were trypsinized. They were collected by centrifugation and the supernatant was decanted. The cell pellet was resuspended in 1.5 ml FBS containing 10% DMSO and frozen down in cryotubes at -80 °C for short-term storage and in liquid nitrogen for long-term storage.

Frozen cells were thawed in a waterbath at 37 °C and taken up in warm medium. Cells were washed with warm medium to remove the freezing medium. Afterwards adherent cells were plated in a 10 cm dish. Suspension cells were seeded in 5 to 10 ml of appropriate medium depending on the amount of cells that were thawed.

2.2.18 Cell counting and determination of cell viability

For cell counts a Neubauer improved counting chamber (Zeiss) was used. For determination of cell viability dye exclusion with tryptan blue was performed. 10 µl of cells in medium were mixed 1:1 with tryptan blue and pipetted into the counting chamber. Tryptan blue is able to penetrate the membrane of dead cells whereas living cells do not absorbe the dye. Hence dead cells appear blue under the microscope whereas living cells appear bright and colorless.

The cell number per ml was calculated as follows:

Average number of cells per main square x chamber factor (10^4) x 2 (dilution factor).

For larger culture volumes cell number and viability was determined using Vi-cell™ provided by the company Beckmann Coulter.

2.2.19 Measuring ROS with DCFDA

To quantify ROS (reactive oxygen species) in cell lines 2´7´-dichlorofluorescin diacetate (CM-H_2DCFDA, Invitrogen) was been used. DCFDA penetrates the cellular membrane and is intracellularly hydrolized by cellular esterases to non-fluorescent DCFH. Oxidation of DCFH by hydrogen peroxides or other ROS produces the fluorescent indicator DCF (Hafer, Iwamoto, & Schiestl, 2008).

The intensity of DCF was measured by FACS at a wavelength of 492-495nm (Invitrogen).

1x10^6 cells were treated with 10µM DCFDA in PBS for 30 min at 37°C. After incubation cells were pelleted and dissolved in FACS-buffer (see materials). DCFDA was dissolved in DMSO. As a negative control, cells treated with DMSO only were used. Sytox blue was added for live-dead staining if not mentioned otherwise.

2.2.20 Annexin V staining

For the detection of apoptosis APC-AnnexinV Apoptosis Kit II provided by BD Pharmingen™ was used.

During the process of apoptosis cells loose their plasma membranes. The membrane phospholipid phosphatidylserine (PS) is located at the inner leaflet of the plasma and is at an early state of apoptosis translocated and exposed to the external cellular enviroment. AnnexinV, Ca^{2+} dependent phospholipid-binding protein has a high affinity to PS and binds to cells exposing PS. For FACS analysis Annexin V is conjugated to fluorochromes to enable the detection of apoptosis. (BD Technical data sheet).

For the Annexin V staining cells were washed twice in PBS and resuspended in 1x of the provided binding buffer that was diluted in distilled water. Cells were resuspended at a concentration of $1x10^6$ per ml. 100 µl of the cellsuspension was stained with 5 µl APC-Annexin V and 5 µl PI for live-dead staining. After incubation for 15 min. at RT in the dark 400 µl 1x binding buffer were added and cells were analyzed by FACS within 1h.

2.2.21 Extraction of murine primary bone marrow cells

Mice were sacrificed using CO_2 and sterilized in 70 % EtOH. Femurs, tibias and hips were taken out and cleaned from the surrounding tissue with scissors and tissue paper. The clean bones were crushed with mortar and pestle in PBS containing 3% FBS. The supernatant containing the bone marrow cells was filtered through a 40-µm filter. The remaining tissue was washed with PBS/3% FBS twice. After centrifugation the pellet was ready for further use.

2.2.22 Cultivation of murine bone marrow

BM was stimulated in DMEM containing 15% FBS and cytokine cocktail (CC) with a final concentration of 10ng/ml mIl-6, 6 ng/ml mIl-3 and 100 ng/ml mCSF. BM cells were cultured at 37 °C, 5% CO_2 in a humified atmosphere.

Cytokine cocktail stock solution (100x)

10 mg/ml mCSF

1 mg/ml mIl-6

600 ng/ml mIl-3

dissolved in DMEM, stored at -20 °C

2.2.23 General FACS staining guidelines

For imunofluorescence analysis cells were centrifuged, dissolved in PBS and stained with the aproppriate amount of antibody for 20 min. in the dark. After staining cells were pelleted and taken up in around 300 µl of Facs-buffer containing 0.05 µl 1M Sytox per 100 µl buffer for live-dead staining. Analysis was performed on a FACS Fortessa.

2.2.24 Subpopulation staining and lineage depletion from mouse bone marrow

Quantification of stem cells, HSC (LSK, CD34, Flk2) and CLPs

10 mice were euthanized and the bone marrow was prepared as described. To remove red blood cells and granulocytes cells were carefully laid on 15 ml ficoll and centrifuged at 1600 rpm at room temperature without brake and acceleration. The buffy coat was removed and cells were washed in cold HBSS containing 10 % FBS.

For depletion of lineage positive cells, 4 µl lineage cocktail per 1 x 10^8 cells was added and incubated on a rocking platform for 25 min.

Lineage cocktail with biotin labeled antibodies:

Taq	Company	CatNo	Dilution
B220	BD biosciences	01122D	1:300
CD5	BD biosciences	01032D	1:200
CD8a	BD biosciences	01042D	1:200
Gr-1	BD biosciences	01212D	1:320
Mac-1	BD biosciences	01712D	1:320

Cells were washed 2 times and resuspended in 2 ml cold HBSS/10%FBS. 1ml Dynabeads per 1 x 10^8 cells were added and incubated at 4 °C for 25 min on a rocking platform. Beads were separated using an Easy Sep magnet offered by Stemcell Technology (#92990) and resuspended in cold HBSS/10% FBS at a concentration of 10^7 cell per ml. FC block (CD16/CD32) in a dilution of 1:100 was added and everything was incubated another 20 min at 4°C on a rocking platform in the dark.

Cells were stained using the following colors and dilutions according to the protocol that was used in our lab:

Tag	Antigen	Dilution
Alexa 700	C-kit	1:200
PECy7	Sca-1	1:600
PE	Flk-2	1:200
V450	Strepavidin	1:300
e660	CD 34	1:200
APC-cy7	Il7Ra	1:200

PI 0.05 µg/ml for live death staining

Staining protocol was performed as described. HSCs and CLPs were sorted using BD FACS Aria.

Isolation of CMPs, GMPs and MEPs

For isolation of CMP, GMP and MEP the same protocol was performed with a different staining:

Tag	Antigen	Dilution
PECy7	Sca-1	1:600
APC	CD34	1:200
eflur450	Strepavidin	1:200
APC-cy7	FC 16/32	1:100
PE	C-kit	1:400

PI 0.05 µg/ml for viability staining

Progenitor cells were sorted using BD FACS Aria. Gating was performed as follows.

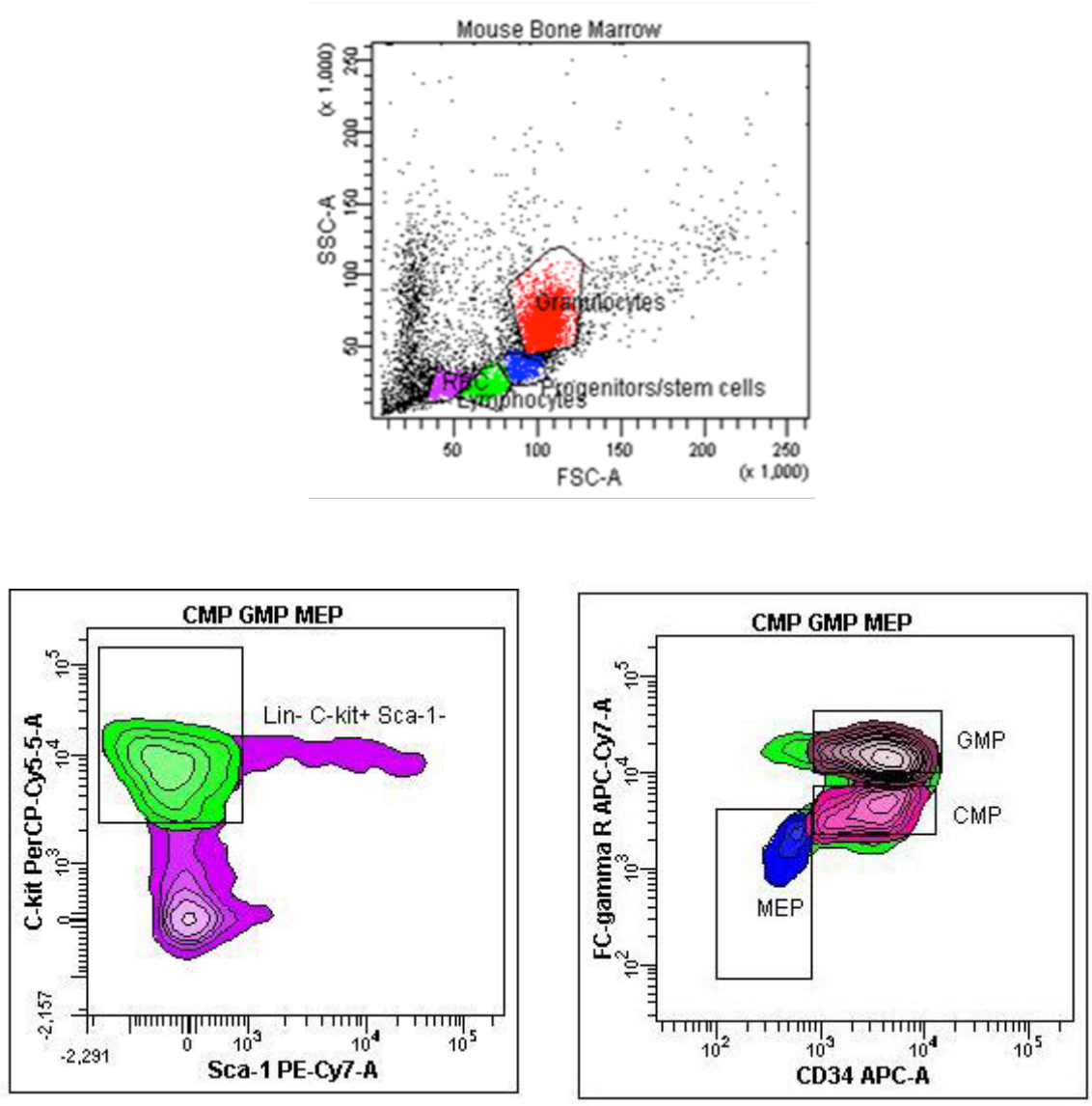

Figure 13 Gating for sort of GMP, CMP and MEP murine progenitor cells from total murine bone marrow.

2.2.25 Retroviral transduction of murine Cell lines

To introduce Plasmids of different constructs into murine cell lines the retroviral packaging cell line phoenix ampho was transfected with Lipofectamine 2000 (Invitrogen).

For a 10 cm dish, 24 µg of DNA was mixed with 1.5 ml Optimem I reduced serum medium in one FACS tube and 60 µl of lipofectamine was prepared in another FACS tube. Both were incubated for 5 min. at room temperature. DNA was added dropwise to the lipofectamine and incubated for another 20 min. The mixture was added to the cells in 10 ml of normal growth medium without antibiotics very carefully. After 4 hours medium was aspirated and 10 ml of normal growth media without antibiotics was added.

VCM (virus containing medium) was aspirated 24 and 48 h after transfection and filtered using a 10 ml syringe and 20 nm filter.

Infection of 32D cells was performed on culture plates coated with Fibronectin.

Fibronectin coating of the culture plates was performed as follows. Recombinant fibronectin fragments were diluted in 2 ml PBS at a concentration of 3 µg/cm^2. The solution was added to a 6 well and incubated over night at 4 °C. Fibronectin was removed and the coated wells were blocked with 2 % BSA for 30 min at room temperature to prevent unspecific bindings. The wells were washed with PBS and 3 ml of VCM was added to the coated wells. Virus was centrifuged in the plates for 45 min at 2500 rpm using a Heraeus Multifuge3S+.

For the infection 1.3 x 10^6 cells were resuspended in 1 ml of normal growth medium with the required cytokines. The cell suspension and additional 2ml of VCM were added to the Fibronectin coated plates and incubated over night at 37 °C.

Next day cells were washed from the plates and cultured under the normal cell culture conditions for 2 more days and then sorted for GFP and Sytox (viability dye) according to the general sorting guidelines mentioned above.

The successful introduction of the construct was tested by PCR.

2.2.26 Lentiviral transduction of human cell lines

Transfection of HEK 293T Lenti X packaging cell line

The knockdown of Gpx4 in human leukemic cell lines with shRNA was performed using the lentiviral packaging cell line HEK 293TLentiX and CalPhos™ Mammalian Transfection Kit provided by Clontech.

LentiX cells were plated in 10 cm dishes one day before transfection to reach a confluency of around 60% by the time of transfection.

Medium was removed before transfection and 9 ml of fresh growth medium was added. DNA and helper plasmids were mixed into a FACS tube as follows.

DNA	15 µg
pMD2	10 µg
psPax	5 µg

87 µl of $CaCl_2$ were added and everything was filled up to 700 µl with destilled water.

700 µl 2x HBS was bubbled with a 2 ml pipette and the DNA mixture was added dropwise. The reagents were incubated for 5 min. at room temperature and then added to the LentiX cells. After 6 to 8 hours the medium was changed to 10 ml of normal growth medium.

The virus-containing medium (VCM) was collected 24 and 48 hours after transfection and was filtered using a 10 ml syringe and 20 µm filter.

Infection of human leukemic cell lines

$1x10^6$ cells were plated in 2 ml of normal growth medium in 6 well plates. 1 ml VCM of the desired construct and 5 µg of polybrene were added per well to enable the viral particles to penetrate the cell membrane easier. After incubation for 8 hours medium was changed to 6 ml of normal growth medium.

The vector contains a puromycin resistancy that enables a selection of transduced cells. Selection was started 48 hours after the end of infection. 2 µg puromycin was used and cells were selected for 3 days. As a control untransduced cells were treated with puromycin. Cell viability was determined with tryptan blue as described earlier. All assays were set up 24 h after the end of selection. Knockdown efficiency was detected by qRT-PCR at the same time point the assays were set up (Figure 14). Knockdown stability was proven at the end point of the assays by qRT-PCR.

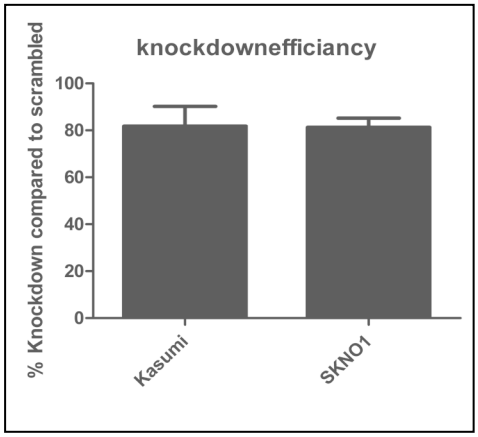

Figure 14: Knockdown efficiency in Kasumi1 and SKNO1 cells after lentiviral knockdown with sh RNA.

2.2.27 Colony forming cell assay (CFC)

To quantify human clonogenic hematopoietic progenitor cells, colony forming cell (CFC) assay using Methocult H4330 was performed. Methocult consists of methycellulose containing EPO (human Erythropoetin) 900 cells in 300 µl normal growth medium containing the appropriate amount of cytokines needed by the cell line was added to 3 ml Methocult, mixed well by vortexing and plated on a 35 mm dish using 3 ml syringes and blunt end needles, 16 Gauch. Two plates with each 1,1 ml of methylcellulose-cell mixture were plated and placed in a 100 mm x 20 mm Petri dish. An additional plate without a lid containing PBS was added to the dish to avoid desiccation. CFCs were incubated at 37 °C in humified atmosphere containing 5 % of CO_2.

After 14 days the number of colonies, colony morphology, absolute cell number and cell morphology were determined. The stability of the knockdown was confirmed by qRT-PCR at the end point of the assay.

2.2.28 Proliferation Assay

To determine the proliferative potential of the cell lines in which *GPX4* was knocked down with sh (small hairpin) RNA 50 000 cells were plated in 6-well plates in 5 ml of appropriate medium, with the addition of cytokines if necessary. Absolute cell number was counted after 48, 96 and 120 hours using a Neubauer improved counting chamber and trypan blue for live-dead staining. The stability of the knockdown was confirmed by qRT-PCR at the end point of proliferation.

2.2.29 Cytospins

To analyze cell morphology around 150 000 – 300 000 cells in 200 µl of PBS were added into the cytofunnel that was placed on a slide with filter paper inbetween. Everything was kept together with a cytoclip. The cytoclips were placed into a Cytospin4 centrifuge and spun for 10 min at 450 rpm.

Slides were air dried and stained for 3 min in Mayer Gruenwald solution followed by a 5 min. washing step with H_2O and 1 h staining in Giemsa solution. The slides were washed 2 times, dried and analyzed under a Nikon Eclipse Ti-S microscope.

3 Results

3.1 *GPX4* in human hematopoiesis and AML

Most of our knowledge about *GPX4* is about its role in embryonal development, in oxidative stress regulation and in neurodegenerative diseases. In order to delineate its role in normal and malignant hematopoiesis, we first investigated *GPX4* expression in normal and leukemic hematopoietic cells.

3.1.1 *GPX4* is highly expressed in CD 34$^+$ cells compared to total MNCs in human bone marrow

We analyzed the sorted bone marrow subpopulations of 3 healthy individuals by qRT-PCR. The expression patterns of pluripotent (CD34$^+$/CD38$^-$), determined stem cells (CD34$^+$/CD38$^-$), myeloid (CD34$^+$/Cd33$^+$), and lymphoid stem cells (CD34$^+$/CD3$^+$, CD34$^+$/CD19$^+$) were analyzed and compared to mononuclear bone marrow cells (MNC) in total Figure 15.

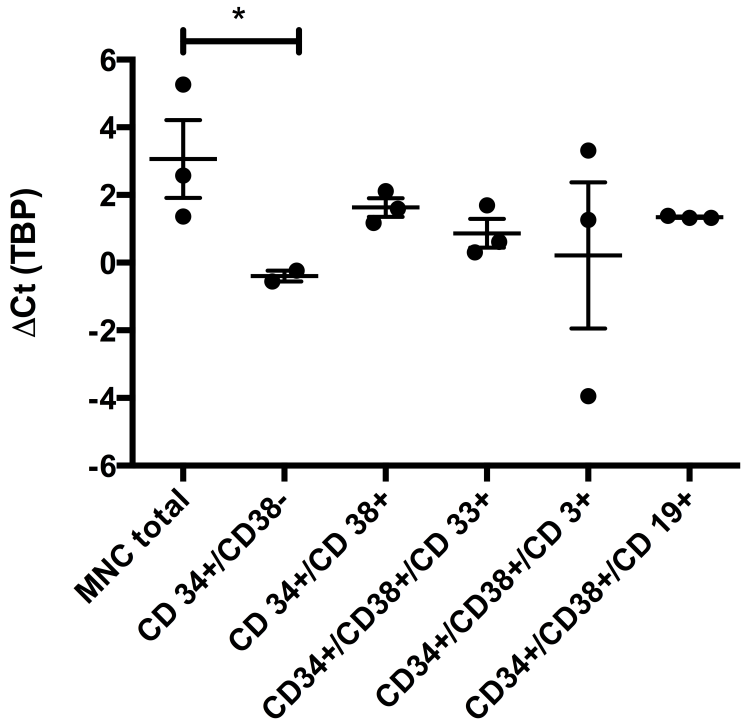

Figure 15 Gene expression of *GPX4* in sorted subpopulations of human bone marrow derived from healthy persons n=3, CD34$^+$/CD38$^-$ n=2 compared to MNCs (mononuclear cells) (The lower the value the higher the expression).

GPX4 is highly expressed in undetermined hematopoietic stem cells ($CD34^+/CD38^-$) (mean ΔCT value of -0.39 ± SEM 0.27) compared to determined, myeloid ($CD33^+$) (mean ΔCT value of 0.87 ± SEM 0.42) and B-lymphoid stem cells (mean ΔCT value of 1,43 ± 0,02). A wide distribution of expression was observed among T-lymphoid stem cells (mean ΔCT value of 0.22 ± 2.16). In all CD34+ cells, *GPX4* expression was significantly higher than in mature bone marrow cells represented by the fraction of total MNCs (p value of 0.0123).

3.1.2 *GPX4* is expressed in all subpopulations of normal karyotype AML patients.

In order to address the role of *GPX4* in malignant hematopoietic cells, we investigated bone marrow subpopulations in AML patients with normal karyotype leukemia. MNCs from 5 AML patients with normal karyotype AML were sorted for $CD34^+/CD38^-$, $CD34^+/CD38^+$, $CD34^-/CD38^+$ (n=5) and $CD34^-/CD38^-$ (n=3). Subpopulations were analyzed for the expression of *GPX4* by qRT-PCR and compared to stem cells ($CD34^+/CD38^-$ and CD34+/CD38+) (n=3) from healthy individuals (Figure 16).
All subpopulations of AML patients with normal karyotype showed similar expression levels. In all AML subfractions, *GPX4* expression was markedly higher than in stem cells of healthy individuals.

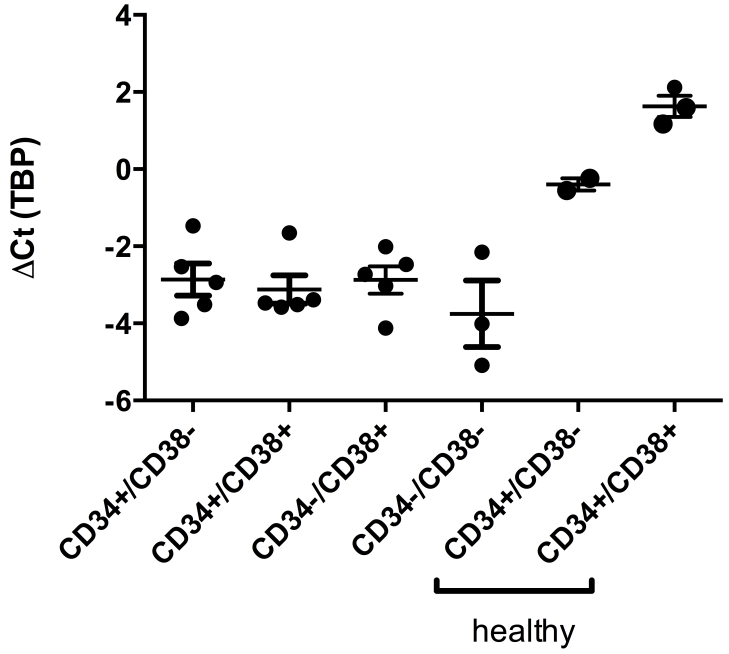

Figure 16: Gene expression of *GPX4* in sorted subpopulations of normal karyotype AML patients compared to those of healthy individuals (the lower the value the higher the expression)

3.1.3 AML1-ETO positive patients show higher expression of *GPX4*

In search of a clinical model for high *GPX4* expression, we analyzed micrroarray data from the Leukemia Gene Atlas (Haferlach, 2010). We compared GPX4 expression in 40 AML samples with AML1-ETO translocation to samples of healthy bone marrow (n=73) and bone marrow derived from AML-patients with various genotypes (n=2096). Our analysis of the microarray data showed high expression of G*PX4* in AML1-ETO positive leukemias compared to healthy individuals (Figure 17).

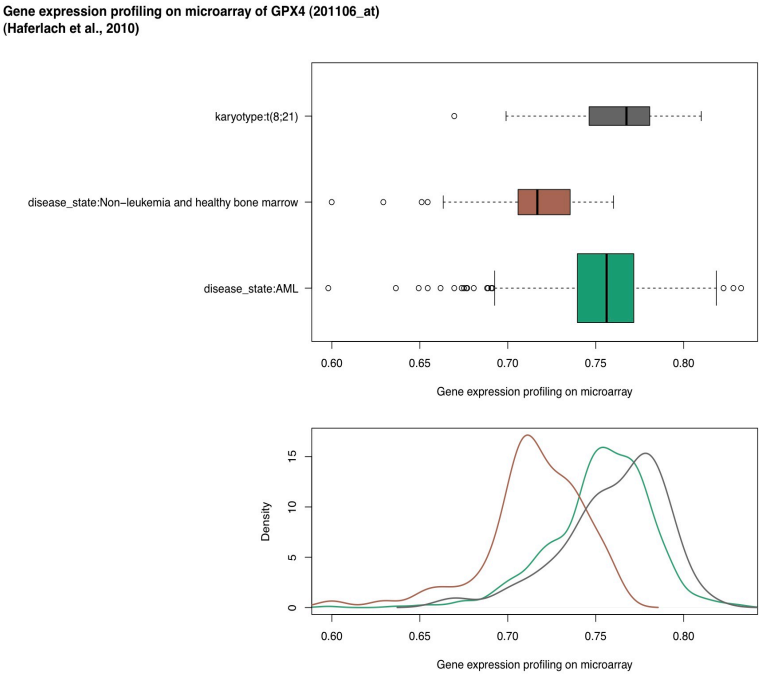

Figure 17 Microarray data on the gene expression of *GPX4* in t(8;21) AML compared to healthy bone marrow and disease state AML (Haferlach et al., 2010, derived from Leukemia Gene Atlas, www.leukemia-gene-atlas.org).

3.1.4 *GPX4* is upregulated in AML1-ETO patients compared to MNCs from healthy individuals

We next analyzed *GPX4* by qRT-PCR in 55 patients with normal and abnormal karyotype including AML1-ETO. The following number of patients that were grouped according to their karyotype were analyzed:

NPM+/FlT3- (n=11), NPM+/FlT3+ (n=10), AML1-ETO (n=14), inv.16 (n=10) and PML/Rara (n=10) (Figure 18).

GPX4 was upregulated in all AML patient samples compared to bone marrow MNCs from healthy individuals (t-test, $p < 0.005$) AML1-ETO positive AMLs revealed comparable expression levels to NPM+/FLT3+ and PML RARA, whereas inv.16 and NPM+/FLT3-patients had an even higher GPX4 expression (Figure 18).

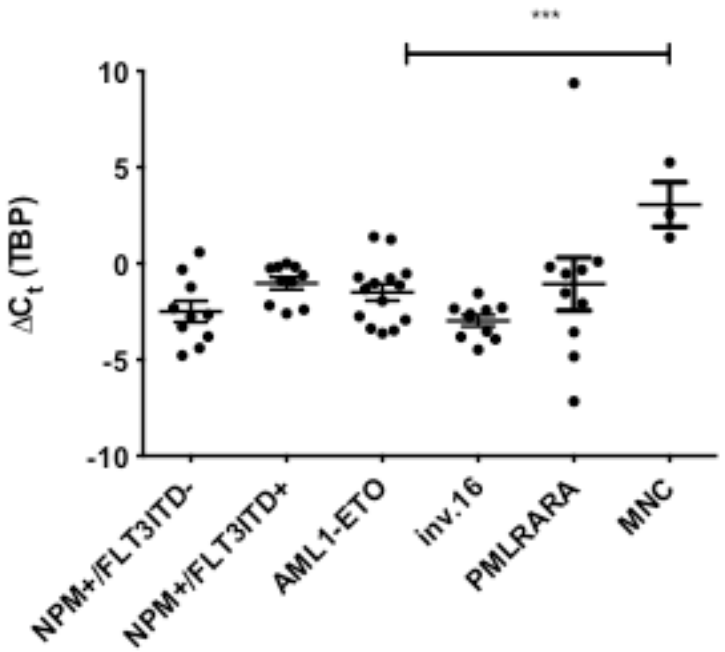

Figure 18: Gene expression of *GPX4* in patients with different karyotypes compared to mononuclear bone marrow cells (MNC) (The lower the value the higher the expression)

3.1.5 *GPX4* expression in AML cell lines

We next analyzed *GPX4* expression by qRT-PCR in 13 AML cell lines harbouring various mutations and compared it to mononuclear cell (MNC).

The expression of *GPX4* was equal in almost all tested AML cell lines. In addition, all cell lines showed an upregulated *GPX4* expression compared to healthy MNCs. The cell lines showed a median ΔCt value of -1.76 (range from -4.79 to 3.10) No AML cell line was negative for *GPX4* or showed a lower expression of *GPX4* than BM MNCs (Figure 19). Of note, NB4 and Molm revealed the lowest *GPX4* expression among the analyzed cell lines.

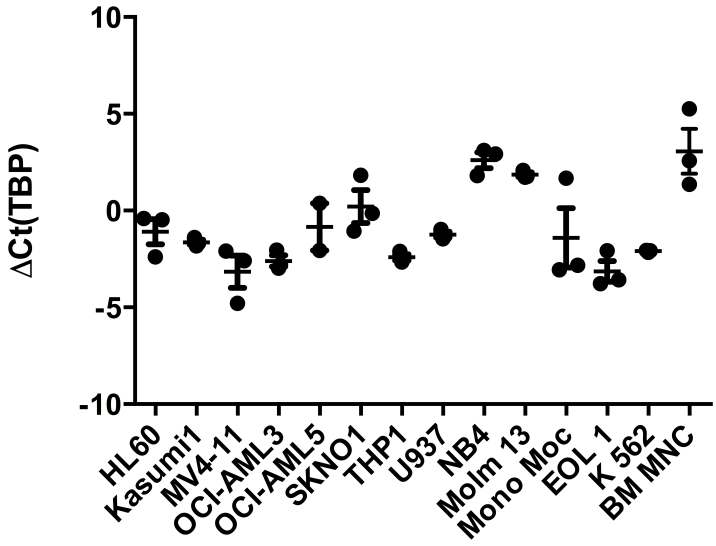

Figure 19 Gene expression of *GPX4* in human AML cell lines compared to mononuclear bone marrow cells n=3 (the lower the value the higher the expression).

3.1.6 GPX4 protein expression in AML cell lines

Since expression of *GPX4* was high in the *AML1-ETO* carrying cell lines Kasumi1 and SKNO1 and patient data in AML ETO leukemias showed high *GPX4* expression as well, we choose these cell lines for further experiments.

To detect to which extend the gene is translated into protein, Western Blot was performed in these cell lines and in addition in U937 cells, a line that shows a similar expression of *GPX4* compared to Kasumi1 but does not carry the AML1-ETO fusion gene (Figure 20).

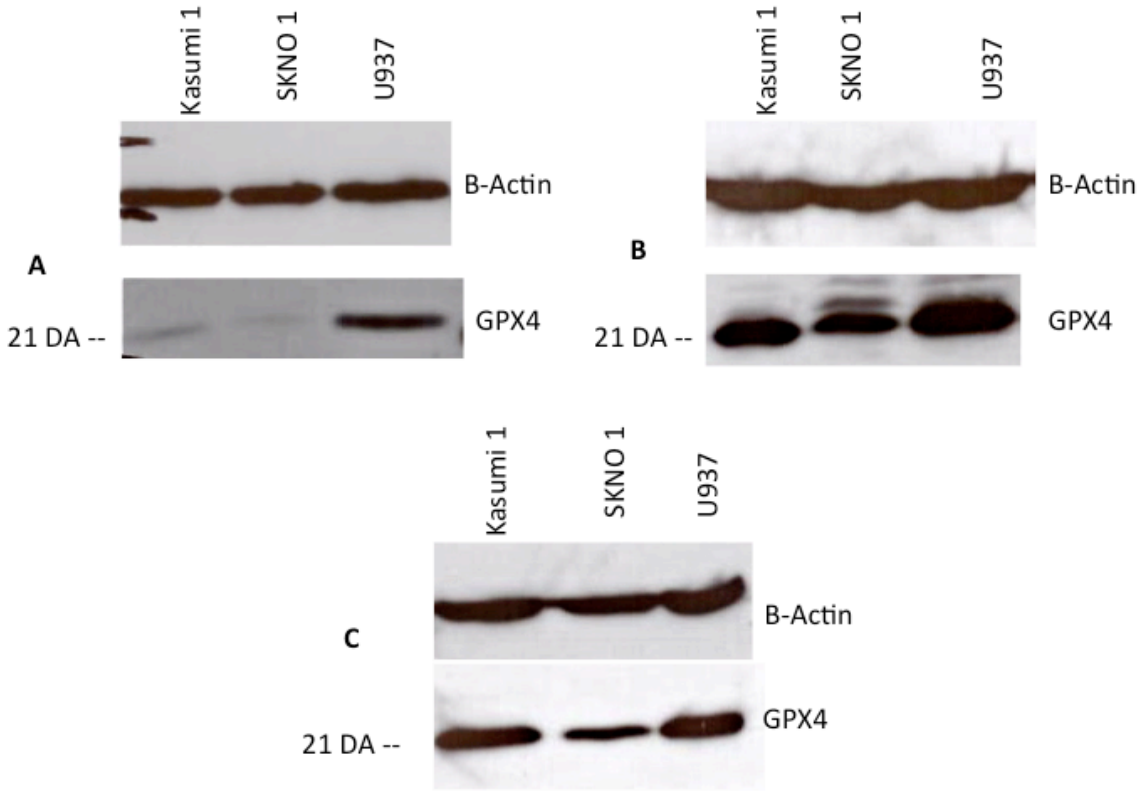

Figure 20 Western Blot of total protein, cytoplasmatic and nuclear extracts from Kasumi1, SKNO1 and U937 cell lines. Protein was blotted on a nitrocellulose membrane and detected with a Gpx4 anti mouse antibody. A) GPX4 detected in total protein B) GPX4 detected in cytoplasmatic extracts C) GPX4 detected in nuclear extracts.

GPX4 protein was expressed in *AML1-ETO* positive Kasumi1 and SKNO1 cells as well as in *AML1-ETO* negative U937 cells in total protein as well as in nuclear and cytoplasmatic extracts, indicating ubiquitous expression of the GPX4 protein.

3.1.7 Knockdown of *GPX4* leads to increased ROS levels in Kasumi1 and SKNO1 cell lines

As *GPX4* was highly expressed in the *AML1-ETO* positive Kasumi1 and SKNO1 cells both on transcript and proteine level, we sought to investigate the functional importance of *GPX4* in this type of leukemia by knocking down the gene with lentiviral based knockdown assays. For this approach, both cell lines were lentivirally transduced with shRNA to achieve a knockdown of *GPX4*. A plko1Puro-sh RNA construct and plko1Puro-shscrambled were used as control. Successfully transduced cells were selected with Puromycin treatment and knockdown efficiency was determined by qRT-PCR.

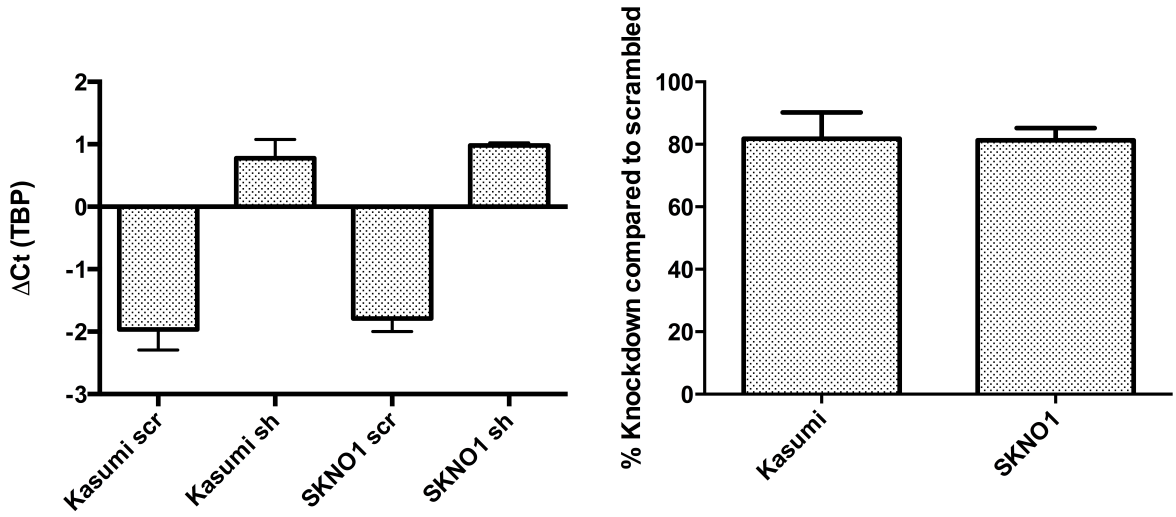

Figure 21 Expression of *GPX4* and knockdown efficiency of sh*GPX4* in Kasumi1 and SKNO1 cells compared to cells transduced with shscrambled.

Kasumi1 and SKNO1 cells expressing the shRNA showed approximately 80% (65%-91%) reduction of *GPX4* transcription levels in comparison to cells that were transduced with scrambled vector (
Figure 21), demonstrating proper function of the knock down system.

To see if the knock down of only one antioxidative enzyme is sufficient to affect ROS, ROS levels were detected by FACS analysis. Cells were stained with DCFDA. Control cells were treated with H_2O_2 prior to the staining in order to produce a maximum increase of ROS levels.

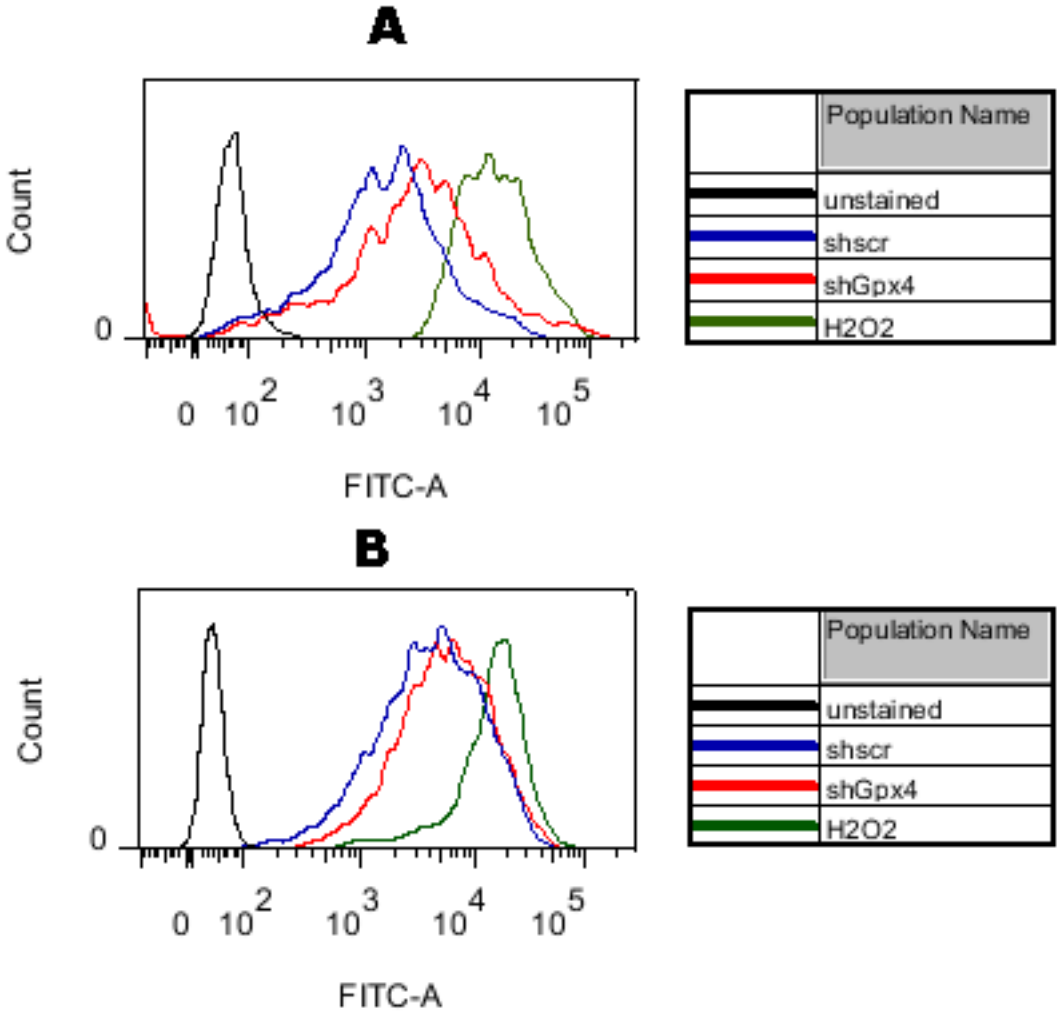

Figure 22: ROS measured with DCFDA in Kasumi (A) and SKNO1 (B) cell lines after lentivirally mediated knockdown of *GPX4*. Cells were stained with DCFDA, which is fluorescing in presence of ROS. Control cells were treated with H_2O to induce maximal ROS levels (positive control).

In both cell lines in which *GPX4* was knocked down, higher ROS levels compared to the scrambled control were observed. A clear shift to the right can be seen in Kasumi1 cells (Figure 22A). The effect is present SKNO1 cells as well. The less prominent induction may be due to the fact, that constitutive ROS levels were already higher in SKNO1.

3.1.8 Knockdown of *GPX4* leads to a decrease of the proliferative potential of Kasumi1 and SKNO1 cells

To determine the proliferative potential of the cells that carry the different constructs, a proliferation assay was set up with 50 000 cells. Total cell numbers were determined after 48, 96 and 120 hours.

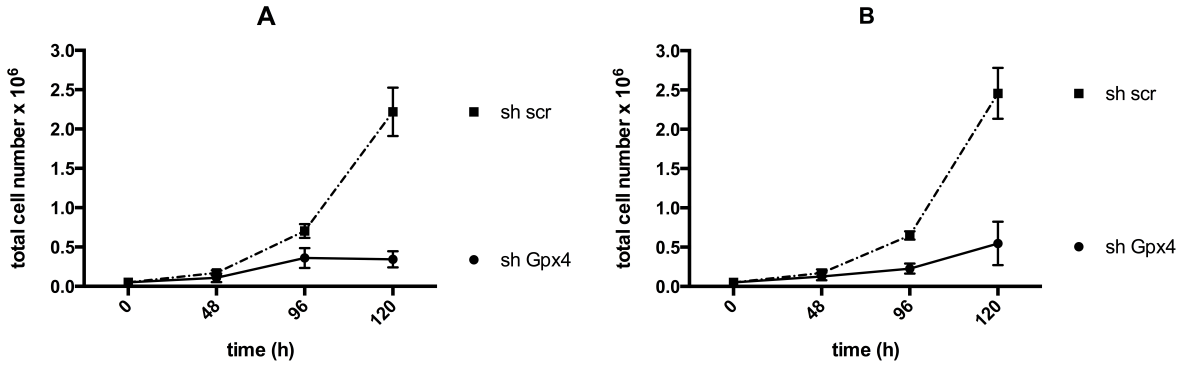

Figure 23 Proliferation of Kasumi and SKNO1 cells after lentiviral knockdown of *GPX4* compared to scrambled. 50 000 cells were seed out per experimental arm. Cells were counted after 48, 96 and 120 hours A) Kasumi1 cells, B) SKNO1 cells.

The knockdown of *GPX4* leads to a strong inhibition of the proliferative potential of the cells, whereas cells that were transduced with scrambled control showed a normal logarithmic growth curve. Inhibition of proliferation was observed in both cell lines. The difference in the growth curves was highly significant in both cell lines at time point 120 h (Kasumi1 p= 0,004, SKNO1 p= 0,01). The percentage of decrease in proliferation was 84.68% for Kasumi1 cells and 79.04% for SKNO1 (Figure 23).

3.1.9 Knockdown of *GPX4* does not lead to major changes in cell morphology.

We next investigated, wheter knockdown of *GPX4* affects cell morphology, particularly with respect to signs of necrosis, apoptosis or differentiation, cytospins were prepared. 150 000 – 300 000 cells were taken at the end point of proliferation assay and spinned on a microscope slide. Slides were stained with Giemsa and were analyzed under the microscope (40x magnification) (Figure 24, Figure 25).

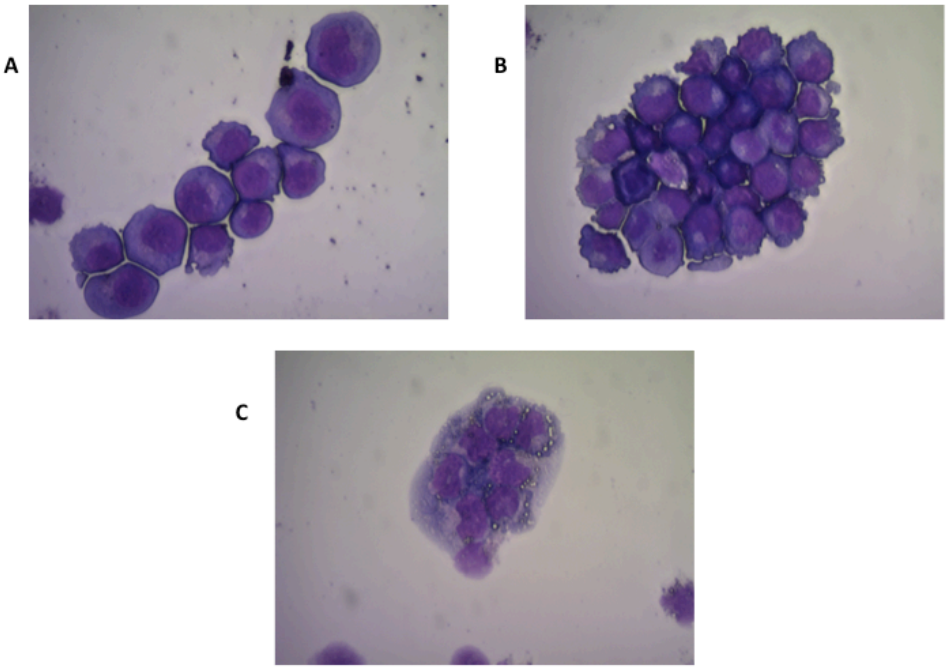

Figure 24 Cytospins of Kasumi1 cells at the end point of proliferation (40x) A) Kasumi1 wildtype, B) Kasumi1 shsscrambled, C) Kasumi1 sh*GPX4*. Representative photos are shown.

As illustrated in Figure 24 and Figure 25, there were no gross changes in morphology, indicating that knockdown of GPX4 has no effect on necrosis, apoptosis or differentiation in these cell lines.

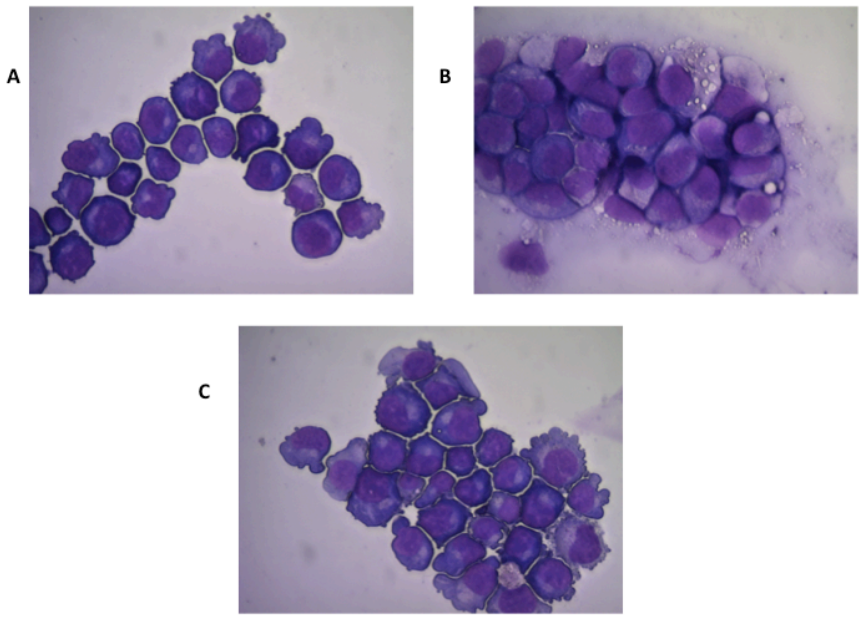

Figure 25 Cytospins of SKNO1 cells at the end point of proliferation analyzed with a 40x lens. A) SKNO1 wildtype, B) SKNO1 shscrambled, C) SKNO1 sh*GPX4*. Representative photos are shown.

3.1.10 The clonogenic potential of Kasumi1 and SKNO1 cells is not affected by knock down of *GPX4*

Next we determined the relevance of *GPX4* for the clonogenic potential of these cell lines. After successful knockdown of *GPX4* 300 cells were plated in methylcellulose containing dishes. The number of colonies was counted after 14 days and is given as a median from two dishes per experimental arm.

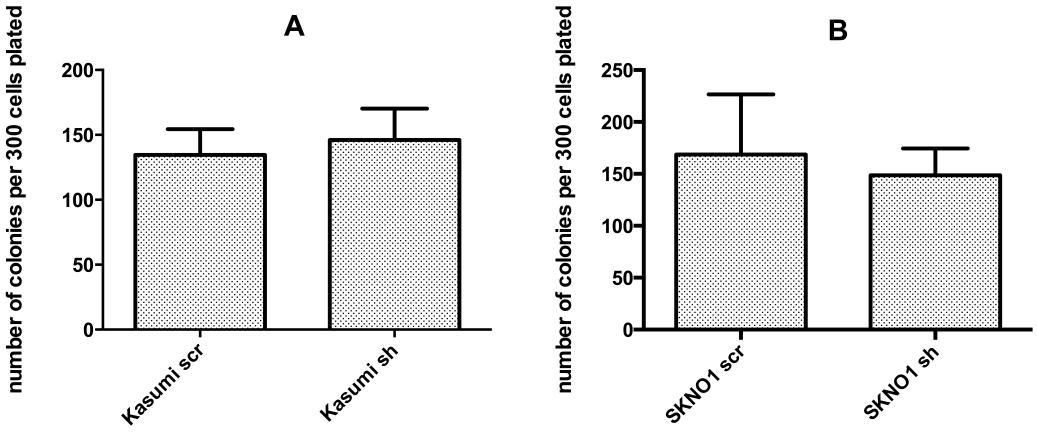

Figure 26 Colonies counted in the CFC assay for Kasumi1 (A) and SKNO1 (B) after lentivirally knockdown of *GPX4* compared to shscrambled. 300 cells were seed per methylcellulose dish in the different experimental arms. The number of colonies was counted after 14 days.

Surprisingly there was no significant difference in the number of colonies after *GPX4* knockdown compared to the scrambled control (Figure 26). In addition, there was no difference in colony size or in morphology (Figure 27).

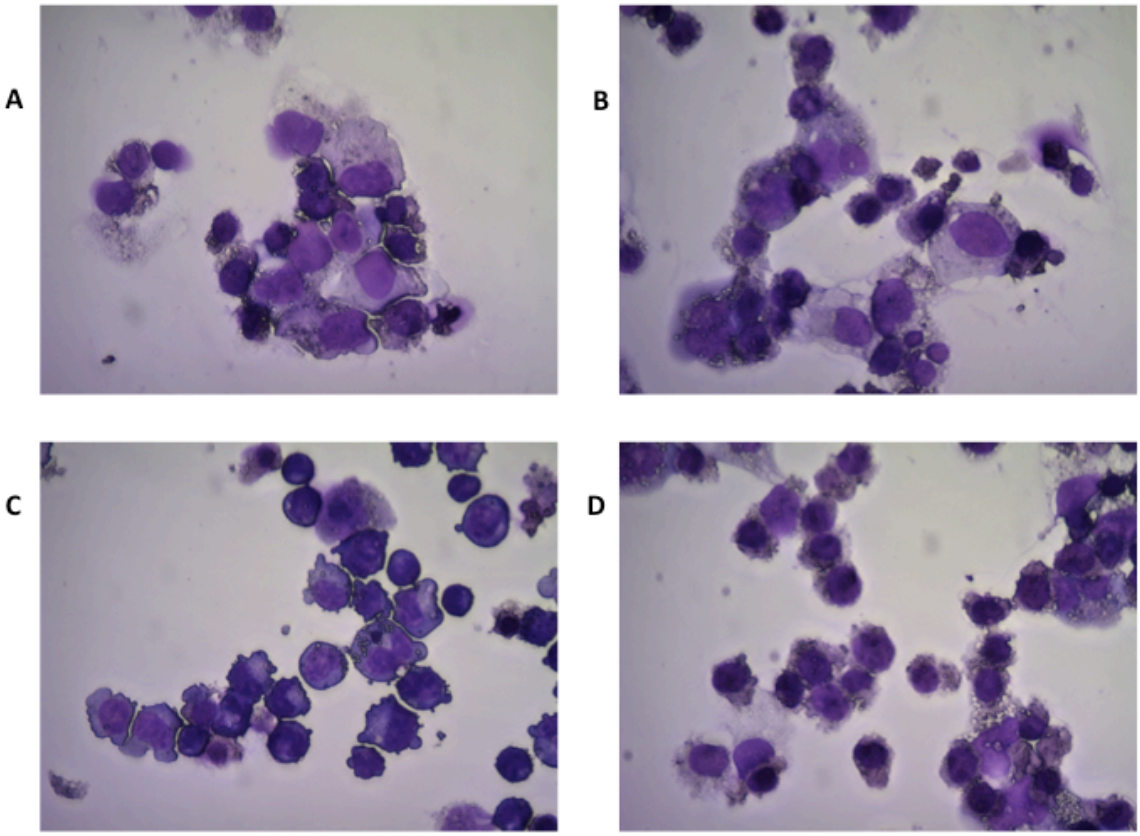

Figure 27: Cytospins of Kasumi1 and SKNO1 cells derived from pooled colonies after knockdown of *GPX4* compared to the scrambled control (at day 7 of the CFC assay). A) Kasumi shscr, B) Kasumi sh*GPX4*, C) SKNO1 shscr, D) SKNO1 sh*GPX4*.

3.1.11 Knockdown of *GPX4* does not lead to an increased rate of apoptosis

As ROS play a major role in apoptosis pathways we wanted to see if the change in ROS level after knockdown of *GPX4* leads to changes in apoptosis. Apoptosis was analyzed by FACS with APC conjugated Annexin V. Cells with a knockdown of *GPX4* and higher ROS levels were compared to scrambled control with lower ROS levels. For live death staining PI was used to separate cells that undergo early apoptosis (lower right quadrant) from debris or necrosis (upper left quadrant) or in late apoptosis (upper right quadrant).

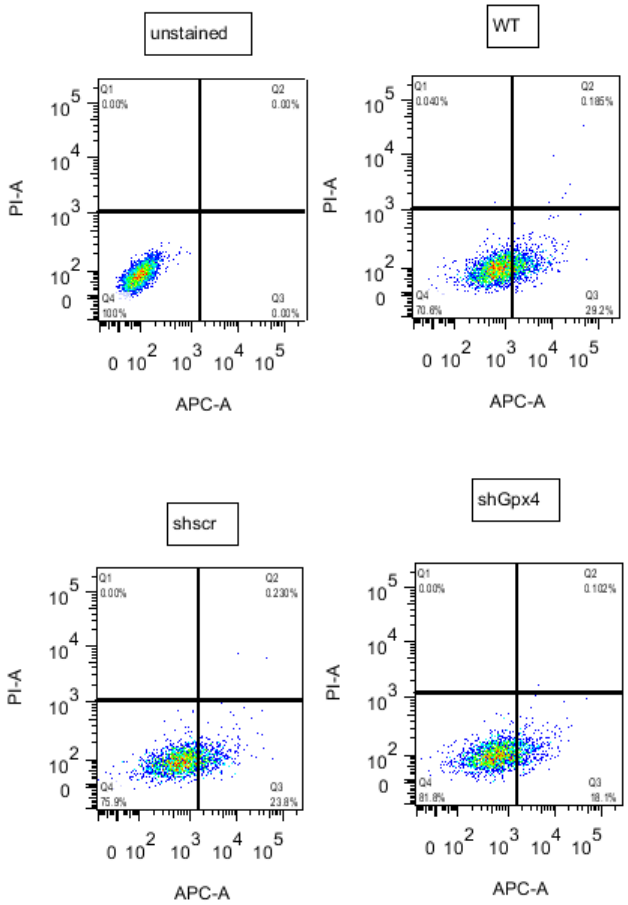

Figure 28: Apoptosis in Kasumi1 cells that carry a *GPX4* knockdown and show higher ROS levels compared to cells of the same cell line that carry the scrambled control vector and show lower ROS levels. Staining was performed using APC conjugated AnnexinV and PI.

No significant difference was found between cells transduced with the different constructs. In Kasumi1 cells transduced with sh scrambled, 23.8% were APC positive and therefore early stages of apoptosis. Only 0.23% of the cells were PI and APC positive indicating late apoptosis. The major part of the population (76.9%) is APC and PI negative and thus alive without any signs of apoptosis. None of the cells were PI single positive. Compared to cells in which *GPX4* was knocked down, similar percentages were observed. The amount of living cells that did not show apoptosis was slightly higher with 81.8%. APC only positive cells (18.1%) and APC and PI double positive (0.102%) were less. Wildtype cells (WT) showed 70.6% double negative cells and the highest percentage (29.2%) of APC only cells. APC and PI double positive cells with 0.185% in between shscr and sh*GPX4* (Figure 28).

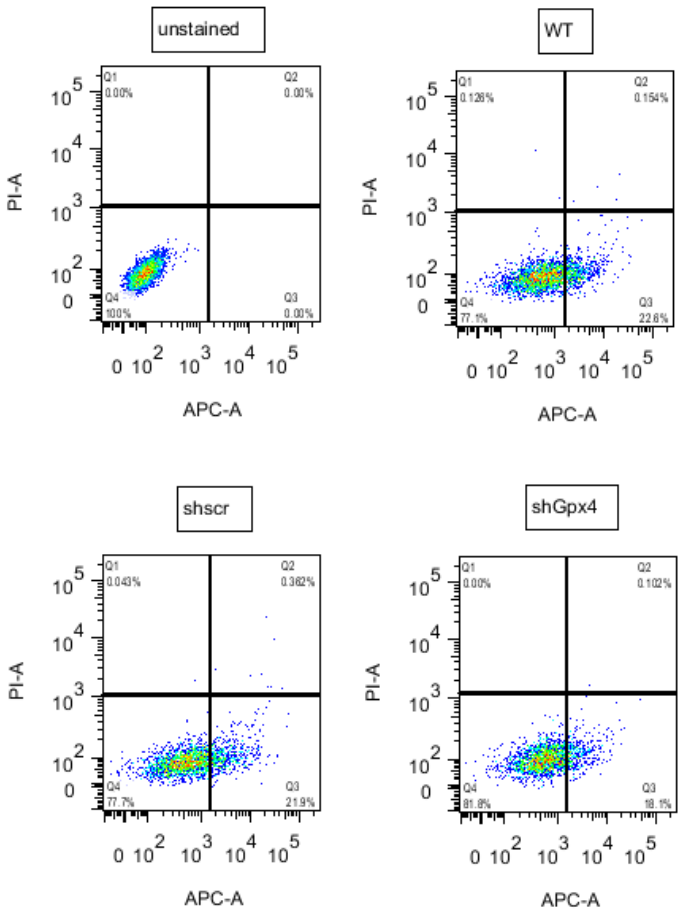

Figure 29: Apoptosis in SKNO1 cells that carry a *Gpx4* knockdown and show higher ROS levels to cells of the same cell line that carry scrambled control vector and show lower ROS levels. Staining was performed using Annexin V that was conjugated to APC and PI for live dead staining.

The pattern looked similarly in SKNO1 cells. In shscr 77.7% of the cells were double negative for APC and PI. 21.9% showed signs of apoptosis and are APC positive and 0.326% were double positive for PI and APC. In contrast to Kasumi1 cells here very few cells (0.043%) that showed neither APC nor PI were found. In shGpx4 cells the amount of double negative cells was higher (81.8%) and the percentage of APC positive (18.1%) and double positives (0.102%) was lower. No cells were only PI positive. Comparing both constructs to WT, WT showed almost the same amount of double negative cells (77.1%) as shscr, the highest number of APC positive cells (22.6%) and double positive cells (0.154%) was in between shscr and shGpx4. With 0.126% the number of PI only was the highest of the three groups (Figure 29).

3.1.12 Gpx4 in murine hematopoiesis and leukemic mouse models

In search for an appropriate mouse model for the analysis of GPX4 in leukemogenesis, we analyzed the role of *Gpx4* in murine normal and malignant hematopoiesis.

3.1.13 *Gpx4* is higher expressed in MEPs compared to GMPs

To determine the expression of *Gpx4* in hematopoietic tissue and especially in hematopoietic progenitor cells, bone marrow from C3H-HeJxB6 mice was collected, stained with specific antibodies for the lineage specific surface markers and sorted by FACS. RNA was analyzed by TaqMan real-time qRT-PCR. Figure 30 shows that *Gpx4* is highly expressed in hematopoietic stem cells (HSC) (mean ΔCt value of 5.89 ± 0.21) as well as in both lymphoid (CLP) (mean ΔCt value of 6.17 ± 0.31) and myeloid (CMP) progenitors (mean ΔCt value of 5.82 ± 0.17). Comparing the two compartments of the myeloid lineage the expression of *Gpx4* is significantly higher in the erythroid lineage.

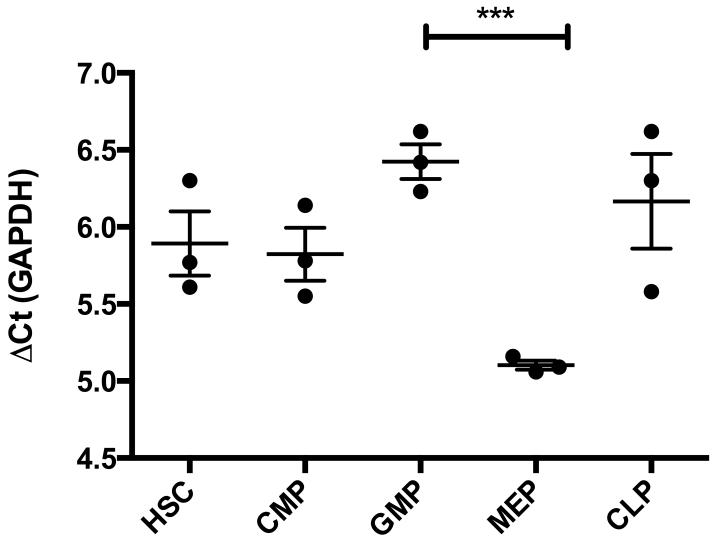

Figure 30: *Gpx4* expression in murine bone marrow subpopulations n=3. The expression of *Gpx4* was determined by TaqMan qRT-PCR and the ΔCt value was calculated by normalization to GAPDH (the lower the value the higher the expression).

3.1.14 Introduction of the *AML1-ETO* full-length fusion gene leads to a down regulation of *Gpx4* in 32D cells.

Based on the results on *AML1-ETO* in the human system we were interested to see whether the the *AML1-ETO* fusion gene induces expression of *Gpx4*. Therefore the murine bone marrow cell line 32D was transduced retrovirally with the full length *AML1-ETO* fusion gene and with the variant *AML1-ETO9a* that is highly leukemogenic. RNA was analyzed with qRT-PCR for *Gpx4* expression (n=3).

32D cells that expressed *AML1-ETO9a* did not show any difference in *Gpx4* expression compared to the control vector. Cells that expressed the full-length *AML1-ETO* fusion gene showed a lower expression of *Gpx4* compared to 32D MIG control (p value 0,032) and 32D AML1-ETO9a (p value 0,0073) (Figure 31). This indicates that in the murine system AML1-ETO does not induce *Gpx4* expression.

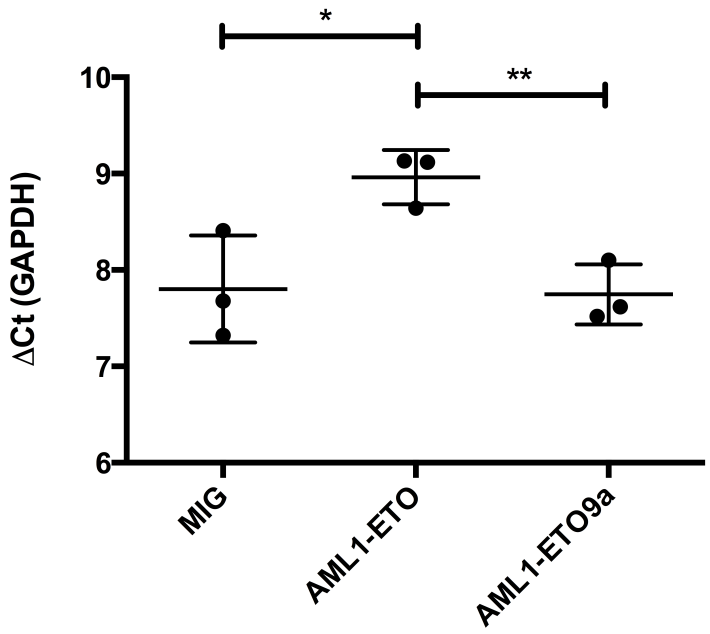

Figure 31 *Gpx4* expression in 32D cells that were retrovirally transduced with the *AML1-ETO* and *AML1-ETO9a* fusion gene compared to 32D cells transduced with the MIG control vector. (The lower the value the higher the expression)

We further investigated the expression of the GPX4 protein in the overexpressing 32D cell lines. Protein lysates of 32DMIG, 32D AML1-ETO and AML1-ETO9a were blotted on a nitrocellulose membrane and detected with GPX4 antibody for the protein of interest and β-Actin as loading control. The expression of the GPX4 protein was similar in 32D MIG and 32D AML1-ETO9a cells correlating with the expression pattern detected by RT-PCR. In 32D AML1-ETO cells GPX4 protein was not detectable (Figure 32), however protein loading was less in this experimental arm as indicated by a weaker band in the β-Actin control.

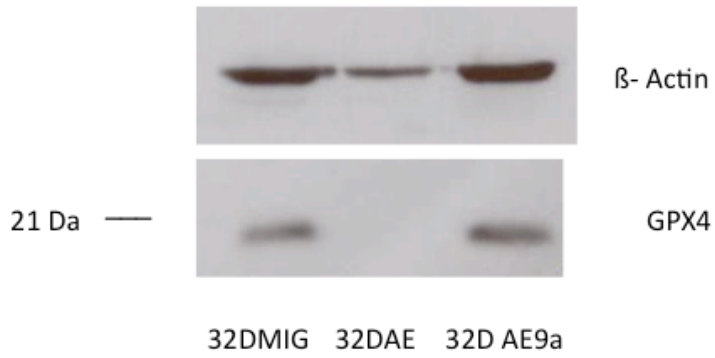

Figure 32 Protein expression in 32D cells that were retrovirally transduced with the *AML1-ETO* and *AML1-ETO9a* fusion gene compared to MIG only vector.

3.1.15 *Gpx4* is expressed in *CALM-AF10*, *HoxA9* and *Cdx2* leukemic murine models

In search for an appropriate mouse model for the analysis of GPX4 in leukemogenesis, we analyzed different types of mouse leukemia cell lines. Cell lines from leukemic mice of different mouse leukemia models that were previously established in our lab and published (Deshpande et al., 2006; Rawat et al., 2004) were analyzed by qRT PCR for expression of *Gpx4*. The three CDX2 cell lines had a very heterogeneous pattern with CDX2 101-394 showing a mean ΔCt value of 7.00 ± 0.59, *Cdx2 78-251* showing a mean ΔCt value of 6.780 ± of 0.07. The third cell line CDX2 *3997* showed a lower expression of *Gpx4* (mean ΔCt value of 9.583 ± 1.5) compared to EGFP bone marrow (mean ΔCt of 7.323 ± 0.15). The CALMAF10 cell line does not show a significant difference (mean ΔCt value of 7.2 ± 0.21), in HOXA*9* cells we found a slightly decreased expression of *Gpx4* (mean ΔCt of 8.17 ± 1.41) (Figure 33).

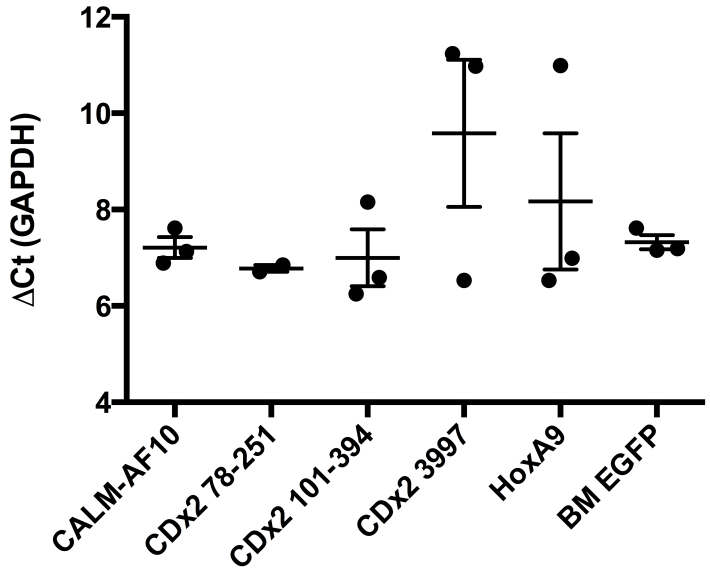

Figure 33 *Gpx4* expression in leukemic bone marrow cell lines compared to EGFP bone marrow n=3 (CDX2 87-251 n=2). Cell lines were established from the bone marrow of mice that were transplanted with bone marrow containing the appropriate vector and were sacrificed when they showed clinical signs of leukemia. (the lower the value the higher the expression)

3.1.16 *Gpx4* is expressed similar in all subpopulations of CALM-AF10leukemic mice

The model of CALM-AF10 murine leukemia allows for the analysis of the LSC hierarchy. The hierarchically subpopulations of primary CALM-AF10 mice were double stained for the surface markers B220 and Mac1, sorted by FACS and were analyzed with qRT-PCR for *Gpx4* expression. All sorted subpopulations showed an expression of *Gpx4*. The LSC population (B220+/Mac1+) seemed to have moderately decreased but not significantly lower expression of *Gpx4* (average ΔCt value of 0.21 ± 0.049) compared to the other non-LSC populations (B220+/Mac1+ and B220-/Mac1+). The expression levels of *Gpx4* were almost at the same level in the other populations (average ΔCt from 0.12 to 0.14)(**Figure 34**).

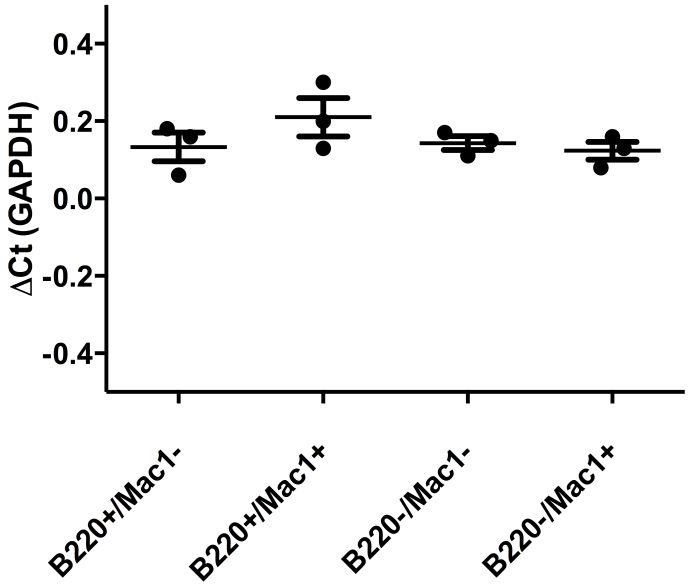

Figure 34 *Gpx4* expression in the bone marrow of primary CALM-AF10 leukemic mice stained for B220 and Mac1. (n=3). Gene expression was detected by Taqman real time PCR and normalized to mGAPDH. (the lower the value the higher the expression).

4 Discussion

GPX4 in human hematopoiesis

Extensive research has been performed on the role of GPX4 in mouse embryogenesis. Homozygous GPX4 depletion leads to embryonic death. The different isoforms are specifically expressed in embryonic brain and heart and play a role in organogenesis of these tissues (Borchert et al., 2006;). Hirotaka Imai et al., 2003; Seiler et al., 2008; Yant et al., 2003).

Further studies addressed the role of GPX4 in different kinds of cancer such as lymphomas (Ran et al., 2007), pancreas carcinoma (Liu et al., 2006; Trachootham et al., 2006) and ovarial cancers (Ding & Lind, 2007). All these studies found that a downregulation of GPX4 leads to retardation of growth and decreases tumorigenic potential of cancer cells indicating that GPX4 is a promising molecular target for anti-cancer therapy (Brielmeier et al., 2001; Liu et al., 2006; Ran et al., 2007; Schneider et al., 2010; Trachootham et al., 2006)

In human hematopoietic cells, GPX4 was first analyzed in platelets demonstrating high expression and activity in these cells (M. Sutherland et al., 2001). In leukemic stem cells, GPX3, another member of the GPX family, has been shown to be positively correlated with leukemic stem cell (LSC) frequency. In mice, high LSC frequency came along with high *Gpx3* expression and low ROS levels in HoxA9 and Meis1- induced leukemias. In patient leukemia cells high *GPX3* expression was associated with poor prognosis (Herault et al., 2012).

In our study, we delineated the *GPX4* expression in human hematopoietic cells, in particular in different bone marrow (BM) subpopulations. Interestingly, we found *GPX4* markedly upregulated in the stem cell compartment compared to total bone marrow MNCs. It is known that HSCs attain long-term protection from oxidative stress in a low oxygenic niche (Jang & Sharkis, 2007) and that the overexpression of ROS-detoxyfying enzymes provides further advantages and protection for HSCs (Miao et al., 2013). The upregulation of *GPX4* may be another mechanism to protect HSCs from oxidative stress in order to keep the quiescence and self-renwing potential of stem cells.

GPX4 in human leukemogenesis

In order to address the role of *GPX4* in malignant hematopoietic cells, we investigated bone marrow subpopulations in AML patients with normal karyotype leukemia. *GPX4* expression was markedly higher in all bone marrow subpopulations of AML patients compared to hematopoietic stem cells in normal bone marrow. Thus, leukemic transformation is associated with elevated *GPX4* expression in all bone marrow cells independent of lineage and maturation. This may be a compensatory mechanism to escape the damaging effects of high ROS levels followed by leukemic transformation. Alternatively it may well be that GPX4 expression increases in line with increased features of "stemness" of leukemia cells strengthening their potential of self renewal.

In search of a clinical model for high *GPX4* expression we analyzed micrroarray data from the Leukemia Gene Atlas (Haferlach, 2010) and found that in leukemias with the *AML1-ETO* fusion, *GPX4* is significantly higher when compared to all other AML subtypes combined. In our gene expression analysis of patients with five different karyotypes including *AML1-ETO* we confirmed that *GPX4* is highly upregulated in all patients. The gene expression was in the same range in all analyzed groups of our study.

Interestingly in our analysis of *GPX4* in human leukemia cell lines the gene was upregulated in all cell lines analyzed except of NB4 and Molm-13 cells. This might be explained by the fact that both cell lines are derived from acute promyelocytic leukemia (APL). APL is a leukemia subtype with a mature phenotype and a high potential for further differentiation (Exner et al., 2000). This is in line with our findings in healthy bone marrow that *GPX4* is lower in mature than in stem cells.

The expression of *GPX4* was high in the *AML1-ETO* carrying cell lines Kasumi1 and SKNO1. Based on the high expression of *GPX4* in patients with this fusion gene shown in the microarray data on *GPX4* and *AML1-ETO* we choose those cell lines for further experiments.

Protein expression of GPX4 in AML1-ETO positive cell lines and in U937 cells was positively correlated with gene expression levels. GPX4 protein was located in all cellular compartements. A difference in cellular subfractions was only detected in Kasumi1 where the protein level was higher in the cytoplasmatic than in the nuclear fraction. Thus, the function of GPX4 in leukemia is not restricted to a single cellular compartment. This is in line with earlier studies of Marcus Conrad (Marcus Conrad et al., 2007) demonstrating ubiquitous distribution of GPX4 in mouse embryogenic cells.

We addressed the role of GPX4 and oxidative stress in leukemogenesis by *GPX4* knock-down. We found that knock-down of *GPX4* alone is sufficient to increase ROS levels in Kasumi1 and SKNO1 cells. In both cell lines a clear shift towards oxidative stress was visible with a stronger effect in Kasumi1 cells. Moreover, we found a higher increase in ROS levels in Kasumi1 cells, which had a higher constitutive expression than SKNO1, indicating a direct correlation of *GPX*4 expression and ROS levels.
Redox imbalance is found in a variety of different cancer types and is associated with carcinogenesis (Marian Valko et al., 2007) In addition, tumor cells in culture produce more ROS than normal cells (Szatrowski & Nathan, 1991). Schumacker et al. claime a role for ROS in tumor promotion, mutagenesis as well as in apoptosis and necrosis of tumor cells. ROS is on one hand necessary for tumor development and on the other hand, might be a potential target for cancer therapy (Schumacker, 2006).
It is known that high ROS levels appear in the state of AML as well as in state of CML. The high ROS levels are partly correlated to specific translocations and oncogenes such as *BCR/ABL, FLT3/ITD* and *AML1-ETO* (Sinenko et al., 2010) Our experiments indicated GPX4 as a regulator for ROS in leukemic cells and especial in AML1-ETO leukemia. Moreover we could show that it was sufficient to target only this one antioxidative mechanism in order to increase ROS levels in a state of disease that is already associated with high ROS. This additional elevation might make the difference between a ROS level that is necessary for the tumor cells and one that causes harm to the cells (Schumacker, 2006), making GPX4 a candidate target for anti-cancer therapy.

Deregulation in cell proliferation, apoptosis and self-renewal are involved in tumorigenesis. GPX4 has been shown to protect Burkitt's lymphoma cells from oxidative stress induced death (Brielmeier et al., 2001) and heterozygous knock-out mice have a latency in developing lymphomas compared to the control group (Ran et al., 2007). A knockdown of *GPX4* is also able to enhance the cytotoxic effect of Docosahexaenoic acid (DHA) in various human cancer cell lines (Ding & Lind, 2007). We hypothesized that knockdown of *GPX4* affects cell proliferation, apoptosis and clonogenicity.

In our experiments knockdown of *GPX4* markedly decreased the proliferative potential of Kasumi1 and SKNO1 cells. Kasumi1 cells showed a stronger effect that might be due to a higher constitutive expression of the gene in the parental cells and therefore a stronger anti-proliferative effect of the knockdown. Since the knockdown efficiency was the same for both cell-lines, this was not due to an imbalance of gene depletion. Our data are in line with the study from Yoo et al. who found that a knock-down of the antioxidative enzyme TRX1 (Thioredoxinreductase 1) in lung carcinoma

cells leads to a loss of their tumorigenic potential and decreases cell proliferation (Yoo et al., 2006).

In our experiments on the role of GPX4 on clonogenicity we found no effect of GPX4 knockdown on the clonogenic potential as measured in CFC assays. This indicates that GPX4 did not affect signaling pathways involved in self-renewal and clonogenicity in this system.

As ROS is known to play a major role in apoptosis pathways and apoptosis induction (Dröge, 2002; M Valko et al., 2006). Brielmeier et al showed that GPX4 protects burkitt lymphoma cells from apoptosis (Brielmeier et al., 2001). We therefore investigated whether the antiproliferative effect of the knock-down of GPX4 is based on an increased apoptosis rate. Surprisingly, there was no difference in the apoptotic rate of cells carrying the knock-down compared to control cells, indicating that the down regulation of GPX4 does not interfere with apoptosis pathways.

ROS act as second messenger molecules for a variety of receptor agonists (Dröge, 2002). Therefore a number of other pathways that affect cell growth and proliferation have to be considered. One possibility is an interaction of ROS with intercellular Ca^{2+}. This signaling pathway regulates cell proliferation and cell cycle arrest. ROS acts here as second messenger in the control of cell proliferation and differentiation (Sauer H, Wartenberg M, 2001).

GPX4 in murine hematopoiesis and leukomogenesis

As in human hematopoiesis, the early steps in mouse hematpoiesis are well defined by monoclonal antibody surface markers. In order to establish an experimental system for GPX4 in pluripotent and determined hematopoietic stem cells, we analyzed whether the function of GPX4 is similar in human and mouse hematopoiesis. In the different lineages of murine hematopoiesis *Gpx4* is constitutively expressed. The gene-expression of *Gpx4* was significantly higher in the erythroid/megakaryopoietic (MEP) compared to the myeloid (GMP) lineage. In line with this, in humans GPX4 activity is elevated in megakaryoblasts and platelets (M. Sutherland et al., 2001). In contrast to human hematopoiesis, we did not find any difference between the myeloid (CMP), the lymphoid (CLP) lineage and the stem cell compartment (HSC). We hereby identified a major difference compared to human hematopoiesis, where *GPX4* is highly expressed in stem cells.

In search for an appropriate mouse model for the analysis of GPX4 in leukemogenesis, we analyzed different types of mouse leukemia cell lines. Cell lines were created by transduction of mouse bone marrow with the CDX2 proto-oncogene, the leukemogenic CALM-AF10 fusion gene, and the AML1-ETO fusion gene, which were then analyzed for *Gpx4* expression. The CDX2 proto-onkogene is expressed in 90% of all AML patients (Scholl et al., 2007). The ectopic expression of the homeobox gene and proto-oncogene CDX2 is the transforming event and leads to the development of leukemia in a mouse model that carries a t(12;13)(p13;q12) translocation (Rawat et al., 2004). Though created by the same proto-oncogene, we found a wide variation in *Gpx4* expression in these leukemia cell lines.

The t(10;11)(p13;q14) translocation causes the highly leukemogenic fusion gene *CALM-AF10*. This model allows for the analysis of the LSC hierarchy. The LSC population is characterized by different expressions of the cell surface marker B220 and Mac1. LSCs with $B220^{+}/Mac1^{-}$ have a LSC frequency of 1 in 36 cells. The $B220^{+}/Mac1^{+}$ population shows a frequency of 1 in 437 cells and $B220^{-}/Mac1^{+}$ has the lowest LSC frequency with 1 in 13906. The double negative cells have no LSC potential (Deshpande et al., 2006). No difference could be found in *Gpx4* expression among all the different LSC populations. The data are in line with our findings in normal mouse bone marrow cells, where *Gpx4* is not upregulated in the stem cell compartment.

The t(8;21) translocation leads to the expression of the AML1-ETO fusion gene, which plays a role in human leukemia. Introduction of AML1-ETO into a drosophila model causes high ROS levels in the hematopoietic precursors (Sinenko et al., 2010). Microarray data show that patients who carry the t(8;21) translocation have a higher expression of the *GPX4* gene compared to healthy individuals (Haferlach, 2010). Instead of an upregulation as expected from our experiments in the human system, the retroviral introduction of the AML1-ETO fusion gene led to a downregulation of *Gpx4* in mouse leukemia cells. The introduction of the spliced variant AML1-ETO9a, which is able to induce leukemia without any additional mutation had no effect at all. These results were also confirmed on protein level.

Taken together, we documented expression of *Gpx4* in murine AML, but did not see any major difference between the different leukemia types or between leukemic stem cells and non-LSCs in the CALM-AF10 model. This might be due to the fact that all these models artificially overexpress the fusion genes by retroviral gene transfer.

5 Summary

Redox systems are a major tool for the organism to deal with oxidative stress and the balance of these systems is crucial for life. The glutathione (GSH) dependent system consists of glutathione, glutathione peroxidases and glutathione reductases and is critically involved in the maintenance of intracellular redox balance. In addition, the glutathione dependent system is a promising target for anti-cancer therapy. In particular, glutathione peroxidase 4, an enzyme that protects cell membranes from lipidperoxidation, plays a major role in proliferation, growth and development as *Gpx4* disruption leads to growth arrest and embryonic death in a mouse model. GPX4 function plays a regulative role in several kinds of cancer and is highly expressed in leukemias, especially in patients carrying the *AML1-ETO* fusion gene. In this work, we delineated the role and expression of GPX4 in hematopoiesis and leukemia and investigated its role as potential target for anti-cancer therapy.

In a state of non-disease glutathionperoxidase 4 is highly expressed in all hematopoietic lineages with the highest expression in the mouse erythroid lineage and is upregulated in the stem cell compartment in human bone marrow.

This suggests that GPX4 is involved as one of the major antioxidative mechanisms in hematopoiesis. In the state of leukemia we could prove an upregulation of the gene in AML1-ETO patients compared to healthy individuals, which was shown by microarray data before.

The present study thus could show that a knock-down of *GPX4* in leukemic cell lines carrying the *AML1-ETO* fusion gene led to a strong anti-proliferative effect but no effect on the clonogenicity of the cells was observed. In addition, the knockdown of only this one antioxidative mechanism was sufficient to increase ROS levels in those cell lines. Apoptosis signaling was not involved in these processes. These data shed new light on the role of GPX4 in normal and malignant hematopoiesis and encourage further studies testing the therapeutic efficacy of GPX4 blockage in human AML.

6 Zusammenfassung

Die Bedeutung von Glutathionperoxidase 4 für die Hämatopoese und Leukämie

Redox Systeme sind ein Hauptwerkzeug des Organismus um oxidativen Stress zu bewältigen und die Balance dieser Systeme ist lebenswichtig. Das Glutathion abhängige System besteht aus Glutathion, Glutathion Peroxidasen und Glutathion Reductasen und spielt eine wichtige Rolle bei der Aufrechterhaltung des intrazellulären Redox Gleichgewichts. Außerdem scheint eine Beeinflussung des Glutathion abhängigen Systems ein vielversprechender Ansatz in der Tumortherapie zu sein. Vor allem Glutathion Peroxidase 4, ein Enzym das Zellmembranen vor Lipidperoxidation schützt spielt eine wichtige Rolle bei Tumorproliferation, -wachstum und -entwicklung. Ein knockdown des Gens führt zu Wachstumsstop und embryonalem Tod im Maus Modell. Es ist bekannt dass GPX4 eine regulative Rolle bei verschiedenen Krebsarten inne hat und dass das Gen in Leukämien hoch exprimiert wird. Dies gilt vor allem für Patienten die Träger des *AML1-ETO* Fusionsgens sind. In dieser Arbeit, „The role of gutathionperoxidase 4 (GPX4) in hematopoiesis and leukemogensis“ zeigen wir die Bedeutung der Glutathionperoxidase 4 in hämatopoetischen Zellen und Leukämien und untersuchen die Rolle dieses speziellen Enzyms als Angriffspunkt für die Krebstherapie.

In gesundem Knochenmark ist Glutathionperoxidase 4 in allen hämatopoetischen Linien hoch exprimiert. Die höchste Expression im murinen System findet sich dabei in der erythroiden Linie. Im humanen Knochenmark ist das Gen ist im Stammzell Kompartiment hochreguliert.

Dies legt den Schluss nahe, dass GPX4 als ein bedeutender antioxidativer Mechanismus an der Hämatopoese beteiligt ist. In Leukämien konnten wir eine Hochregulierung des Gens in AML1-ETO Patienten verglichen mit mononuklearen Zellen gesunder Menschen bestätigen. Dies wurde zuvor im Mikroarray gezeigt.

Die vorliegende Studie zeigt außerdem, dass ein knock-down von *GPX4* in Leukämiezellinien die das *AML1-ETO* Fusionsgen tragen einen starken antiproliferativen Effekt hat. Die Klonogenität der Zellen wurde dabei nicht beeinflusst. Außerdem ist ein knockdown dieses einzelnen antioxidativen Enzyms ausreichend um den oxidativen Stress, das ROS Level in den Zellen zu erhöhen. Apoptose spielte hierbei keine Rolle. Diese Daten stellen die Rolle von GPX4 in der normalen und malignen Hämatopoese in einem neuen Licht dar und fordern weitere Studien die den therapeutischen Effekt einer Blockade von GPX4 in humanen AML erforschen.

7 References

Andresen, M., Regueira, T., Bruhn, A., Perez, D., Strobel, P., Dougnac, A., … Leighton, F. (2008). Lipoperoxidation and protein oxidative damage exhibit different kinetics during septic shock. *Mediators of Inflammation*, *2008*, 168652. doi:10.1155/2008/168652

Arai, M., Imai, H., Koumura, T., Yoshida, M., Emoto, K., Umeda, M., … Nakagawa, Y. (1999). Mitochondrial phospholipid hydroperoxide glutathione peroxidase plays a major role in preventing oxidative injury to cells. *The Journal of Biological Chemistry*, *274*(8), 4924–33. Retrieved from http://www.ncbi.nlm.nih.gov/pubmed/9988735

Arai, M., Imai, H., Sumi, D., Imanaka, T., Takano, T., Chiba, N., & Nakagawa, Y. (1996). Import into mitochondria of phospholipid hydroperoxide glutathione peroxidase requires a leader sequence. *Biochemical and Biophysical Research Communications*, *227*(2), 433–9. doi:10.1006/bbrc.1996.1525

Asetskaia, I. L., Egorov, D. I., Kozlov, A. v, Nalivaĭko, E. S., Markin, S. S., Sergienko, V. I., … Lopukhin, I. M. (1990). [Ceruloplasmin-transferrin antioxidant system in in experimental and clinical atherosclerosis]. *Vestnik Akademii Meditsinskikh Nauk SSSR*, (12), 41–5. Retrieved from http://www.ncbi.nlm.nih.gov/pubmed/2291327

Banning, A., Schnurr, K., Böl, G. F., Kupper, D., Müller-Schmehl, K., Viita, H., … Brigelius-Flohé, R. (2004). Inhibition of basal and interleukin-1-induced VCAM-1 expression by phospholipid hydroperoxide glutathione peroxidase and 15-lipoxygenase in rabbit aortic smooth muscle cells. *Free Radical Biology & Medicine*, *36*(2), 135–44. Retrieved from http://www.ncbi.nlm.nih.gov/pubmed/14744625

Borchert, A., Savaskan, N. E., & Kuhn, H. (2003). Regulation of expression of the phospholipid hydroperoxide/sperm nucleus glutathione peroxidase gene. Tissue-specific expression pattern and identification of functional cis- and trans-regulatory elements. *The Journal of Biological Chemistry*, *278*(4), 2571–80. doi:10.1074/jbc.M209064200

Borchert, A., Wang, C. C., Ufer, C., Schiebel, H., Savaskan, N. E., & Kuhn, H. (2006). The role of phospholipid hydroperoxide glutathione peroxidase isoforms in murine embryogenesis. *The Journal of Biological Chemistry*, *281*(28), 19655–64. doi:10.1074/jbc.M601195200

Bradford, M. M. (1976). A rapid and sensitive method for the quantitation of microgram quantities of protein utilizing the principle of protein-dye binding. *Analytical Biochemistry*, *72*, 248–54. Retrieved from http://www.ncbi.nlm.nih.gov/pubmed/942051

Brielmeier, M., Béchet, J. M., Suppmann, S., Conrad, M., Laux, G., & Bornkamm, G. W. (2001). Cloning of phospholipid hydroperoxide glutathione peroxidase (PHGPx) as an anti-apoptotic and growth promoting gene of Burkitt lymphoma cells. *BioFactors (Oxford, England)*, *14*(1-4), 179–90. Retrieved from http://www.ncbi.nlm.nih.gov/pubmed/11568455

Brigelius-Flohé, R., Friedrichs, B., Maurer, S., Schultz, M., & Streicher, R. (1997). Interleukin-1-induced nuclear factor kappa B activation is inhibited by overexpression of phospholipid hydroperoxide glutathione peroxidase in a human endothelial cell line. *The Biochemical Journal*, *328 (Pt 1*, 199–203. Retrieved from http://www.pubmedcentral.nih.gov/articlerender.fcgi?artid=1218906&tool=pmcentrez&rendertype=abstract

Brigelius-Flohé, R., Maurer, S., Lötzer, K., Böl, G., Kallionpää, H., Lehtolainen, P., … Ylä-Herttuala, S. (2000). Overexpression of PHGPx inhibits hydroperoxide-induced oxidation, NFkappaB activation and apoptosis and affects oxLDL-mediated proliferation of rabbit aortic smooth muscle cells. *Atherosclerosis*, *152*(2), 307–16. Retrieved from http://www.ncbi.nlm.nih.gov/pubmed/10998458

Burton, G. W., & Traber, M. G. (1990). Vitamin E: antioxidant activity, biokinetics, and bioavailability. *Annual Review of Nutrition*, *10*, 357–82. doi:10.1146/annurev.nu.10.070190.002041

Cammarata, G., Augugliaro, L., Salemi, D., Agueli, C., La Rosa, M., Dagnino, L., … Santoro, A. (2010). Differential expression of specific microRNA and their targets in acute myeloid leukemia. *American Journal of Hematology*, *85*(5), 331–9. doi:10.1002/ajh.21667

Campisi, J., & Vijg, J. (2009). Does damage to DNA and other macromolecules play a role in aging? If so, how? *The Journals of Gerontology. Series A, Biological Sciences and Medical Sciences*, *64*(2), 175–8. doi:10.1093/gerona/gln065

Challen, G. A., & Goodell, M. A. (2011). Bridge over troubled stem cells. *Molecular Therapy : The Journal of the American Society of Gene Therapy*, *19*(10), 1756–8. doi:10.1038/mt.2011.184

Chen, C. J., Huang, H. S., Lin, S. B., & Chang, W. C. (2000). Regulation of cyclooxygenase and 12-lipoxygenase catalysis by phospholipid hydroperoxide glutathione peroxidase in A431 cells. *Prostaglandins, Leukotrienes, and Essential Fatty Acids*, *62*(4), 261–8. doi:10.1054/plef.2000.0153

Chen, C.-J., Huang, H.-S., & Chang, W.-C. (2003). Depletion of phospholipid hydroperoxide glutathione peroxidase up-regulates arachidonate metabolism by 12S-lipoxygenase and cyclooxygenase 1 in human epidermoid carcinoma A431 cells. *FASEB Journal : Official Publication of the Federation of American Societies for Experimental Biology*, *17*(12), 1694–6. doi:10.1096/fj.02-0847fje

Chinta, S. J., & Andersen, J. K. (2008). Redox imbalance in Parkinson's disease. *Biochimica et Biophysica Acta*, *1780*(11), 1362–7. doi:10.1016/j.bbagen.2008.02.005

Conrad, M., Moreno, S. G., Sinowatz, F., Ursini, F., Kölle, S., Roveri, A., … Bornkamm, G. W. (2005). The nuclear form of phospholipid hydroperoxide glutathione peroxidase is a protein thiol peroxidase contributing to sperm chromatin stability. *Molecular and Cellular Biology*, *25*(17), 7637–44. doi:10.1128/MCB.25.17.7637-7644.2005

Conrad, M., Schneider, M., Seiler, A., & Bornkamm, G. W. (2007). Physiological role of phospholipid hydroperoxide glutathione peroxidase in mammals. *Biological Chemistry*, *388*(10), 1019–25. doi:10.1515/BC.2007.130

Cozzio, A., Passegué, E., Ayton, P. M., Karsunky, H., Cleary, M. L., & Weissman, I. L. (2003). Similar MLL-associated leukemias arising from self-renewing stem cells and short-lived myeloid progenitors. *Genes & Development*, *17*(24), 3029–35. doi:10.1101/gad.1143403

Cumano, A., & Godin, I. (2007). Ontogeny of the hematopoietic system. *Annual Review of Immunology*, *25*, 745–85. doi:10.1146/annurev.immunol.25.022106.141538

Dalle-Donne, I., Rossi, R., Colombo, R., Giustarini, D., & Milzani, A. (2006). Biomarkers of oxidative damage in human disease. *Clinical Chemistry*, *52*(4), 601–23. doi:10.1373/clinchem.2005.061408

Dash, A., & Gilliland, D. G. (2001). Molecular genetics of acute myeloid leukaemia. *Best Practice & Research. Clinical Haematology*, *14*(1), 49–64. doi:10.1053/beha.2000.0115

Deshpande, A. J., Cusan, M., Rawat, V. P. S., Reuter, H., Krause, A., Pott, C., … Buske, C. (2006). Acute myeloid leukemia is propagated by a leukemic stem cell with lymphoid characteristics in a mouse model of CALM/AF10-positive leukemia. *Cancer Cell*, *10*(5), 363–74. doi:10.1016/j.ccr.2006.08.023

Dhalla, N. S., Temsah, R. M., & Netticadan, T. (2000). Role of oxidative stress in cardiovascular diseases. *Journal of Hypertension*, *18*(6), 655–73. Retrieved from http://www.ncbi.nlm.nih.gov/pubmed/10872549

Ding, W.-Q., & Lind, S. E. (2007). Phospholipid hydroperoxide glutathione peroxidase plays a role in protecting cancer cells from docosahexaenoic acid-induced cytotoxicity. *Molecular Cancer Therapeutics*, *6*(4), 1467–74. doi:10.1158/1535-7163.MCT-06-0608

Dröge, W. (2002). Free radicals in the physiological control of cell function. *Physiological Reviews*, *82*(1), 47–95. doi:10.1152/physrev.00018.2001

Eliades, A., Matsuura, S., & Ravid, K. (2012). Oxidases and reactive oxygen species during hematopoiesis: a focus on megakaryocytes. *Journal of Cellular Physiology*, *227*(10), 3355–62. doi:10.1002/jcp.24071

Exner, M., Thalhammer, R., Kapiotis, S., Mitterbauer, G., Knöbl, P., Haas, O. A., … Schwarzinger, I. (2000). The "typical" immunophenotype of acute promyelocytic leukemia (APL-M3): does it prove true for the M3-variant? *Cytometry*, *42*(2), 106–9. Retrieved from http://www.ncbi.nlm.nih.gov/pubmed/10797447

Falini, B., & Martelli, M. P. (2011). NPM1-mutated AML: targeting by disassembling. *Blood*, *118*(11), 2936–8. doi:10.1182/blood-2011-07-366146

Falini, B., Nicoletti, I., Martelli, M. F., & Mecucci, C. (2007). Acute myeloid leukemia carrying cytoplasmic/mutated nucleophosmin (NPMc+ AML): biologic and clinical features. *Blood*, *109*(3), 874–85. doi:10.1182/blood-2006-07-012252

Fathi, A. T., & Chen, Y.-B. (2011). Treatment of FLT3-ITD acute myeloid leukemia. *American Journal of Blood Research*, *1*(2), 175–89. Retrieved from http://www.pubmedcentral.nih.gov/articlerender.fcgi?artid=3301423&tool=pmcentrez&rendertype=abstract

Gentles, A. J., Plevritis, S. K., Majeti, R., & Alizadeh, A. A. (2010). Association of a leukemic stem cell gene expression signature with clinical outcomes in acute myeloid leukemia. *JAMA : The Journal of the American Medical Association*, *304*(24), 2706–15. doi:10.1001/jama.2010.1862

Ghaffari, S. (2008). Oxidative stress in the regulation of normal and neoplastic hematopoiesis. *Antioxidants & Redox Signaling*, *10*(11), 1923–40. doi:10.1089/ars.2008.2142

Gilliland, D. G., & Tallman, M. S. (2002). Focus on acute leukemias. *Cancer Cell*, *1*(5), 417–420. doi:10.1016/S1535-6108(02)00081-8

Godeas, C., Tramer, F., Micali, F., Roveri, A., Maiorino, M., Nisii, C., … Panfili, E. (1996). Phospholipid hydroperoxide glutathione peroxidase (PHGPx) in rat testis nuclei is bound to chromatin. *Biochemical and Molecular Medicine*, *59*(2), 118–24. Retrieved from http://www.ncbi.nlm.nih.gov/pubmed/8986633

Griendling, K. K., & Ushio-Fukai, M. (2000). Reactive oxygen species as mediators of angiotensin II signaling. *Regulatory Peptides*, *91*(1-3), 21–27. doi:10.1016/S0167-0115(00)00136-1

Hafer, K., Iwamoto, K. S., & Schiestl, R. H. (2008). Refinement of the dichlorofluorescein assay for flow cytometric measurement of reactive oxygen species in irradiated and bystander cell populations. *Radiation Research*, *169*(4), 460–8. doi:10.1667/RR1212.1

Haferlach. (2010). Leukemia Gene Atlas. Retrieved September 09, 2013, from http://www.leukemia-gene-atlas.org/LGAtlas/

Haidar, R., Mhaidli, H., & Taher, A. T. (2010). Paraspinal extramedullary hematopoiesis in patients with thalassemia intermedia. *European Spine Journal : Official Publication of the European Spine Society, the European Spinal Deformity Society, and the European Section of the Cervical Spine Research Society*, *19*(6), 871–8. doi:10.1007/s00586-010-1357-2

Halliwell, B a. G., J. M. . (1989). Free radicals in biology and medicine: Oxford University Press, Oxford.

Haraguchi, C. M., Mabuchi, T., Hirata, S., Shoda, T., Yamada, A. T., Hoshi, K., & Yokota, S. (2003). Spatiotemporal changes of levels of a moonlighting protein, phospholipid hydroperoxide glutathione peroxidase, in subcellular compartments during spermatogenesis in the rat testis. *Biology of Reproduction*, *69*(3), 885–95. doi:10.1095/biolreprod.102.013524

Herault, O., Hope, K. J., Deneault, E., Mayotte, N., Chagraoui, J., Wilhelm, B. T., … Sauvageau, G. (2012). A role for GPx3 in activity of normal and leukemia stem cells. *The Journal of Experimental Medicine*, *209*(5), 895–901. doi:10.1084/jem.20102386

Imai, H., Hirao, F., Sakamoto, T., Sekine, K., Mizukura, Y., Saito, M., … Nakagawa, Y. (2003). Early embryonic lethality caused by targeted disruption of the mouse PHGPx gene. *Biochemical and Biophysical Research Communications*, *305*(2), 278–86. Retrieved from http://www.ncbi.nlm.nih.gov/pubmed/12745070

Imai, H., Narashima, K., Arai, M., Sakamoto, H., Chiba, N., & Nakagawa, Y. (1998). Suppression of leukotriene formation in RBL-2H3 cells that overexpressed phospholipid hydroperoxide glutathione peroxidase. *The Journal of Biological Chemistry*, *273*(4), 1990–7. Retrieved from http://www.ncbi.nlm.nih.gov/pubmed/9442035

Imlay, J. A. (2008). Cellular defenses against superoxide and hydrogen peroxide. *Annual Review of Biochemistry*, *77*, 755–76. doi:10.1146/annurev.biochem.77.061606.161055

Jang, Y.-Y., & Sharkis, S. J. (2007). A low level of reactive oxygen species selects for primitive hematopoietic stem cells that may reside in the low-oxygenic niche. *Blood*, *110*(8), 3056–63. doi:10.1182/blood-2007-05-087759

Jenner, P. (1996). Oxidative stress in Parkinson's disease and other neurodegenerative disorders. *Pathologie-Biologie*, *44*(1), 57–64. Retrieved from http://www.ncbi.nlm.nih.gov/pubmed/8734302

Karihtala, P., & Soini, Y. (2007). Reactive oxygen species and antioxidant mechanisms in human tissues and their relation to malignancies. *APMIS : Acta Pathologica, Microbiologica, et Immunologica Scandinavica*, *115*(2), 81–103. doi:10.1111/j.1600-0463.2007.apm_514.x

Kerksick, C., & Willoughby, D. (2005). The antioxidant role of glutathione and N-acetyl-cysteine supplements and exercise-induced oxidative stress. *Journal of the International Society of Sports Nutrition*, *2*, 38–44. doi:10.1186/1550-2783-2-2-38

Kim, J. H., Chu, S. C., Gramlich, J. L., Pride, Y. B., Babendreier, E., Chauhan, D., … Sattler, M. (2005). Activation of the PI3K/mTOR pathway by BCR-ABL contributes to increased production of reactive oxygen species. *Blood*, *105*(4), 1717–23. doi:10.1182/blood-2004-03-0849

Krieger-Brauer, H. I., & Kather, H. (1995). The stimulus-sensitive H2O2-generating system present in human fat-cell plasma membranes is multireceptor-linked and under antagonistic control by hormones and cytokines. *The Biochemical Journal*, *307 (Pt 2*, 543–8. Retrieved from http://www.pubmedcentral.nih.gov/articlerender.fcgi?artid=1136682&tool=pmcentrez&rendertype=abstract

Liao, E. C., Trede, N. S., Ransom, D., Zapata, A., Kieran, M., & Zon, L. I. (2002). Non-cell autonomous requirement for the bloodless gene in primitive hematopoiesis of zebrafish. *Development (Cambridge, England)*, *129*(3), 649–59. Retrieved from http://www.ncbi.nlm.nih.gov/pubmed/11830566

Liu, J., Du, J., Zhang, Y., Sun, W., Smith, B. J., Oberley, L. W., & Cullen, J. J. (2006). Suppression of the malignant phenotype in pancreatic cancer by overexpression of phospholipid hydroperoxide glutathione peroxidase. *Human Gene Therapy*, *17*(1), 105–16. doi:10.1089/hum.2006.17.105

Lo, Y. Y., & Cruz, T. F. (1995). Involvement of reactive oxygen species in cytokine and growth factor induction of c-fos expression in chondrocytes. *The Journal of Biological Chemistry*, *270*(20), 11727–30. Retrieved from http://www.ncbi.nlm.nih.gov/pubmed/7744816

Lu, J., Chew, E.-H., & Holmgren, A. (2007). Targeting thioredoxin reductase is a basis for cancer therapy by arsenic trioxide. *Proceedings of the National Academy of Sciences of the United States of America*, *104*(30), 12288–93. doi:10.1073/pnas.0701549104

Maiorino, M., Aumann, K. D., Brigelius-Flohé, R., Doria, D., van den Heuvel, J., McCarthy, J., … Flohé, L. (1995). Probing the presumed catalytic triad of selenium-containing peroxidases by mutational analysis of phospholipid hydroperoxide glutathione peroxidase (PHGPx). *Biological Chemistry Hoppe-Seyler*, *376*(11), 651–60. Retrieved from http://www.ncbi.nlm.nih.gov/pubmed/8962674

Maiorino, M., Bosello, V., Ursini, F., Foresta, C., Garolla, A., Scapin, M., … Flohe, L. (2003). Genetic variations of gpx-4 and male infertility in humans. *Biology of Reproduction*, *68*(4), 1134–41. doi:10.1095/biolreprod.102.007500

Maiorino, M., Wissing, J. B., Brigelius-Flohé, R., Calabrese, F., Roveri, A., Steinert, P., … Flohé, L. (1998). Testosterone mediates expression of the selenoprotein PHGPx by induction of spermatogenesis and not by direct transcriptional gene activation. *FASEB Journal : Official Publication of the Federation of American Societies for Experimental Biology*, *12*(13), 1359–70. Retrieved from http://www.ncbi.nlm.nih.gov/pubmed/9761779

Mauri, P., Benazzi, L., Flohé, L., Maiorino, M., Pietta, P. G., Pilawa, S., … Ursini, F. (2003). Versatility of selenium catalysis in PHGPx unraveled by LC/ESI-MS/MS. *Biological Chemistry*, *384*(4), 575–88. doi:10.1515/BC.2003.065

May, J. M., & de Haën, C. (1979). Insulin-stimulated intracellular hydrogen peroxide production in rat epididymal fat cells. *The Journal of Biological Chemistry*, *254*(7), 2214–20. Retrieved from http://www.ncbi.nlm.nih.gov/pubmed/429281

Miao, W., Xufeng, R., Park, M.-R., Gu, H., Hu, L., Kang, J. W., … Cheng, T. (2013). Hematopoietic stem cell regeneration enhanced by ectopic expression of ROS-detoxifying enzymes in transplant mice. *Molecular Therapy : The Journal of the American Society of Gene Therapy*, *21*(2), 423–32. doi:10.1038/mt.2012.232

Moreno, S. G., Laux, G., Brielmeier, M., Bornkamm, G. W., & Conrad, M. (2003). Testis-specific expression of the nuclear form of phospholipid hydroperoxide glutathione peroxidase (PHGPx). *Biological Chemistry*, *384*(4), 635–43. doi:10.1515/BC.2003.070

Mulder, K. M. (2000). Role or Ras and MAPKs in TGF beta signaling. *Cytokine Growth Fact. Rev.*, 23–35.

Nakamura, T., Imai, H., Tsunashima, N., & Nakagawa, Y. (2003). Molecular cloning and functional expression of nucleolar phospholipid hydroperoxide glutathione peroxidase in mammalian cells. *Biochemical and Biophysical Research Communications*, *311*(1), 139–48. Retrieved from http://www.ncbi.nlm.nih.gov/pubmed/14575705

Nerlov, C., & Graf, T. (1998). PU.1 induces myeloid lineage commitment in multipotent hematopoietic progenitors. *Genes & Development*, *12*(15), 2403–2412. doi:10.1101/gad.12.15.2403

Neufeld, G., Cohen, T., Gengrinovitch, S., & Poltorak, Z. (1999). Vascular endothelial growth factor (VEGF) and its receptors. *FASEB J*, *13*(1), 9–22. Retrieved from http://www.fasebj.org/content/13/1/9.long

Niwa, T. (2007). Protein glutathionylation and oxidative stress. *Journal of Chromatography. B, Analytical Technologies in the Biomedical and Life Sciences*, *855*(1), 59–65. doi:10.1016/j.jchromb.2006.12.029

Nordberg, J., & Arnér, E. S. J. (2001). Reactive oxygen species, antioxidants, and the mammalian thioredoxin system1 1This review is based on the licentiate thesis "Thioredoxin reductase—interactions with the redox active compounds 1-chloro-2,4-dinitrobenzene and lipoic acid" by Jonas Nordberg,. *Free Radical Biology and Medicine*, *31*(11), 1287–1312. doi:10.1016/S0891-5849(01)00724-9

Ozben, T. (2007). Oxidative stress and apoptosis: impact on cancer therapy. *Journal of Pharmaceutical Sciences*, *96*(9), 2181–96. doi:10.1002/jps.20874

Packer, J. E., Slater, T. F., & Willson, R. L. (1979). Direct observation of a free radical interaction between vitamin E and vitamin C. *Nature*, *278*(5706), 737–738. doi:10.1038/278737a0

Petrie, K., & Zelent, A. (2007). AML1/ETO, a promiscuous fusion oncoprotein. *Blood*, *109*(10), 4109–4110. doi:10.1182/blood-2007-02-075804

Pfeifer, H., Conrad, M., Roethlein, D., Kyriakopoulos, A., Brielmeier, M., Bornkamm, G. W., & Behne, D. (2001). Identification of a specific sperm nuclei selenoenzyme necessary for protamine thiol cross-linking during sperm maturation. *FASEB Journal : Official Publication of the Federation of American Societies for Experimental Biology*, *15*(7), 1236–8. Retrieved from http://www.ncbi.nlm.nih.gov/pubmed/11344099

Pineault, N., Buske, C., Feuring-Buske, M., Abramovich, C., Rosten, P., Hogge, D. E., … Humphries, R. K. (2003). Induction of acute myeloid leukemia in mice by the human leukemia-specific fusion gene NUP98-HOXD13 in concert with Meis1. *Blood*, *101*(11), 4529–38. doi:10.1182/blood-2002-08-2484

Piwkowska, A., Rogacka, D., Audzeyenka, I., Jankowski, M., & Angielski, S. (2011). High glucose concentration affects the oxidant-antioxidant balance in cultured mouse podocytes. *Journal of Cellular Biochemistry*, *112*(6), 1661–72. doi:10.1002/jcb.23088

Pushpa-Rekha, T. R., Burdsall, A. L., Oleksa, L. M., Chisolm, G. M., & Driscoll, D. M. (1995). Rat phospholipid-hydroperoxide glutathione peroxidase. cDNA cloning and identification of multiple transcription and translation start sites. *The Journal of Biological Chemistry*, *270*(45), 26993–9. Retrieved from http://www.ncbi.nlm.nih.gov/pubmed/7592947

Ran, Q., Liang, H., Gu, M., Qi, W., Walter, C. A., Roberts, L. J., … Van Remmen, H. (2004). Transgenic mice overexpressing glutathione peroxidase 4 are protected against oxidative stress-induced apoptosis. *The Journal of Biological Chemistry*, *279*(53), 55137–46. doi:10.1074/jbc.M410387200

Ran, Q., Liang, H., Ikeno, Y., Qi, W., Prolla, T. A., Roberts, L. J., … Richardson, A. (2007). Reduction in glutathione peroxidase 4 increases life span through increased sensitivity to apoptosis. *The Journals of*

Gerontology. Series A, Biological Sciences and Medical Sciences, *62*(9), 932–42. Retrieved from http://en.wikipedia.org/wiki/Glutathione_peroxidase

Raskind, W. H., Steinmann, L., & Najfeld, V. (1998). Clonal development of myeloproliferative disorders: clues to hematopoietic differentiation and multistep pathogenesis of cancer. *Leukemia*, *12*(2), 108–16. Retrieved from http://www.ncbi.nlm.nih.gov/pubmed/9519769

Rawat, V. P. S., Cusan, M., Deshpande, A., Hiddemann, W., Quintanilla-Martinez, L., Humphries, R. K., … Buske, C. (2004). Ectopic expression of the homeobox gene Cdx2 is the transforming event in a mouse model of t(12;13)(p13;q12) acute myeloid leukemia. *Proceedings of the National Academy of Sciences of the United States of America*, *101*(3), 817–22. doi:10.1073/pnas.0305555101

Reikvam, H., Hatfield, K. J., Kittang, A. O., Hovland, R., & Bruserud, Ø. (2011). Acute myeloid leukemia with the t(8;21) translocation: clinical consequences and biological implications. *Journal of Biomedicine & Biotechnology*, *2011*, 104631. doi:10.1155/2011/104631

Reya, T., Morrison, S. J., Clarke, M. F., & Weissman, I. L. (2001). Stem cells, cancer, and cancer stem cells. *Nature*, *414*(6859), 105–11. doi:10.1038/35102167

Roche, M., Rondeau, P., Singh, N. R., Tarnus, E., & Bourdon, E. (2008). The antioxidant properties of serum albumin. *FEBS Letters*, *582*(13), 1783–7. doi:10.1016/j.febslet.2008.04.057

Rosenbauer, F., & Tenen, D. G. (2007). Transcription factors in myeloid development: balancing differentiation with transformation. *Nature Reviews. Immunology*, *7*(2), 105–17. doi:10.1038/nri2024

Roveri, A., Casasco, A., Maiorino, M., Dalan, P., Calligaro, A., & Ursini, F. (1992). Phospholipid hydroperoxide glutathione peroxidase of rat testis. Gonadotropin dependence and immunocytochemical identification. *The Journal of Biological Chemistry*, *267*(9), 6142–6. Retrieved from http://www.ncbi.nlm.nih.gov/pubmed/1556123

Sakamoto, H., Imai, H., & Nakagawa, Y. (2000). Involvement of phospholipid hydroperoxide glutathione peroxidase in the modulation of prostaglandin D2 synthesis. *The Journal of Biological Chemistry*, *275*(51), 40028–35. doi:10.1074/jbc.M003191200

Sallmyr, A., Fan, J., Datta, K., Kim, K.-T., Grosu, D., Shapiro, P., … Rassool, F. (2008). Internal tandem duplication of FLT3 (FLT3/ITD) induces increased ROS production, DNA damage, and misrepair: implications for poor prognosis in AML. *Blood*, *111*(6), 3173–82. doi:10.1182/blood-2007-05-092510

Sato, H., Tamba, M., Okuno, S., Sato, K., Keino-Masu, K., Masu, M., & Bannai, S. (2002). Distribution of Cystine/Glutamate Exchange Transporter, System xc-, in the Mouse Brain. *J. Neurosci.*, *22*(18), 8028–8033. Retrieved from http://www.jneurosci.org/content/22/18/8028.short

Sattler, M., Winkler, T., Verma, S., Byrne, C. H., Shrikhande, G., Salgia, R., & Griffin, J. D. (1999). Hematopoietic growth factors signal through the formation of reactive oxygen species. *Blood*, *93*(9), 2928–35. Retrieved from http://www.ncbi.nlm.nih.gov/pubmed/10216087

Sauer H, Wartenberg M, H. J. (2001). Reactive Oxygen Species as Intracellular Messengers During Cell Growth and Differentiation - Karger Publishers. *Cell Physiol Biochemistry*, *11*(4), 173–86. Retrieved from http://www.karger.com/Article/Pdf/47804

Savaskan, N. E., Ufer, C., Kühn, H., & Borchert, A. (2007). Molecular biology of glutathione peroxidase 4: from genomic structure to developmental expression and neural function. *Biological Chemistry*, *388*(10), 1007–17. doi:10.1515/BC.2007.126

Sayre, L. M., Smith, M. A., & Perry, G. (2001). Chemistry and biochemistry of oxidative stress in neurodegenerative disease. *Current Medicinal Chemistry*, *8*(7), 721–38. Retrieved from http://www.ncbi.nlm.nih.gov/pubmed/11375746

Schneider, M., Vogt Weisenhorn, D. M., Seiler, A., Bornkamm, G. W., Brielmeier, M., & Conrad, M. (2006). Embryonic expression profile of phospholipid hydroperoxide glutathione peroxidase. *Gene Expression Patterns : GEP*, *6*(5), 489–94. doi:10.1016/j.modgep.2005.11.002

Schneider, M., Wortmann, M., Mandal, P. K., Arpornchayanon, W., Jannasch, K., Alves, F., … Beck, H. (2010). Absence of glutathione peroxidase 4 affects tumor angiogenesis through increased 12/15-lipoxygenase activity. *Neoplasia (New York, N.Y.)*, *12*(3), 254–63. Retrieved from http://www.pubmedcentral.nih.gov/articlerender.fcgi?artid=2838443&tool=pmcentrez&rendertype=abstract

Scholl, C., Bansal, D., Döhner, K., Eiwen, K., Huntly, B. J. P., Lee, B. H., … Fröhling, S. (2007). The homeobox gene CDX2 is aberrantly expressed in most cases of acute myeloid leukemia and promotes leukemogenesis. *The Journal of Clinical Investigation*, *117*(4), 1037–48. doi:10.1172/JCI30182

Schumacker, P. T. (2006). Reactive oxygen species in cancer cells: live by the sword, die by the sword. *Cancer Cell*, *10*(3), 175–6. doi:10.1016/j.ccr.2006.08.015

Seiler, A., Schneider, M., Förster, H., Roth, S., Wirth, E. K., Culmsee, C., … Conrad, M. (2008). Glutathione peroxidase 4 senses and translates oxidative stress into 12/15-lipoxygenase dependent- and AIF-mediated cell death. *Cell Metabolism*, *8*(3), 237–48. doi:10.1016/j.cmet.2008.07.005

Shah AM, C. K. (2004). Free radicals and redox signalling in cardiovascular disease. *Heart*.

Shidoji, Y., Okamoto, K., Muto, Y., Komura, S., Ohishi, N., & Yagi, K. (2006). Prevention of geranylgeranoic acid-induced apoptosis by phospholipid hydroperoxide glutathione peroxidase gene. *Journal of Cellular Biochemistry*, *97*(1), 178–87. doi:10.1002/jcb.20627

Sinenko, S. a, Hung, T., Moroz, T., Tran, Q.-M., Sidhu, S., Cheney, M. D., … Banerjee, U. (2010). Genetic manipulation of AML1-ETO-induced expansion of hematopoietic precursors in a Drosophila model. *Blood*, *116*(22), 4612–20. doi:10.1182/blood-2010-03-276998

Stocker, R., Yamamoto, Y., McDonagh, A. F., Glazer, A. N., & Ames, B. N. (1987). Bilirubin is an antioxidant of possible physiological importance. *Science (New York, N.Y.)*, *235*(4792), 1043–6. Retrieved from http://www.ncbi.nlm.nih.gov/pubmed/3029864

Sutherland, M., Shankaranarayanan, P., Schewe, T., & Nigam, S. (2001). Evidence for the presence of phospholipid hydroperoxide glutathione peroxidase in human platelets: implications for its involvement in the regulatory network of the 12-lipoxygenase pathway of arachidonic acid metabolism. *The Biochemical Journal*, *353*(Pt 1), 91–100. Retrieved from http://www.pubmedcentral.nih.gov/articlerender.fcgi?artid=1221546&tool=pmcentrez&rendertype=abstract

Sutherland, J. V, & Bailar, J. C. (1984). The multihit model of carcinogenesis: etiologic implications for colon cancer. *Journal of Chronic Diseases*, *37*(6), 465–80. Retrieved from http://www.ncbi.nlm.nih.gov/pubmed/6725500

Szatrowski, T. P., & Nathan, C. F. (1991). Production of Large Amounts of Hydrogen Peroxide by Human Tumor Cells. *Cancer Res.*, *51*(3), 794–798. Retrieved from http://cancerres.aacrjournals.org/content/51/3/794

Tatla, S., Woodhead, V., Foreman, J. C., & Chain, B. M. (1999). The role of reactive oxygen species in triggering proliferation and IL-2 secretion in T cells. *Free Radical Biology & Medicine*, *26*(1-2), 14–24. Retrieved from http://www.ncbi.nlm.nih.gov/pubmed/9890636

Tothova, Z., Kollipara, R., Huntly, B. J., Lee, B. H., Castrillon, D. H., Cullen, D. E., … Gilliland, D. G. (2007). FoxOs are critical mediators of hematopoietic stem cell resistance to physiologic oxidative stress. *Cell*, *128*(2), 325–39. doi:10.1016/j.cell.2007.01.003

Trachootham, D., Zhou, Y., Zhang, H., Demizu, Y., Chen, Z., Pelicano, H., … Huang, P. (2006). Selective killing of oncogenically transformed cells through a ROS-mediated mechanism by beta-phenylethyl isothiocyanate. *Cancer Cell*, *10*(3), 241–52. doi:10.1016/j.ccr.2006.08.009

Truscott, R. J. (2000). Age-related nuclear cataract: a lens transport problem. *Ophthalmic Research*, *32*(5), 185–94. Retrieved from http://www.ncbi.nlm.nih.gov/pubmed/10971179

Ufer, C., & Wang, C. C. (2011). The Roles of Glutathione Peroxidases during Embryo Development. *Frontiers in Molecular Neuroscience*, *4*, 12. doi:10.3389/fnmol.2011.00012

Ursini, F., Maiorino, M., Valente, M., Ferri, L., & Gregolin, C. (1982). Purification from pig liver of a protein which protects liposomes and biomembranes from peroxidative degradation and exhibits glutathione peroxidase activity on phosphatidylcholine hydroperoxides. *Biochimica et Biophysica Acta*, *710*(2), 197–211. Retrieved from http://www.ncbi.nlm.nih.gov/pubmed/7066358

Valko, M., Leibfritz, D., Moncol, J., Cronin, M. T. D., Mazur, M., & Telser, J. (2007). Free radicals and antioxidants in normal physiological functions and human disease. *The International Journal of Biochemistry & Cell Biology*, *39*(1), 44–84. doi:10.1016/j.biocel.2006.07.001

Valko, M., Rhodes, C. J., Moncol, J., Izakovic, M., & Mazur, M. (2006). Free radicals, metals and antioxidants in oxidative stress-induced cancer. *Chemico-Biological Interactions*, *160*(1), 1–40. doi:10.1016/j.cbi.2005.12.009

Vardiman, J. W. (2010). The World Health Organization (WHO) classification of tumors of the hematopoietic and lymphoid tissues: an overview with emphasis on the myeloid neoplasms. *Chemico-Biological Interactions*, *184*(1-2), 16–20. doi:10.1016/j.cbi.2009.10.009

Vardiman, J. W., Thiele, J., Arber, D. A., Brunning, R. D., Borowitz, M. J., Porwit, A., … Bloomfield, C. D. (2009). The 2008 revision of the World Health Organization (WHO) classification of myeloid neoplasms and acute leukemia: rationale and important changes. *Blood*, *114*(5), 937–51. doi:10.1182/blood-2009-03-209262

Varela, B. L., Chuang, C., Woll, J. E., & Bennett, J. M. (n.d.). Modifications in the classification of primary myelodysplastic syndromes: the addition of a scoring system. *Hematological Oncology*, *3*(1), 55–63. Retrieved from http://www.ncbi.nlm.nih.gov/pubmed/3857211

Veal, E. A., Day, A. M., & Morgan, B. A. (2007). Hydrogen peroxide sensing and signaling. *Molecular Cell*, *26*(1), 1–14. doi:10.1016/j.molcel.2007.03.016

Viarengo, A., Burlando, B., Ceratto, N., & Panfoli, I. (2000). Antioxidant role of metallothioneins: a comparative overview. *Cellular and Molecular Biology (Noisy-Le-Grand, France)*, *46*(2), 407–17. Retrieved from http://www.ncbi.nlm.nih.gov/pubmed/10774929

Waris, G., & Ahsan, H. (2006). Reactive oxygen species: role in the development of cancer and various chronic conditions. *Journal of Carcinogenesis*, *5*, 14. doi:10.1186/1477-3163-5-14

Weissman, I. L., & Shizuru, J. A. (2008). The origins of the identification and isolation of hematopoietic stem cells, and their capability to induce donor-specific transplantation tolerance and treat autoimmune diseases. *Blood*, *112*(9), 3543–53. doi:10.1182/blood-2008-08-078220

Wen, H., Li, Y., Malek, S. N., Kim, Y. C., Xu, J., Chen, P., … Wang, S. M. (2012). New fusion transcripts identified in normal karyotype acute myeloid leukemia. *PloS One*, *7*(12), e51203. doi:10.1371/journal.pone.0051203

Winkler, B. S., Boulton, M. E., Gottsch, J. D., & Sternberg, P. (1999). Oxidative damage and age-related macular degeneration. *Molecular Vision*, *5*, 32. Retrieved from http://www.pubmedcentral.nih.gov/articlerender.fcgi?artid=1773059&tool=pmcentrez&rendertype=abstract

Yagi, K., Komura, S., Kojima, H., Sun, Q., Nagata, N., Ohishi, N., & Nishikimi, M. (1996). Expression of human phospholipid hydroperoxide glutathione peroxidase gene for protection of host cells from lipid hydroperoxide-mediated injury. *Biochemical and Biophysical Research Communications*, *219*(2), 486–91. doi:10.1006/bbrc.1996.0260

Yagi, K., Shidoji, Y., Komura, S., Kojima, H., & Ohishi, N. (1998). Dissipation of mitochondrial membrane potential by exogenous phospholipid monohydroperoxide and protection against this effect by transfection of cells with phospholipid hydroperoxide glutathione peroxidase gene. *Biochemical and Biophysical Research Communications*, *245*(2), 528–33. doi:10.1006/bbrc.1998.8417

Yang, D., Elner, S. G., Bian, Z.-M., Till, G. O., Petty, H. R., & Elner, V. M. (2007). Pro-inflammatory cytokines increase reactive oxygen species through mitochondria and NADPH oxidase in cultured RPE cells. *Experimental Eye Research*, *85*(4), 462–72. doi:10.1016/j.exer.2007.06.013

Yant, L. J., Ran, Q., Rao, L., Van Remmen, H., Shibatani, T., Belter, J. G., … Prolla, T. A. (2003). The selenoprotein GPX4 is essential for mouse development and protects from radiation and oxidative damage insults. *Free Radical Biology & Medicine*, *34*(4), 496–502. Retrieved from http://www.ncbi.nlm.nih.gov/pubmed/12566075

Yoo, M.-H., Xu, X.-M., Carlson, B. A., Gladyshev, V. N., & Hatfield, D. L. (2006). Thioredoxin reductase 1 deficiency reverses tumor phenotype and tumorigenicity of lung carcinoma cells. *The Journal of Biological Chemistry*, *281*(19), 13005–8. doi:10.1074/jbc.C600012200

8 Appendix

Acknowledgements

Finally I'd love to thank all the people who supported me during this project and especially those who made my every day life as a PhD student easier by answering each and every single question that occurred during my work.

My first gratitude goes to Prof. Dr. Christian Buske for the opportunity to work at his institute; his inputs and experiences were extremely valuable for the prosperity of the study. Special thanks to my supervisor Dr. Naidu Vegi for his continuos support in study and research.

I'd also like to say thank you to Prof. Dr. Eckhard Wolf for his unlimited support.

I thank all my lab members for support, discussion and lots of fun during day-to-day work and after-work. I'd like to mention especially Katrin Edmaier who was always willing to share her knowledge with each and eyery single new method and experiment, as well as Heather Murany and Deidra Daria for carefully reading and correcting the manuscript.

Last but not least thanks to my family for always supporting me in every new project life brings. To mention especially my dad; Thanks for your expertise, discussion and support!